Title

Epigenetic Regulation Of Thermogenesis By Adipose Specific Tet1 And Role Of Dnmt3a In Endurance Exercise By Suppressing Aldh1l1-mediated Oxidative Stress

Author

Damal Villivalam, Sneha

Publication Date

2021

Peer reviewed|Thesis/dissertation

Epigenetic Regulation Of Thermogenesis By Adipose Specific Tet1 And Role Of Dnmt3a In Endurance Exercise By Suppressing Aldh1l1-mediated Oxidative Stress

By

Sneha Damal Villivalam

A dissertation submitted in partial satisfaction of the

requirements for the degree of

Doctor of Philosophy

in

Endocrinology

in the

Graduate Division

of the

University of California, Berkeley

Committee in charge:

Professor Sona Kang, Chair
Professor Hei Sook Sul
Professor Jen-Chywan Wang

Summer 2021

Abstract

Epigenetic Regulation Of Thermogenesis By Adipose Specific Tet1 And Role Of Dnmt3a In Endurance Exercise By Suppressing Aldh1l1-mediated Oxidative Stress

By

Sneha Damal Villivalam

Doctor of Philosophy in Endocrinology

University of California, Berkeley

Professor Sona Kang, Chair

The first part of the thesis reports the role of Ten-eleven translocation methylcytosine dioxygenase 1 (TET1) in beige adipocyte thermogenesis. It has been suggested that beige fat thermogenesis is tightly controlled by epigenetic regulators that sense environmental cues such as temperature. We report that subcutaneous adipose expression of the DNA demethylase TET1 is suppressed by cold and other stimulators of beige adipocyte thermogenesis. TET1 acts as an autonomous repressor of key thermogenic genes, including *Ucp1* and *Ppargc1a*, in beige adipocytes. Adipose-selective Tet1 knockout mice generated by using Fabp4-Cre improves cold tolerance and increases energy expenditure and protects against diet-induced obesity and insulin resistance. Moreover, the suppressive role of TET1 in the thermogenic gene regulation of beige adipocytes is largely DNA demethylase–independent. Rather, TET1 coordinates with HDAC1 to mediate the epigenetic changes to suppress thermogenic gene transcription. Taken together, TET1 is a potent beige-selective epigenetic breaker of the thermogenic gene program. Our findings from this chapter may lead to a therapeutic strategy to increase energy expenditure in obesity and related metabolic disorders.

The second part of the thesis demonstrates the role of DNA (cytosine-5)-methyltransferase 3A (DNMT3A) in exercise regulation. Exercise can alter the skeletal muscle DNA methylome, yet little is known about the role of the DNA methylation machinery in exercise capacity. Here, we show that DNMT3A expression in oxidative red muscle increases greatly following a bout of endurance exercise. Muscle-specific *Dnmt3a* knockout mice have reduced tolerance to endurance exercise, accompanied by reduction in oxidative capacity and mitochondrial respiration. Moreover, *Dnmt3a* deficient muscle overproduces reactive oxygen species (ROS), the major contributors to muscle dysfunction. Mechanistically, we show that DNMT3A suppresses the *Aldh1l1* transcription by binding to its promoter region, altering its epigenetic profile. Forced expression of ALDH1L1 elevates NADPH levels, which results in overproduction of ROS by the action of NADPH oxidase complex, ultimately resulting in mitochondrial defects in myotubes. Thus, inhibition of ALDH1L1 pathway can

rescue oxidative stress and mitochondrial dysfunction from *Dnmt3a* deficiency in myotubes. Finally, we show that *in vivo* knockdown of *Aldh1l1* largely rescues exercise intolerance in *Dnmt3a* deficient mice. Together, we establish that DNMT3A in skeletal muscle plays a pivotal role in endurance exercise by controlling intracellular oxidative stress.

The aim of this dissertation work was to identify and characterize the role of adipose Tet1 in the epigenetic regulation of thermogenesis and the role of skeletal muscle Dnmt3a in exercise metabolism and oxidative stress. This may lead to a therapeutic strategy in obesity, related metabolic disorders and exercise intolerance.

Chapter 1 provides a detailed understanding of the mechanisms of DNMT3A and TET2, which may lead to identifying novel targets for the treatment of IR and relevant human diseases. Even though a plethora of studies have found that changes in DNA methylation are associated with metabolic dysregulation, the functional role is poorly understood. Here, I will review the currently available literature and point out the remaining questions to be answered in order to gain a better understanding of the mechanisms of DNMT3a and TET2.

Chapter 2 exhibits my efforts in characterizing the epigenetic role of DNA demethylase TET1 in suppressing key thermogenic genes. TET1 suppresses the thermogenic activation of beige adipocytes. Moreover, adipose-specific TET1 loss-of function in vivo led to increased energy expenditure and protection from diet-induced obesity, insulin resistance, and glucose tolerance. TET1 coordinates with HDAC1 to suppress thermogenic gene transcription in a DNA demethylase-independent manner. These findings will open new avenues for developing therapeutic strategies to increase energy expenditure in obesity and related metabolic disorders.

Chapter 3 shows the previously unknown role of DNMT3A in endurance exercise skeletal muscle mitochondrial biology. DNMT3A expression in oxidative red muscle increases greatly following a bout of endurance exercise. Mechanistically, we reveal that ALDH1L1 serves as a novel molecular link that contributes to oxidative stress and mitochondrial dysfunction following the loss of *Dnmt3a* in red muscle. This is of great importance from the standpoint of exercise physiology, as physical activity is strongly encouraged as a key strategy for preventing and treating a wide range of human diseases.

Chapter 4 concludes my work on the role of epigenetic enzymes TET1 and DNMT3A in metabolism and related disorders. Further, it also presents future directions and additional questions to get a further understanding.

Table of contents

List of figures

List of Tables

Acknowledgments

First and foremost, thanks to my adviser and mentor, Dr. Sona Kang for taking a chance on me and giving me the greatest opportunity of my life. Her drive, knowledge and exacting attention to detail has been an inspiration and kept my work on track from the first day of my graduate study. I would not have developed as a well-rounded researcher without her mentorship and persistence in me. Being her first PhD student, I worked very closely with her over the years. She taught me how to multitask, grasp techniques fast, and execute experiments without errors. I also express my deepest gratitude for taking the time to guide me for not only my research work but also providing me with instant feedbacks on my scientific writing, motivating me to mentor undergraduate students, and training me to give scientific presentations. She coached me to be a team player by involving me in multiple collaboration projects both within our lab and other labs. She actively created opportunities for me to learn several new techniques and always pushed me to achieve beyond my limits. I would not have been able to accomplish nearly as much as I have without her.

A special thanks to Dr. Hei Sook Sul, being a great pillar of support throughout my PhD. I would not have made it this far without her motivation. My sincere gratitude for truly caring about me and taking the time to help me through the various stages of my graduate school. I will always be indepted for her kindness. I would like to thank Dr. Wally Wang for his support and guidance over the years. His positive comments and reassurance during my qualifying exams and endocrinology seminars helped me moved forward.

During my PhD I was fortunate to work with amazing former and current lab members. My Sincere thanks to my colleagues in the lab, Dr. You, Dr. Jung, Dr. Ma, Dr. Bian, Jinse Kim and Han Xu who have stood by me through thick and thin. All of them have made great contribution to all the projects. I'm also glad to have worked with wonderful undergraduate students Sarah Fung, Lilian Kim, Anna Pi, Tabitha Tcheau, Sarah Ampaloor, Mrinalini Jain, Pouya Amin and Camella Alvarez.

I will not be who I am today without the inspiration and affection of my loving parents, amazing husband, our wonderful family and friends. They have helped me focus on my PhD by taking care of every other aspect in my life. Thanks for spending sleepless nights with me, helping me prepare for important presentations, providing me emotional support and much more. I will forever cherish their love and endless support.

Chapter 1:
DNMT3a and TET2 in adipocyte insulin sensitivity

DNMT3a and TET2 in adipocyte insulin sensitivity

Abstract

Insulin resistance (IR) is a key pathogenic feature of type 2 diabetes and occurs in a wide array of other maladies including obesity, aging, cardiovascular disease, and certain typesof cancer. It results from an intricate interaction between genetic make-up and environment, suggesting it's orchestrated by epigenetic mechanisms. In fact, a plethora of studies have found that changes in DNA methylation are associated with metabolic dysregulation [1,2], but methylation's functional role is poorly understood. In this chapter we will review in detailthe known mechanisms of DNA methylation activity of DNMT3a and TET2 in IR. Further, list the outstanding questions that still remain unanswered.

Role of DNMT3A in insulin resistance

DNA methylation is an epigenetic mark involving the covalent transfer of a methyl group tothe C-5 position (5mC) of cytosine by DNA methyltransferases (DNMTs). The initial findingthat DNMT levels are significantly increased in diet-induced obesity and genetically obeseob/ob mice led us to postulate that it plays a large role in IR [3]. We found that DNMT3a, inparticular, is both necessary and sufficient to mediate IR in cultured mouse and human adipocytes. Indeed, adipose-specific Dnmt3a knockout mice are protected from diet-induced IR and glucose intolerance, with no change in their body weight or composition. Through RNA-seq studies, we found that an important downstream target is Fgf21, which is known to facilitate glucose uptake in adipocytes. In patients with diabetes, DNA methylation at the FGF21 locus is elevated in association with decreased expression of FGF21 in adipose tissue. Importantly, FGF21 expression partially rescues Dnmt3a- mediated IR in vitro, indicating that it is helping mediate the effect of DNMT3a on IR.

Role of TET2 in insulin resistance

DNMTs methylate DNA, but this methylation can be erased by the TET proteins (TET1, 2,and 3), which oxidize 5mC to hydroxymethylcytosine (5hmC), which is then converted to unmethylated cytosine (5C) through base excision repair (BER) and thymidine DNA glycosylase (TDG) [4]. Given the functional role of DNMT3a in the development of IR, we hypothesized that the TET proteins play a counter-regulatory role. Indeed, adipose expression of TET2 is significantly decreased in diet-induced IR [5], and TET2 gain-of-function promotes insulin sensitivity while loss-of-function is necessary for insulin sensitization of PPARγ agonist, Rosiglitazone (Rosi). TET2 is required for Rosi-dependent gene activation of certain PPARγ targets, which is accompanied by changes in the DNA demethylation profile at their promoter regions (Figure 1). Furthermore, TET2 physically interacts with PPARγ to sustain PPARγ binding to target loci upon PPARγ activation with Rosi (Figure 1). Together, these studies suggest that TET2 facilitates the transcriptional activity and insulin-sensitizing efficacy of PPARγ.

In line with these findings, Wu et al recently published work revealing a novel axis between TET2 and AMPK in the regulation of glucose homeostasis [6]. This study found that hyperglycemia destabilizes TET2 through inhibiting AMPK-mediated TET2 phosphorylation at Ser99, which leads to downregulation of global 5hmC levels in the blood of diabetic patients. Furthermore, hyperglycemia-promoted tumor growth was suppressed by TET2, and the anti-tumor effect of Metformin appears to require the AMPK-TET2-5hmC axis. Together, these studies suggest that TET2 is a critical epigenetic sensor/regulator of glucose in the cell. It will be of great importance to find out whether this regulatory loop can be found in adipose and other metabolic tissues in the context of obesity and diabetes

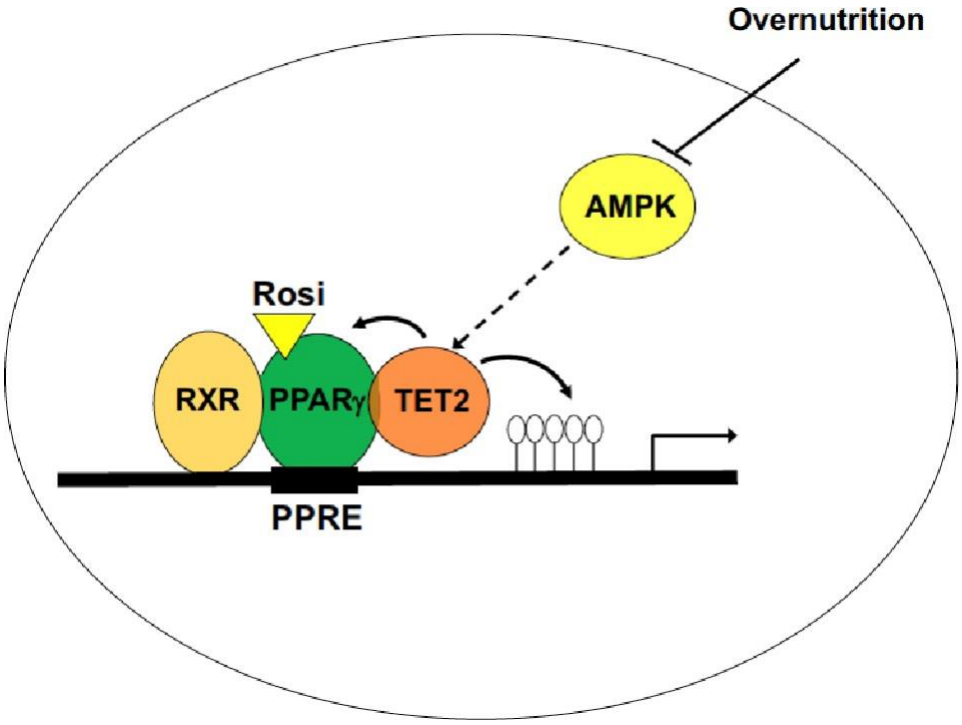

Figure 1: Proposed model of TET2 as a regulator of PPARγ-dependent transcriptionin adipocytes. TET2 physically interacts with PPARγ to sustain PPARγ binding at PPARγ responsive elements (PPREs) and to facilitate the transcriptional activation of PPARγ in response to Rosiglitazone (Rosi). TET2 causes demethylation at the promoter regions of some PPARγ target genes such as Adipoq in a site-specific manner, which canaffect insulin sensitivity. Based upon recent finding by Wu et al, it is postulated that AMPKmay act as an upstream of TET2 in adipocytes (Open circle; demethylated CpG).

Outstanding Questions

Several important questions still remain: 1) Do DNMT3a and TET2 directly converge to regulate insulin sensitivity? They functionally oppose one another, but physical interaction between the two was not detectable by co-immunoprecipitation, and most of their gene targets do not overlap [3,3,5]. 2) What is the in vivo role of TET2 in adipose and other tissues? Studies on TET2 were conducted using cultured adipocyte models, thus physiological validation using tissue-specific knockout and transgenic mouse models will
be critical. It will be intriguing to investigate whether adipose-specific Tet2- knockout mice are refractory to Rosi-driven insulin sensitization. 3) How do DNMT3a and TET2 affect theadipose epigenome?

Conclusion

Investigation into the DNA methylation activity of DNMT3a and TET2 has been limited to the promoter regions of key target genes, but gene bodies and enhancers may also be methylated, having different impacts on gene regulation depending on the function of the region and CpG density. To gain a more comprehensive understanding, global DNA methylation profiling studies will be necessary, ideally using in vivo models. Answering these questions will lead to a more detailed understanding of the mechanisms of DNMT3a and TET2, which may lead to identifying novel targets for the treatment of IR and relevant human diseases.

References

1 Barres, R. and Zierath, J.R. (2011) DNA methylation in metabolic disorders. *Am. J. Clin. Nutr.* 93, 897S – 900

2 Davegårdh, C. *et al.* (2018) DNA methylation in the pathogenesis of type 2 diabetes in humans. *Mol. Metab.* 14, 12–25

3 You, D. *et al.* (2017) Dnmt3a is an epigenetic mediator of adipose insulin resistance. *elife* 6,

4 Benner, C. *et al.* (2015) New roles for DNA cytosine modification, eRNA, anchors, and superanchors in developing B cell progenitors. *Proc Natl Acad Sci USA*112, 12776–12781
5 Bian, F. *et al.* (2018) TET2 facilitates PPARγ agonist-mediated gene regulation and insulin sensitization in adipocytes. *Metab. Clin. Exp.* 89, 39–47
6 Wu, D. *et al.* (2018) Glucose-regulated phosphorylation of TET2 by AMPKreveals a pathway linking diabetes to cancer. *Nature* 559, 637–641

Chapter 2:
TET1 is a beige adipocyte-selective epigenetic suppressor of thermogenesis

TET1 is a beige adipocyte-selective epigenetic suppressor of thermogenesis

Abstract

It has been suggested that beige fat thermogenesis is tightly controlled by epigenetic regulators that sense environmental cues such as temperature. Here, we report that subcutaneous adipose expression of the DNA demethylase TET1 is suppressed by cold and other stimulators of beige adipocyte thermogenesis. TET1 acts as an autonomous repressor of key thermogenic genes, including *Ucp1* and *Ppargc1a*, in beige adipocytes. Adipose-selective Tet1 knockout mice generated by using Fabp4-Cre improves cold tolerance and increases energy expenditure and protects against diet-induced obesity and insulin resistance. Moreover, the suppressive role of TET1 in the thermogenic gene regulation of beige adipocytes is largely DNA demethylase–independent. Rather, TET1 coordinates with HDAC1 to mediate the epigenetic changes to suppress thermogenic gene transcription. Taken together, TET1 is a potent beige-selective epigenetic breaker of the thermogenic gene program. Our findings may lead to a therapeutic strategy to increase energy expenditure in obesity and related metabolic disorders.

Introduction

Mammals have at least two types of thermogenic adipocytes, brown and beige, that play a central role in regulating energy homeostasis[1,2]. In rodents, classical brown adipose tissue (BAT) exists in discrete anatomical depots, such as the interscapular regions, while beige adipocytes sporadically arise within white adipose tissue (WAT)[1,2]. These two thermogenic adipocyte subtypes are similar in multiple respects: both contain multilocular lipid droplets, have a high mitochondrial content, and express key thermogenic genes such as *Ucp1*, *Ppargc1a*, and *Cidea[1,2]*. At the same time, beige and brown adipocytes have several distinct characteristics that distinguish them as two different cell types. For instance, their developmental origins are different. While classical brown adipocytes derive from Myf5-positive precursors during embryonic development, beige adipocytes postnatally develop in the WAT depots of adults and derive from multiple origins depending on the depot[3–7]. In addition, molecular profiling studies highlight significant differences between the gene signatures of brown vs. beige adipocytes[8,9]. Lastly, the plasticity of thermogenic activity remarkably differs between these two cell types. Brown adipocytes are constitutively active and express high levels of UCP1 and other thermogenic genes. Their thermogenic activity can be further increased to a moderate degree upon stimulation. On the other hand, beige adipocytes express very low levels of thermogenic genes but robustly induce their expression in response to external stimuli, thus displaying a greater degree of thermogenic plasticity[1,2].

Beige fat formation, also called “browning” or “beiging”, is induced by various environmental cues, including cold exposure, exercise, and PPARγ agonist[1,2], and it results in the production of heat by burning stored fat. Conversely, beige adipocytes also

undergo “whitening”, returning them to a white adipocyte–like phenotype, in response to thermoneutrality[10], impaired β-adrenergic signaling[11], triglyceride hydrolase deficiency[12] , and other cues[13]. In mice, beige fat contains one tenth the amount of UCP1, a key thermogenic protein, than brown fat[14]; however, the total amount of beige fat can be greater than brown fat and can have a bigger impact on energy homeostasis, as it can be recruited en masse in many white depots[14]. Notably, recent studies have identified additional mechanisms through which beige fat modulates whole-body metabolism such as creatine cycling[15] and Serca2b-mediated calcium cycling[16]. In humans, although still debatable, a substantial number of studies suggest that thermogenic adipocytes are recruited upon cold acclimatization[17,18] leading to increased energy expenditure and a beneficial impact on glucose metabolism[18,19]. Due to this remarkable plasticity and the relevance to human obesity, beige adipocytes are an attractive therapeutic target for obesity and related metabolic diseases.

The browning and whitening of beige and brown fat involves dramatic changes in morphology, transcription, and chromatin landscape[10,20–25]. Therefore, epigenetic regulators are likely to play a key role in this process. The ten-eleven translocation (TET) proteins (TET1, 2, and 3) are the enzymes that oxidize methylated cytosine. In addition to participating in the initial step of DNA demethylation, TETs play versatile roles in transcription regulation[26] by acting as both transcriptional co-activators and co-repressors[26]. Notably, the transcriptional regulation activity of TET proteins can be dependent or independent of their demethylase activity through interacting with other transcriptional regulators and chromatin modifiers[27–31].

Here, we report that TET1 expression in subcutaneous adipose tissue shows reciprocal regulation with Ucp1 in response to ambient temperature changes and cAMP signaling. We demonstrate that *Tet1* loss-of-function leads to cell-autonomous increases in cAMP-induced expression of thermogenic genes, including *Ucp1*, and increases in mitochondrial respiration in beige adipocytes. Consistent with this, conditional deletion of *Tet1* in adipose tissue increases browning of subcutaneous fat, leading to reduced adiposity and improved cold tolerance, glucose tolerance, and insulin sensitivity. Moreover, the knockout mice are protected from diet-induced obesity and metabolic impairment. Mechanistically, we identify that TET1 collaborates with HDAC1 to mediate the epigenetic changes that suppress thermogenic gene transcription in a DNA demethylase–independent manner. Together, our results suggest that TET1 is a potent epigenetic sensor of ambient temperature and modulates the temperature-mediated browning of beige adipocytes.

Results

Adipose TET1 levels in response to temperature and cAMP.

First, we compared the expression of Tets across tissues and noted that all three Tets are moderately expressed in inguinal and epididymal white adipose tissues (iWAT and eWAT) and less expressed in BAT (**Figs. 1a-d**). To identify a potential role for the DNA

methylation machinery in the temperature-induced plasticity of beige and brown adipocytes, we examined how TET expression in adipose tissue is affected by changes in ambient temperature. Inguinal white adipose tissue (iWAT), epididymal WAT (eWAT), interscapular brown fat tissue (BAT) were taken from wild-type C57BL/6J mice that were housed at RT (23°C) before being subjected to cold (4°C) or thermoneutral (TN, 30°C) temperatures for 24 hours. As expected, *Ucp1* levels overall went up in all three depots when mice were housed for 24 hours at cold (4°C) and down when housed at thermoneutrality (TN, 30°C) (**Fig. 1e**). Importantly, the expression of *Tet1* was most dramatically regulated by the changes in ambient temperature, especially in iWAT (**Fig. 1f)**. Heat increased the mRNA expression of *Tet1* by ~ 20 fold whereas cold reduced it by ~60% (**Fig. 1f)**. The temperature-sensitive regulation of TET1 in iWAT was also confirmed by western blotting (**Fig. 1f**).

Similar to *Tet1*, the expression of *Tet2* was also changed but to a lesser degree in iWAT (**Fig. 1g**). On the contrary, *Tet3* levels did not show consistent changes between depots; they had a ~3 fold increase in iWAT (**Fig. 1h)** under cold conditions. The anti-correlation between *Tet1* levels with *Ucp1 in vivo* prompted us to determine their expression levels in three different shades of adipocyte cell lines: 3T3-L1 cells (considered 'white') and immortalized 'beige' and 'brown' adipocytes. As expected, UCP1 protein expression was not detectable in mature 3T3-L1 adipocytes, had intermediate expression in mature beige adipocytes, and high expression in mature brown adipocytes (**Fig. 1l)**. Interestingly, TET1 expression was increased during white adipogenesis and reduced during beige and brown adipogenesis, displaying an anti-correlation with UCP1 levels (**Figs. 1i-1l**). On the other hand, both the expression of TET2 and TET3 was overall higher in all three types of mature adipocytes compared to that of preadipocytes (**Figs. 1i-1l**). As we noted that *Tet1* expression was relatively higher in iWAT compared to BAT (**Figs. 1a, d**), we looked into how the regulation of *Tet1* expression is regulated in response to thermogenic stimulators (cAMP-inducing forskolin and norepinephrine) in *in vitro*–differentiated primary inguinal adipocytes. Consistent with *in vivo*, *Tet1* mRNA expression was reciprocally regulated with *Ucp1* expression in response to the thermogenic stimulators (**Figs. 1m, n**). Together, our expression data suggested that TET1 and TET2 have a functional role in the regulation of thermogenesis in beige fat, thus we sought to test the effects of their downregulation in beige adipocyte thermogenesis.

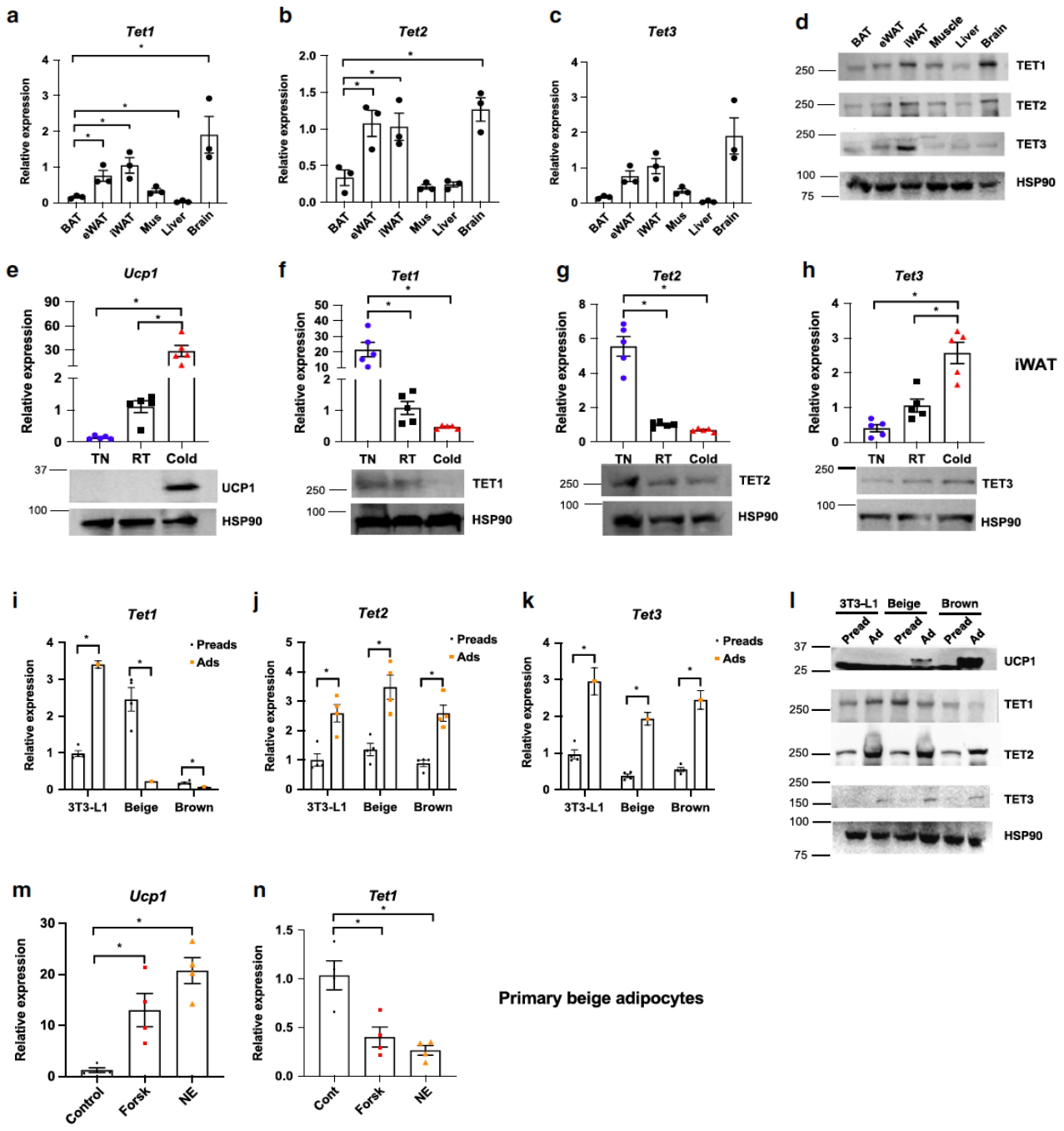

Fig. 1 Subcutaneous adipose Tet1 expression is regulated by ambient temperature and cAMP signaling. a–d Various tissues from wild-type C57BL/6 mice housed at room temperature (RT) were collected to measure Tets mRNA (a–c) and protein expression d (a–c); n =3 per group. Data are expressed as means ± SEM. *denotes $p < 0.05$, determined by two-tailed Student's t test and one-way ANOVA). e–h Tet and Ucp1 mRNA and protein expression in iWAT from wild-type male C57BL/6J mice housed at room temperature (RT) and exposed to cold or thermoneutrality (TN) for 24 h (n = 5 per group. Data are expressed as means ± SEM. *denotes $p < 0.05$, determined by two-tailed

Student's t test and one-way ANOVA followed by Bonferroni post-hoc testing). i–l Tets mRNA and protein expression were measured in 3T3-L1 and immortalized beige and brown preadipocytes at confluence and after differentiation (i–k; n = 4 per group. Data are expressed as means ± SEM. *denotes $p < 0.05$, determined by two-tailed Student's t test). m, n Ucp1 and Tet1mRNA expression with and without 1 μM forskolin (Forsk) or 1 μM norepinephrine (NE) stimulation for 3 h in mature primary beige adipocytes (n = 4 pergroup, Data are expressed as means ± SEM. *denotes $p < 0.05$, determined by two-tailed Student's t test and one-way ANOVA followed by Bonferroni post-hoc testing).

TET1 suppresses the thermogenic activation of beige adipocytes.

To test the cell-autonomous role of TETs in the regulation of thermogenic genes, we performed gain- and loss-of-function studies of individual TETs using an immortalized beige cell line. Since TETs are pro-adipogenic [32] we conducted the studies in fully mature beige adipocytes using short hairpin RNAs (shRNAs) to avoid any effect on differentiation. Remarkably, knockdown of *Tet1*, but not *Tet2* or *Tet3*, enhanced the forskolin-stimulated expression of *Ucp1* and some of key thermogenic markers including *Ppargc1a*, *Cidea*, and *Elovl3* (**Figs. 2a-d**). Notably, there was no change in the expression levels of general adipocyte markers such as *Pparg* and *Fabp4* (**Figs. 2e, f**). *Tet1* knockdown in beige adipocytes increased the rate of mitochondrial respiration in the presence and absence of norepinephrine (**Figs. 2g-i**). Conversely, lentiviral overexpression of *Tet1* in mature beige adipocytes suppressed the expression of thermogenic genes (**Figs. 3a-d**) without altering the expression of general adipocyte markers (*Pparg* and *Fabp4*) (**Figs. 3e, f**) and suppressed mitochondrial respiration in the presence and the absence of norepinephrine (**Figs. 3g-i**). Together, our results suggest that TET1 suppresses adipocyte thermogenesis in a cell-autonomous manner in beige adipocytes.

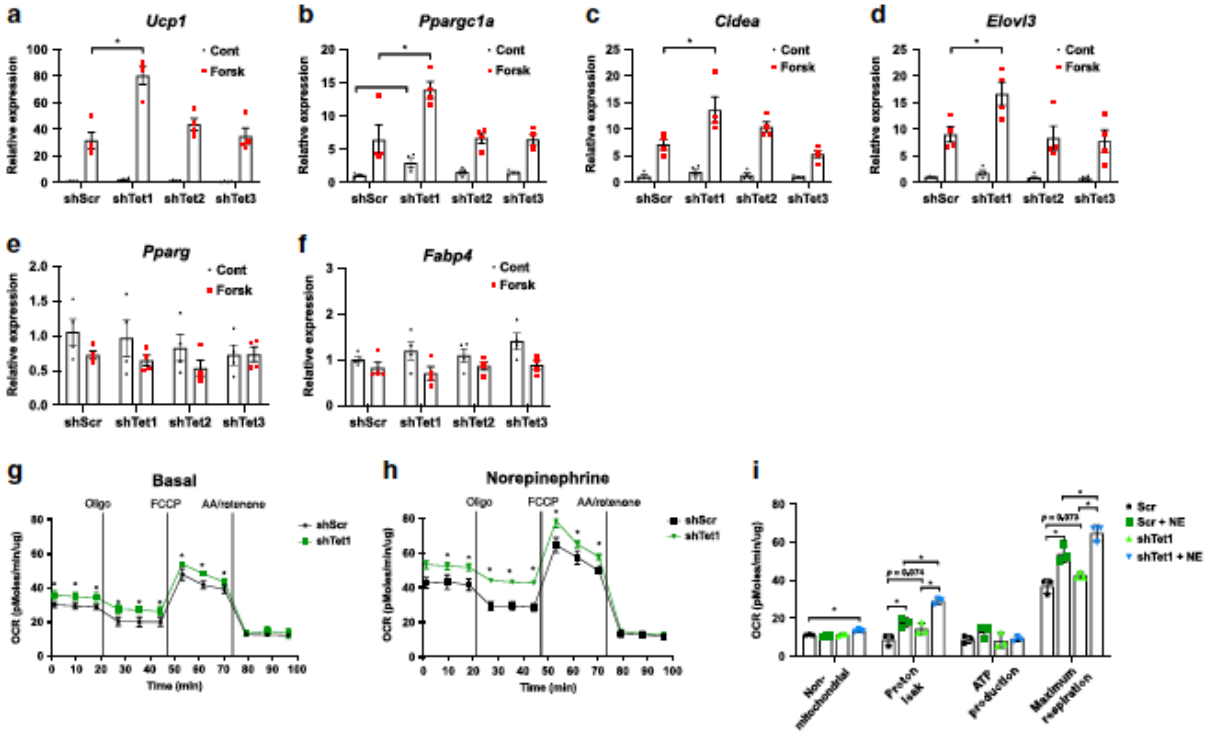

Fig. 2 Tet1 loss-of-function in vitro increases thermogenesis in beige adipocytes. a–f Differentiated beige adipocytes were transduced with hairpins against Tet1, 2, and 3 and scrambled control shRNA (shScr). The basal- and forskolin-stimulated levels of key adipocyte thermogenic gene transcripts were measured by qPCR (n =4 per group. Data are expressed as means ± SEM. *denotes $p < 0.05$, determined by two-tailed Student's t test and two-way ANOVA followed by Bonferroni post-hoc testing). g–i Basal and norepinephrine (NE)-stimulated mitochondrial respiration under various drug treatments was measured in Tet1 knockdown and scramble beige adipocytes (n= 3 per group. Data are expressed as means ± SEM. *denotes $p < 0.05$, determined by two-tailed Student's t test and one-way ANOVA). (Oligo; Oligomycin, AA; antimycin A). i Shown are the various components of oxygen consumption rates with and without NE stimulation from (g, h). (n = 3 per group. Data are expressed as means ± SEM. *denotes $p < 0.05$, determined by two-tailed Student's t test and two-way ANOVA followed by Bonferroni post-hoc testing)

***Tet1* KO mice display increased cold tolerance and energy expenditure.**

To determine the *in vivo* role of *Tet1* in the regulation of adipose plasticity and the thermogenic gene program, we initially generated adipose-selective *Tet1* knockout mice (AdipoQ-Tet1KO) using adiponectin-Cre mice[33]. However, these knockout mice had poor knockdown efficiency (~10%) even when specifically assessing adipocytes. Therefore, we used Fabp4-Cre[34] to generate an adipose-selective knockout (Adi-Tet1KO) mouse, in which *Tet1* mRNA levels were knocked down by more than 80% in the purified adipocyte fraction obtained from iWAT, eWAT, and BAT.

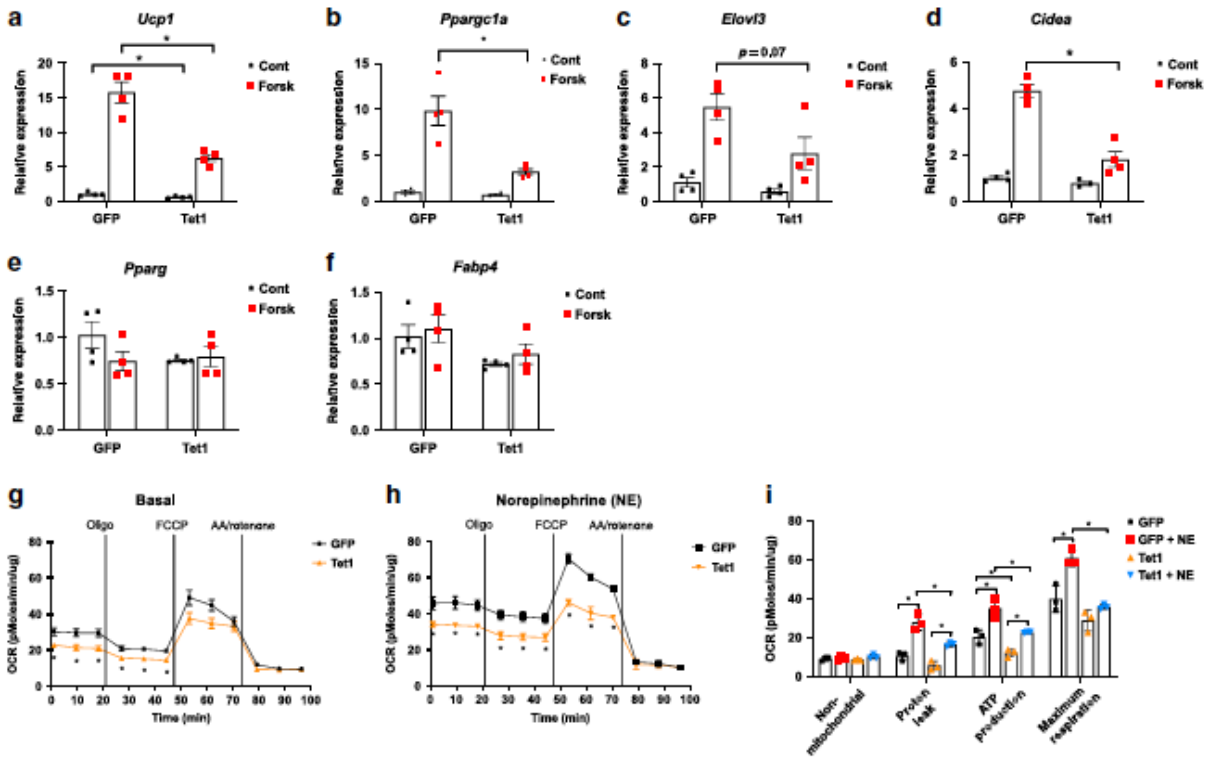

Fig. 3 Tet1 gain-of-function in vitro suppresses thermogenesis in beige adipocytes. a–f Differentiated beige adipocytes were transduced with lentiviral expression plasmids for Tet1 and GFP. The basal- and forskolin-stimulated levels of key adipocyte thermogenic gene transcripts were measured by qPCR (n = 4 per group. Data are expressed as means ± SEM. *denotes $p < 0.05$, determined by two-tailed Student's t test and two-way ANOVA followed by Bonferroni post-hoc testing). g, h Basal and norepinephrine (NE)-stimulated mitochondrial respiration under various drug treatments was measured in Tet1 overexpression and GFP beige adipocytes (n = 3 per group. Data are expressed as means ± SEM. *denotes $p < 0.05$, determined by two-tailed Student's t test and one-way ANOVA). (Oligo; Oligomycin, AA; antimycin A). i Shown are the various components of oxygen consumption rates with and without NE stimulation from g, h. (n = 3 per group. Data are expressed as means ± SEM. *denotes $p < 0.05$, determined by two-tailed Student's t test and two-way ANOVA followed by Bonferroni post-hoc testing).

To examine whether TET1 is necessary for temperature-mediated adipose plasticity, we exposed Adi-Tet1KO and WT mice to different ambient temperatures. To assess their cold tolerance, we monitored the rectal temperature of individual mice placed into a 4°C cold chamber. Adi-Tet1KO mice maintained their core body temperature better than WT

mice under cold conditions (**Fig. 4a**). Consistent with the increased tolerance to cold, the KO mice had a significant increase in oxygen consumption upon cold exposure and a trend towards increased oxygen consumption at RT and TN, as compared to controls (**Figs. 4b, c**). In addition, the serum release of glycerol was elevated in KO mice upon cold exposure (**Fig. 4d**), likely due to increased lipolysis to provide fuel for the increased adaptive thermogenesis. We also noted that KO iWAT had more multilocular brown-like adipocytes after 7 days of cold exposure (**Fig. 4e**), whereas there was no marked difference between WT and KO BAT (**Fig. 4e**). Also notably, the increased rates of basal and norepinephrine-stimulated respiration was more pronounced in the KO iWAT (**Fig. 4f**). This depot-biased effect was also observed at molecular levels; increased expression of UCP1 and PGC1α was found in iWAT (**Fig. 4g**). This suggests that TET1 is acting selectively on beige adipocytes, which are present in iWAT.

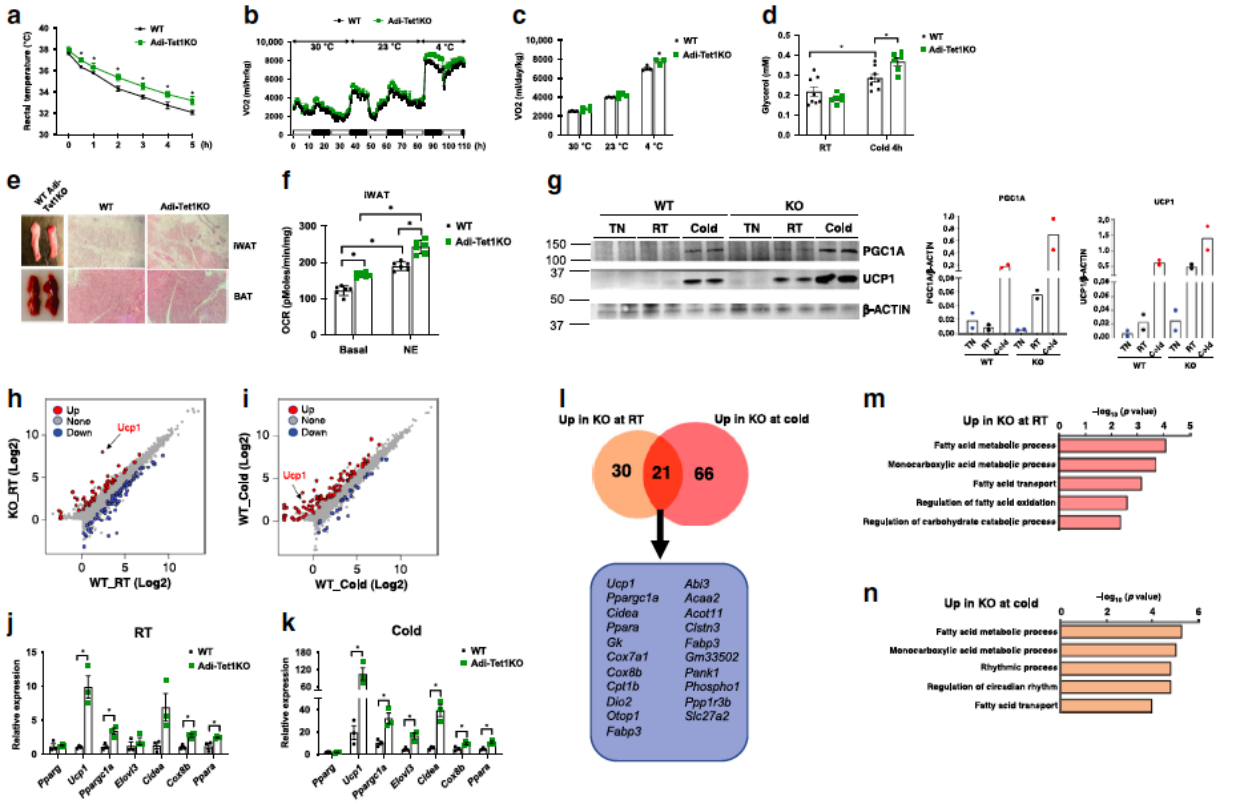

Fig. 4 Adipose-specific Tet1-KO mice show improved cold tolerance. a Rectal core body temperatures of Adi-Tet1-KO and WT mice under cold conditions at indicated time points (n =5 per group. Data are expressed as means ± SEM. *denotes $p < 0.05$, determined by two-tailed Student's t test and one-way ANOVA). b, c Shown is the whole-body oxygen consumption rate (VO2, b) and averaged VO2 c (n = 4 per group. Data are expressed as means ± SEM. *denotes $p < 0.05$, determined by two-tailed Student's t test and two-way ANOVA followed by Bonferroni post-hoc testing). d Serum levels of glycerol were measured from WT and KO mice that were housed at RT or exposed to cold for 24 h (n= 8 WT, n = 6 KO. Data are expressed as means ± SEM. *denotes $p < 0.05$,

determined by two-tailed Student's t test and two-way ANOVA followed by Bonferroni post-hoc testing). e Whole tissue and H&E staining of iWAT and BAT from WT and KO mice that were exposed to cold for 7 days. f Oxygen consumption rate of iWAT from WT and KO mice was measured with and without stimulation of NE. Average basal respiration rate is presented with or without norepinephrine addition (n = 6 per group. Data are expressed as means ± SEM. *denotes $p < 0.05$, determined by two-tailed Student's t test and two-way ANOVA followed by Bonferroni post-hoc testing). g Immunoblot of UCP1 and PGC1A from WT and KO iWAT from RT, exposed to TN or cold for 7 days. The relative expression is shown by normalizing to β-ACTIN (n =2 per group. Data are presented as means of the two). h, i Scatter plot showing differentially regulated genes in inguinal KO adipocytes from WT and KO mice held at RT and exposed to cold for 4 h (n = 2 per group for RT, n = 3 WT, n = 2 KO for Cold, FC > 1.5, FDR < 0.05). j, k q-PCR analysis of key thermogenic genes from WT and KO inguinal adipocytes from WT and KO mice at RT and cold exposed for 4 h (n = 3 per group. Data are expressed as means ± SEM. *denotes $p < 0.05$, determined by two-tailed Student's t test). l Venn diagram of the upregulated genes in the KO adipocytes at RT vs cold conditions and the gene names that are commonly upregulated in the KO adipocytes at both temperatures (n= 2 per group for RT, n = 3 WT, n = 2 KO for Cold). Gene list is provided in Supplementary Table 1. m, n Commonly upregulated biological pathways in the KO adipocytes from RT and cold.

TET1 acts as a repressor of the thermogenic gene program.
To investigate the mechanism of how TET1 suppresses the thermogenic gene program, we used RNA-Seq to identify the adipocyte-specific target genes of TET1. In short, we profiled fractionated inguinal adipocytes from WT and KO mice held at RT and exposed to cold for 4 hours (**Figs. 4h-n**). We found that 51 genes were significantly upregulated and 73 genes were downregulated in the KO inguinal adipocytes at RT, and 87 genes were upregulated and 26 genes downregulated after a 4-hr cold exposure (**Figs. 4h-j**). This suggests that TET1 acts as both a gene repressor and activator in inguinal adipocytes. Interestingly, the upregulated genes in the KO adipocytes greatly overlapped between RT and cold conditions (**Fig. 4j**), and many of those are involved in thermogenesis (e.g., *Ucp1*, *Pgc1a*, *Cidea*, and *Elovl3).* These were validated by qPCR analysis (**Figs. 4k, l**). This suggests that the transcriptional regulation of key thermogenic genes in the KO is already primed under RT, which is mildly cold for mice. Gene Ontology term analysis found that the commonly upregulated pathways in KO inguinal adipocytes are relevant to thermogenesis, such as fatty acid metabolism, under both RT and cold (**Figs. 4m, n**).

***Tet1* KO mice are protected against diet-induced obesity.**
Increased browning leads to increased energy expenditure and improved glucose homeostasis[18,19]. Thus, we assessed whether the increased browning during adipose-selective *Tet1* deficiency leads to metabolic improvement. Despite the body weight of Adi-Tet1KO remaining unchanged (**Fig. 5a**), their fat mass was significantly reduced compared to their littermate controls on a chow diet (**Fig. 5b**). Reduced adiposity in Adi-Tet1KO mice on chow was accompanied by improved glucose tolerance, insulin sensitivity, and hypoinsulinemia (**Figs. 5c-e**). Next, we asked whether adipose-selective

Tet1 deficiency confers protection against diet-induced obesity and impaired glucose tolerance by placing cohort mice on a high-fat diet (HFD, 60% calories from fat). The body weights of the two groups began to significantly diverge after 6 weeks of HFD feeding (**Fig. 5f**). The KO had reduced fat mass (**Fig. 5g**), and their tissue mass of inguinal and mesenteric WAT was significantly decreased (**Fig. 5h**). Consistent with the lean phenotype, KO mice were more glucose tolerant and insulin sensitive than controls, having reduced insulin levels at fed and fast states on HFD (**Figs. 5i-k**).

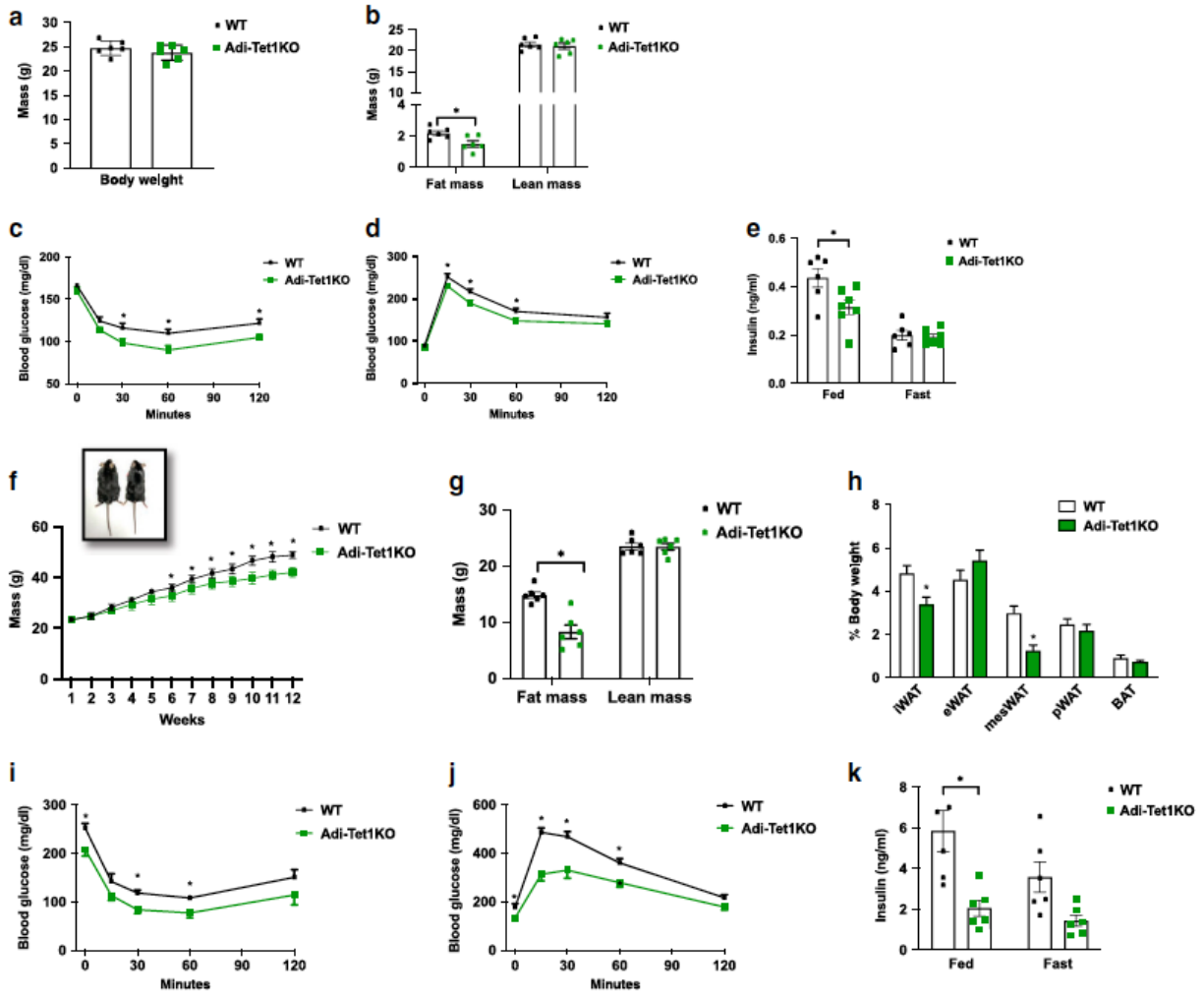

Fig. 5 Adipose-specific Tet1-KO mice are protected from diet-induced obesity and metabolic dysregulation. a, b Body weight (a) and body composition by EchoMRI (b) of 8-week-old WT and KO mice on a chow diet (n = 6 per group. Data are expressed as means ± SEM. *denotes $p < 0.05$, determined by two-tailed Student's t test). c, d Insulin tolerance test (c) and glucose tolerance test (d) on chow diet (n = 8 WT, n = 6 KO. Data are expressed as means ± SEM. *denotes $p < 0.05$, determined by two-tailed Student's t test). e Fed and fasted insulin levels from a chow-fed cohort (n = 6 per group. Data are expressed as means ± SEM. *denotes $p < 0.05$, determined by two-tailed Student's t test and two-way ANOVA followed by Bonferroni post-hoc testing). f Weekly body weight of

WT and KO mice on a high-fat diet (n = 7 per group. Data are expressed as means ± SEM. *denotes p < 0.05, determined by two-tailed Student's t test). g Body composition after 10 weeks of HFD (n = 6 per group, Data are expressed as means ± SEM. *denotes p < 0.05, determined bytwo-tailed Student's t test). h Adipose tissue weight from HFD cohort (n= 6 per group. Data are expressed as means ± SEM. *denotes p < 0.05, determined by two-tailed Student's t test). i, j Insulin tolerance test (i) and glucose tolerance test (j) after 10 or 11 weeks on HFD, respectively (n =6 per group, Data are expressed as means ± SEM. *denotes p < 0.05, determined by two-tailed Student's t test). k Fed and fasted insulin levels from high-fat-fed mice (n =6 per group. Data are expressed as means ± SEM. *denotes p < 0.05, determined by two-tailed Student's t test and Two-way ANOVA followed by Bonferroni post-hoc testing).

TET1 acts in a DNA demethylase–independent manner.

TETs mediate their biological functions in both DNA demethylase–dependent and –independent manners[27–31]. Thus, we addressed whether demethylation activity is necessary for TET1 to suppress the thermogenic program in beige adipocytes. First, as a genetic approach, we generated various Tet1 mutant alleles (**Fig. 6a**). Lentiviral overexpression of a Tet1 mutant allele that lacks c-terminal catalytic activity (Tet1ΔCD)[42] (**Fig. 6b**) still repressed Ucp1 transcription to a similar degree as the wild-type allele (Tet1WT) (**Fig. 6c**). On the other hand, overexpressing either the truncation mutant that contains only the catalytic domain (Tet1CD) or the catalytically inactive mutant with two critical amino acid substitutions (Tet1CDM)[43] was not able to repress Ucp1 expression (**Fig. 6c**). Both wild-type Tet1 and Tet1ΔCD equally inhibited mitochondrial respiration in the presence of norepinephrine (**Figs. 6d, e**).

Second, we performed *Tet1* loss-of-function studies in cells that had all three DNA methyltransferases (DNMTs) knocked down to reduce the level of 5mC, which is the enzymatic substrate for TET. If DNA demethylation activity was critical, the effect of *Tet1* loss-of-function would be diminished in these cells. Interestingly, knocking down the Dnmts alone resulted a trend toward an increase in the *Ucp1* expression, and double knockdown with *Tet1* further increased the expression of *Ucp1* (**Fig. 6f**). Third, we manipulated TET demethylase activity at the co-factor level. Alpha-ketoglutarate (α-KG), a key metabolite from the TCA cycle, acts as a co-factor for the demethylation activity of TETs, whereas another TCA intermediate, succinate, inhibits TET activity[44,45]. We treated mature brown and beige adipocytes with cell-permeable forms of α-KG and diethyl-succinate then subjected them to forskolin treatment. Neither metabolite had any significant impact on forskolin-stimulated *Ucp1* expression **(Fig. 6g**).

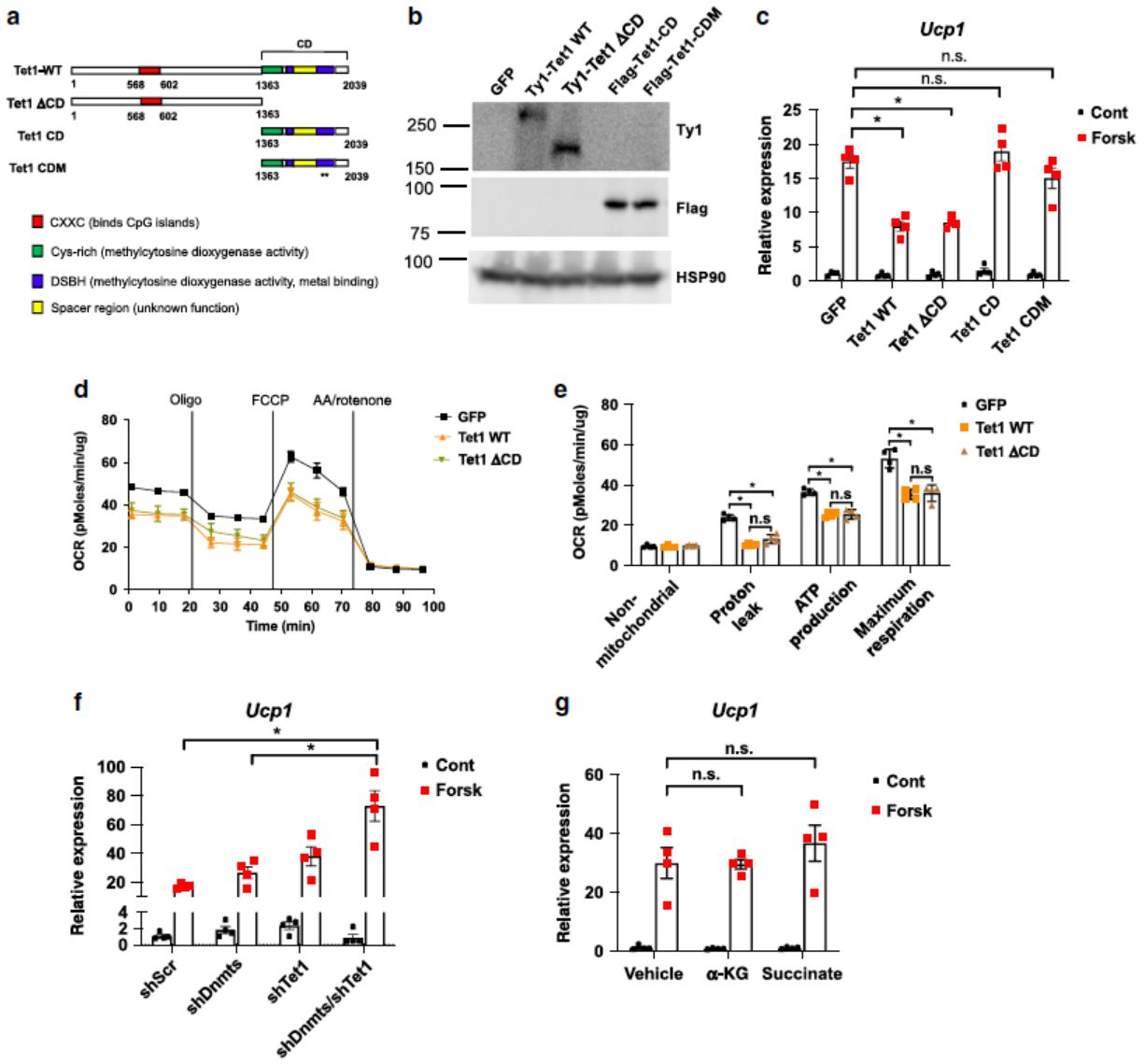

Fig. 6 TET1 suppresses the thermogenic gene program in a DNA demethylase–independent manner. a The protein map showing Tet1 wild-type and mutant alleles: the Tet1 wild-type (Tet1 WT) allele, a truncation mutant that lacks DNA demethylase activity (Tet1 ΔCD), a mutant that contains only DNA demethylase activity (Tet1 CD), and a catalytically inactive form (Tet1 CDM). b Mature beige adipocytes were transduced with lentiviral expression plasmids for the various Tet1 alleles from (a). c The basal- and forskolin-stimulated levels of Ucp1 were measured by qPCR from (b) (n = 4 per group. Data are expressed as means ± SEM. *denotes $p < 0.05$, determined by two-tailed Student's t test and one-way ANOVA followed by Bonferroni post-hoc testing). d, e Mitochondrial respiration is measured by Seahorse from beige adipocytes that overexpress Tet1 WT, Tet1 ΔCD, or GFP. (n = 4 per group. Data are expressed as means ± SEM. *denotes $p < 0.05$, determined by two-tailed Student's t test and two-way ANOVA followed by Bonferroni post-hoc testing). f Beige adipocytes were transduced with hairpins against Dnmt1, 3a, and, 3b or control scramble RNA (shScr), and differentiated beige adipocytes were transduced with shTet1. The basal- and

forskolin-stimulated levels of Ucp1 were measured by qPCR (n= 4 per group. Data are expressed as means ± SEM. *denotes $p < 0.05$, determined by two-tailed Student's t test and two-way ANOVA followed by Bonferroni post-hoc testing). g Alpha-KG (α-KG), diethyl-succinate (Succinate), or a vehicle was used to pre-treat mature beige adipocytes for 3 hr. The basal- and forskolin-stimulated levels of Ucp1 were measured by qPCR (n =4 per group. Data are expressed as means ± SEM. *denotes $p < 0.05$, determined by two-tailed Student's t test and two-way ANOVA followed by Bonferroni post-hoc testing).

TET1 coordinates with HDAC1 to mediate the thermogenic gene repression.
It has been proposed that the repressor role of TET1 in gene regulation in other cell types is accomplished through interacting with other repressor proteins like polycomb repressive complex 2 (PRC2)[50], HDACs[51], and SIN3A[52]. Since genetic and pharmacological inhibition of HDAC1 increases UCP1 and PGC1α expression and oxidative metabolism[53–55]. we sought to determine whether TET1-mediated repression involves interacting with HDAC1. First, we detected an interaction between TET1 and HDAC1 by co-immunoprecipitating in HEK293T cells **(Fig. 7a).** Interestingly, the interaction with HDAC1 still existed with Tet1ΔCD, which lacks DNA demethylase activity at the c-terminal region (Fig. 7a). We examined whether TET1 and HDAC1 are recruited to the same gene regulatory regions of Ucp1 and Ppargc1a[55]. Since we were not able to identify a high-quality antibody against endogenous TET1, we immunoprecipitated TET1 tagged with of Ty1 tag from overexpressor cells. With ChIP-reChIP analysis, we confirmed the simultaneous binding of HDAC1 and TET1 at these regulatory regions **(Fig. 7b)** and that both TET1 and HDAC1 binding at these sites was greatly diminished with forskolin stimulation **(Figs. 7c-e).**

HDAC1 deacetylates histones, which prevents transcription. Therefore, to examine the downstream epigenetic changes that Tet1 loss-of-function confers, we performed ChIP-PCR using the active histone mark H3K27ac in WT and KO adipose tissue harvested from different temperature conditions. As expected, in WT iWAT samples, H3K27ac enhancer activity was higher at RT and highest during cold exposure as compared to TN. Overall, this temperature-dependent H3K27ac enhancer activity was even more dramatic in KO iWAT (**Figs. 7f-h**), in concert with increased expression of *Ucp1* and *Ppargc1a* (**Figs. 4j, k**). Lastly, we assayed the role of HDAC1 in TET1-mediated thermogenic gene suppression. CRISPR-Cas-mediated knockout of HDAC1 fully rescued TET1-mediated repression of *Ucp1* (**Figs. 7i, j**). Together, our results suggest that the role of TET1 as a suppressor of the thermogenic gene program is in large part due to HDAC1.

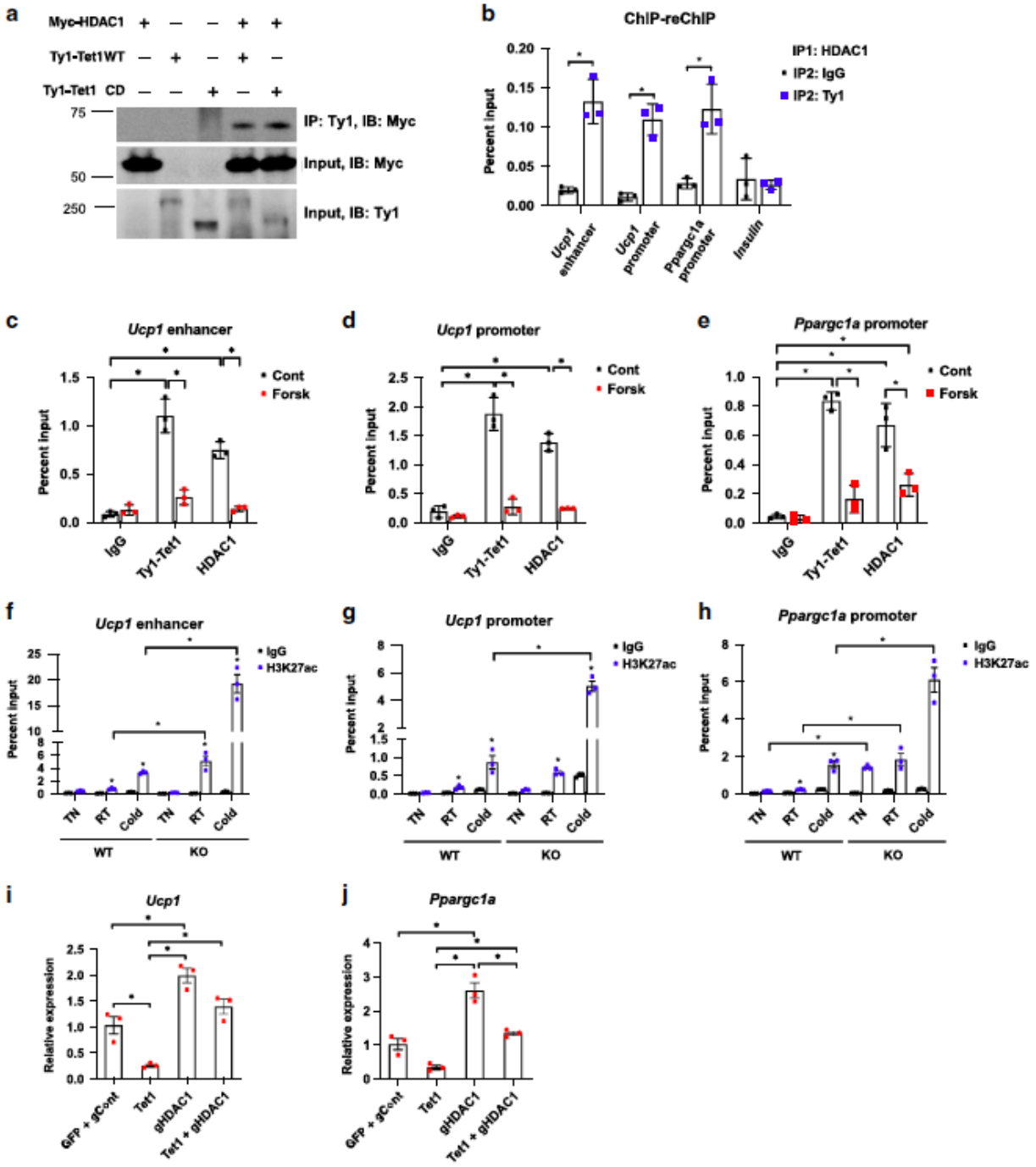

Fig. 7 TET1 coordinates the epigenetic remodeling of the regulatory regions of Ucp1 and Ppargc1a by coordinating with HDAC1. a Coimmunoprecipitation assay was performed using protein lysates from HEK293T cells that were co-transfected with vectors expressing Ty1-Tet1 WT, Ty1- Tet1deltaCD, and Myc-HDAC1. b ChIP-reChIP qPCR analysis was performed on beige adipocytes that were transduced with Ty1-Tet1 WT or GFP using HDAC1 (1st IP), Ty1 (2nd IP), or IgG as a control. The enrichment efficiency is presented as a percent input at the indicated binding sites (n =3 per group. Data are expressed as means ± SEM. *denotes $p < 0.05$, determined by two-tailed Student's t test followed by Bonferroni post-hoc testing). c–e Ty1 and HDAC1 ChIP-qPCR analysis was

performed in cells that express Ty1-Tet1 WT with and without forskolin stimulation (n = 3 per group. Data are expressed as means ± SEM. *denotes $p < 0.05$, determined by two-tailed Student's t test and two-way ANOVA followed by Bonferroni post-hoc testing). f–h H3K27ac ChIP-qPCR analysis was performed in WT and KO iWAT from RT or exposed to TN or cold for 7 days (n = 3 per group). Data are expressed as means ± SEM. *denotes $p < 0.05$, determined by two-tailed Student's t test and two-way ANOVA followed by Bonferroni post-hoc testing. i, j Beige adipocytes were transduced with either Tet1 overexpressor, gRNA against Hdac1, both, or control plasmids. The forskolin-stimulated level of Ucp1 and Ppargc1a was measured by qPCR (n =4 per group, Data are expressed as means ± SEM. *denotes $p < 0.05$, determined by two-tailed Student's t test and two-way ANOVA followed by Bonferroni post-hoc testing).

Discussion

While classical brown and beige adipocytes share many fundamental features in morphology and function, discrete characteristics have been identified, including the plasticity of beige thermogenesis[1]. A recent epigenomic profiling study demonstrated that the temperature-mediated plasticity of subcutaneous fat is accompanied by profound changes in chromatin state[10]. To add to these results, we identified TET1 as a beige fat–selective epigenetic repressor of the thermogenic gene program.

We demonstrated that TET1 represses thermogenic gene regulation in a largely DNA demethylase–independent manner. In support of this notion, transcriptional changes induced by overexpression of TET1 were highly similar to those induced by its demethylation activity–dead mutant in differentiated cell lines. Other studies have demonstrated that TETs, in addition to modifying cytosine methylation, can act as gene regulators through a DNA methylation–independent manner[28]. The repressive role of TET1 in transcriptional regulation has been proposed to derive from its interaction with other repressor proteins. In ES cells, but not in somatic cells, TET1 contributes to silencing some genes by interacting with polycomb repressive complex 2 (PRC2), which targets repressive histone mark H3K27me3[50]. TET1 is also found in the repressor complex containing SIN3A and HDAC1/2 in both mESCs and HEK293T cells, and its localization greatly overlaps with the SIN3A binding profile genome-wide[30]. Thus, our results are in line with these studies, as TET1 cooperates with HDAC1 to repress some of the key thermogenic genes like *Ucp1* and *Ppargc1a*. We speculate that such interaction facilitates local epigenetic modifications and regulates other transcription factors and co-factors to regulate transcriptional activity.

There is also indirect evidence that DNA demethylation and TETs are also required for the development of interscapular BAT[56]. In this study, the authors suggested that TET proteins mediate demethylation at the promoter region of *Prdm16[56]*, a key developmental gene that is critical for the brown adipogenic lineage and maintains brown adipocyte identity. Moreover, reducing the level of α-ketoglutarate (α-KG), a co-factor for the TET enzymes, leads to reduced demethylation of *Prdm16* and impaired brown adipocyte development and function in mutant mice carrying loss-of-function AMPKa1[56]. Given the pro-adipogenic function of TET1 in white and brown

adipogenesis, our results demonstrating TET1 is an inhibitor of thermogenic genes may seem contradictory. However, such dual roles have been reported with other 'whitening' transcription factors. For example, Zfp423, preferentially expressed in white adipocytes, is a pro-adipogenic commitment factor *in vitro* and *in vivo[57]*, but it also acts as a molecular gate keeper that maintains white cell identity while suppressing browning in mature adipocytes[58]. Interestingly, a recent study reported that the glucocorticoid receptor (GR) drives beige adipocyte whitening as an upstream regulator of Zfp423[10]. TLE3, another whitening transcription factor, promotes adipose conversion during early differentiation by interacting with PPARγ and antagonizing Wnt signaling[59]. But a recent study identified its novel role as a suppressor of thermogenic gene expression in beige adipocytes[60]. Notably, both Zfp423 and TLE3 inhibit the activity of pro-browning transcription factor early B-cell factor 2 (EBF2)[58,60], which cooperates with PPARγ and epigenetic modifiers, such as the chromatin remodelers BRG1 and BAF, and a long noncoding RNA, Blnc1[61]. Future studies are warranted to determine whether TET1-mediated gene repression converges with these known transcriptional regulators.

Notably, two global studies suggest that differences in the DNA methylation profile is not a major contributor to cell type–specific gene expression in white vs beige or brown adipocytes[62,63]. The first global study employed restriction landmark genomic scanning (RLGS)[63], the method by which methylation-sensitive restriction enzymes preferentially cut CpG islands in regulatory regions[63]. In this study, authors also did not find a dramatic difference in the DNA methylation profile between primary white vs. brown adipocytes. The other global study profiled *in vitro*–differentiated white and brown adipocytes from inguinal and brown adipose depots using reduced representation bisulfite sequencing (RRBS)[62,63], which focuses on CpG-rich promoter methylation. Although an overall negative correlation between promoter methylation and gene expression was observed when comparing white and brown adipocytes, dramatic differences in DNA methylation at the thermogenic genes were not reported. Consistent with these reports, we did not detect dramatic changes in DNA demethylation at the key thermogenic genes. However, we observed that some of the CpG sites displayed simultaneous hyper- or hypo-methylation depending on temperature changes at the *Ucp1* promoter region. Thus, genome-wide methylation profiling studies are warranted to more accurately understand the DNA methylation profile under different temperature conditions. Moreover, functional validation studies will be necessary at the level of individual CpGs.

One of the major caveats of our study is the use of Fabp4-Cre, which is expressed in several other non-adipose tissues[35,64] . Thus, we conducted additional experiments to assess whether there is an additional contribution from non-adipose tissues to the increased thermogenesis in Adi-Tet1 KO mice. First, our *in vitro* gain- and loss-of-function studies showed that *Tet1* knockdown and overexpression have a beige adipocyte–autonomous effect on thermogenic gene regulation and mitochondrial respiration. Second, we showed that inguinal-selective knockdown of *Tet1* by AAV8-hAdi-Cre and noted a similar effect on thermogenesis. Third, to address if there is input from macrophage cells in Adi-Tet1 KO mice, we conducted co-culture experiments using beige adipocytes and primary macrophages isolated from Adi-Tet1 KO vs. WT mice. There were no significant changes in basal and forskolin-induced thermogenic gene expression.

Lastly, we report no major phenotypic changes in thermogenesis and energy homeostasis in the PDGFRa-Tet1 KO generated using PDGFRa-Cre, which is expressed in preadipocytes and a variety of tissues, including the lung, heart, intestine, skin, and cranial facial mesenchyme[37–39,65–67]. We, however, note that it is still possible that there could be an additional contribution on top of that from adipose tissues.

In summary, we identified TET1 as an important epigenetic regulator of the thermogenic gene program in beige adipocytes that coordinates with HDAC1. Adipose-specific TET1 loss-of-function led to increased energy expenditure and protection from diet-induced obesity, insulin resistance, and glucose tolerance.

Methods

Cell culture

Immortalized beige and brown adipocytes were maintained and differentiated with an adipogenic cocktail (0.5mM IBMX, 5uM Rosiglitazone, 5mg/ml insulin, 1mM dexamethasone). To generate lentivirus particles, lentiviral constructs were co-transfected with pM2DG- and psPAX-expressing plasmids into 293T cells. After 48 h, virus-containing supernatant was collected, filtered through 0.45 μm filters, and added to mature day 5 adipocytes for 48 h along with 8 μg/ml Polybrene. Transduction efficiency was determined by comparing to cells transduced in parallel with a GFP-expressing lentivirus. For the *ex vivo* system, subcutaneous WAT and iBAT from wild-type C57BL/6 mice was fractionated with digestion buffer (10 mg/ml collagenase D, 2.4 units of dispase II, 10 mM $CaCl_2$ in PBS). The stromal-vascular fraction (SVF) were isolated by 1.5u/ml collagenase and plated in culture and differentiated with adipogenic cocktail. For co-culture experiment, beige adipocytes were cultured in 6-well plates and differentiated at day 8, and macrophages (2×10^5 cells/well) were plated onto the transwell insert containing a 0.4 μm polyethylene terephthalate membrane (Costar, Corning, USA) in serum free medium. After incubation together for 24 h, the transwell was removed and beige adipocytes were harvested for analysis. 3T3-L1 adipocytes were differentiated in 12-well plates and then treated with conditioned medium from LPS-activated macrophages from WT and KO mice. 3T3-L1 adipocytes were cultured for 24 hours before gene expression analysis.

Reagents

Insulin, dexamethasone, isobutylmethylxanthine (IBMX), α-KG, CL316, 243, diethyl succinate, and thyroid hormone (T3) were purchased from Sigma. Rosiglitazone was purchased from Cayman. Antibodies were purchased from GeneTex (Tet1, GTX1242071), Thermo Fisher (β-actin, MA5-14739), Cell Signaling (HSP-90, 4874), GenScript (Ty1, A01004), Covance (HA, MMS-101R), Sigma (Flag, F3165), Santa Cruz (Myc, SC-40), Abcam (UCP1, Ab10983; PGC1α: Ab54481; H3K27ac: Ab4729),

Biolegend (CD45-PerCP/Cy5.5,103131; F4/80-PE/Cy7, Cat# 123113; Cd11b-Pacific Blue, 101223; CD301-APC, 145707 and eBioscience (Cd11c-PE,12-0114-81).

Animals

Tet1$^{f/f}$ mice were obtained from Dr. Anjana Rao laboratory at UCSD. Mice were maintained under a 12hr light /12hr dark cycle at room temperature (23°C) with free access to food and water. For thermal challenge, mice were placed in a cold chamber (4°C) for up to 1 week or at thermoneutrality (30°C). Body temperature was measured using a rectal probe (Physitemp). For high-fat feeding studies, male C57BL/6J mice were put on the diet beginning at 8 weeks of age and continuing for up to three months. Blood and various tissue samples were collected. For the CL316,243 studies, animals were given the drug by IP injection for 5 consecutive days at RT and euthanized for the gene expression analysis. For histology, adipose tissues were fixed with neutral-buffered formalin and embedded in paraffin, and sections were stained with H&E.

iWAT-specific *Tet1* Adi-CRE mice were generated by injecting adeno-associated virus (AAV) expressing Adiponectin CRE (AAV8-hAdp-iCre, Vector Biolabs) or control Null (AAV8-Null) into inguinal WAT level. Briefly, mice were anesthetized and maintained using isoflurane. Area around iWAT was shaved on either side of the mice and cleaned with Betadine (#19-027132,) and Ethanol. A small incision was made to expose the iWAT pads. AAV was injected into both the iWAT depot at 10 different locations per depot of *Tet1*f/f adult mice using hamilton microsyringe. Viral titer of 5.0×10^{11} genomic copies (GC) per mouse. After injection, the incision was closed using suture (#101-7137, Henry Schein). Efficacy of viral infection and knockdown was evaluated by quantification of TET1 expression. All animal work was approved by the UC Berkeley ACUC.

Protein analysis

Whole-cell protein lysates were prepared using RIPA lysis buffer (1% Triton X-100, 1% Sodium deoxycholate, 0.1% SDS, 0.15M NaCl, 50mM Tris (pH 7.2) and protease inhibitor cocktail (Complete Mini-EDTA free, 11836170001**,** Roche). Protein was resolved using Tris-glycine gels and transferred to PVDF membrane. After blocking with 5% nonfat dried milk in TBS-Tween (0.25%), the membranes were incubated with the appropriate primary antibodies and loading control. Immunoblots were quantified by the ImageJ program.

Immunoprecipitation

HEK-293T cells were transfected with various DNA constructs using Lipofectamine 3000 (Invitrogen). A day after transfection, cells were lysed with RIPA buffer with protease inhibitor cocktail. 500 mg of protein was incubated with the appropriate antibodies overnight. The next day, protein A/G PLUS-Agarose (SC-2003, Santa Cruz) was added and incubated for 2 hr, washed with lysis buffer five times and PBS once. Beads were eluted with non-reducing SDS/PAGE loading buffer and subjected to SDS/PAGE and western blotting.

Indirect Calorimetry

Metabolic rate was measured by indirect calorimetry in open-circuit Oxymaxchambers, a component of the Comprehensive Lab Animal Monitoring System (CLAMS; Columbus

Instruments). Mice were housed individually at various temperatures under a 12 hr light/12 hr dark cycle. Food and water were available ad libitum.

Cellular and tissue respiration

For cellular respiration, lentivirally transduced beige adipocytes were plated on XF24 Cell Culture Microplates. For tissue respiration, freshly isolated iWAT and iBAT were rinsed in sterile saline and dissected with a microdisector to 2 mm per well. Oxygen consumption rate (OCR) was determined using an XF24 Extracellular Flux Analyzer (Seahorse Bioscience). Uncoupled and maximal OCR was determined using oligomycin (4 μM) and FCCP (4 μM). Antimycin A and rotenone (2 uM each) were used to inhibit Complex III– and Complex I–dependent respiration.

ChIP-qPCR

Cells were crosslinked with 1% formaldehyde for 10 min at room temperature. Cross-linked chromatin was sonicated using an S220 Ultrasonicator (Covaris) to generate DNA fragments of ~200–500 bp. Inputs were taken from cleared lysates, and the rest were rotated O/N at 4°C with Ty1, HDAC1, and IgG antibodies for immunoprecipitation. An aliquot of 20 μl of pre-washed Dynabeads Protein G was added per IP and rotated 1 hr at 4°C. Beads were successively washed in low-salt RIPA buffer (20 mM Tris-HCl [pH 8.0], 1 mM EDTA, 1% Triton x-100, 0.1% SDS, 140 mM NaCl, 0.1% Na deoxycholate), high-salt RIPA buffer (20 mM Tris-HCl [pH 8.0], 1 mM EDTA, 1% Triton x-100, 0.1% SDS, 500 mM NaCl, 0.1% Na deoxycholate), LiCl buffer (250 mM LiCl, 0.5% NP40, 0.5% Na deoxycholate, 1 mM EDTA, 10 mM Tris-HCl [pH 8.0]) and TE buffer (10 mM Tris-HCl [pH 8.0] and 1 mM EDTA). Each reaction was then incubated in digestion buffer (50 mM Tris-HCl [pH 8.0], 1 mM EDTA, 100 mM NaCl, 0.5% SDS, proteinase K) for a minimum of 4 hr at 65°C to reverse cross-links. DNA was recovered using a phenol-chloroform extraction. ChIP-reChIP was performed in essentially the same way as ChIP, except that the first elution was carried out in a digestion buffer (50 mM Tris, pH 8.0, 1 mM EDTA, 1% SDS, 50mM $NaHCO_3$) at 65°C for 10 minutes. After saving the supernatant, the beads were with 40 ul 10 mM DTT for 30 minutes at 37°C. The combined elutes were subjected to the second IP. Real-time qPCR primers are listed in **Supplementary Table 2**. All data were normalized to input.

RNA extraction and quantitative PCR

Total RNA was extracted from cells or tissues using TRIzol reagent according to the manufacturer's instructions. cDNA was reverse-transcribed from 1 μg of RNA using the RETROscript first strand synthesis kit (Ambion). Quantitative PCR (qPCR) was performed with SYBR Green qPCR Master Mix (Applied Biosystems) using a 7900HT Fast Real-Time PCR System (Applied Biosystems) and CFX96 Touch (BioRad). Primer sequences are listed in **Supplemental Table 2.** The relative amount of mRNA normalized to cyclophilin B was calculated using the delta–delta method[68].

RNA-Seq analysis

RNA samples were extracted using the RNeasy Mini kit (Qiagen, 74104) following the manufacturer's protocol. Libraries were prepared using the BGI Library Preparation Kit, and sequencing was performed on the BGISEQ. RNA-Seq reads were aligned to UCSC

mm10 genome using STAR aligner[69] with an option, "--outFilterMultimapNmax 1". Mitochondrial reads were filtered out to avoid sequencing depth bias due to mitochondrial abundance. Then, raw read count for each gene was measured using Feature Counts. Differential gene expression analysis was performed using edgeR. Hierarchical clustering was performed using group-wise average gene expression levels to identify distinct functional modules of genes using Ward's criterion and Pearson correlation as a similarity measure. Gene ontology analysis was done using EnrichR.

5hmC-Seal analysis

Genomic DNA (250ng) was sonicated to ~100-500bp with a Bioruptor PICO sonicator (Diagenode). Sonicated DNA was end-repaired, A-tailed, and ligated to paired-end adapters following the standard Illumina protocol. The glucosylation reactions were performed in a 50 µl solution containing 1x glucosylation buffer, above adapter-ligated DNA, 200 µM UDP-Azide-Glucose (Active Motif, 55020), and 5 U T4 ß-glucosyltransferase (Thermofisher, EO0831), at 37°C for 1 hr. After glucosylation, the reaction was purified by Zymo DNA clean & concentrator Kit (Zymo, D4014) and eluted into 45ul ddH2O. Then, 1.5µl DBCO-PEG4-Biotin (Click Chemistry Tools, A105. 4.5 mM stored in DMSO, dilute from 30mM stock before use) was added to the 45ul glusosylated DNA and the reactions were incubated at 37°C for 2 hr. Next, the DNA was purified by Zymo DNA clean & concentrator Kit and eluted in 10ul ddH2O. The purified DNA was pulled down by 5µl streptavidin C1 beads (Thermofisher, 65001) for 15 min according to the manufacture's instruction. The beads were subsequently undergone ten washes with 1x binding-washing buffer and two washes with ddH2O and were re-suspended in 15ul ddH2O. All binding and washing were done at room temperature. The captured DNA fragments were amplified with 12 cycles of PCR amplification using the Phusion DNA polymerase. The PCR products were purified using 1.0X AMPure XP beads according to the manufacture's instruction. DNA concentration of each library was measured with a Qubit fluorometer (Life Technologies) and sequencing was performed on the Next-Seq instrument (Illumina). 5hmC-seq analysis: Sequencing reads was trimmed adapter using cutadapt (https://cutadapt.readthedocs.io/en/stable/), aligned to mouse genome mm10 using BWA with default parameters http://bio-bwa.sourceforge.net/. MethylQA was used to process the aligned BAM files. Concordantly aligned read-pairs were selected and deduplicated using Picard tool (https://broadinstitute.github.io/picard/). Genome browser tracks were created in bigwig files using "makeUCSCfile" in Homer and bedGraphToBigWig in UCSC toolkit.

Plasmids

Hairpins against Dnmt1, Dnmt3a, and Dnmt3b are from Sigma. HDAC1 was subcloned to pcDNA3.1 at EcoRI/NotI for Myc-HDAC1. Lentiviral overexpression vectors for Tet1WT, Tet1ΔCD, Tet1CD, and Tet1CDM were subcloned into pCDH using various multicloning sites (XbaI/NotI for Ty1-Tet1WT, Ty1-Tet1ΔCD, XbaI/NheI for Flag-Tet1CD, Flag-Tet1CDM). Hairpins targeting Tet1 were subcloned at AgeI/EcoRI or purchased from Open Biosystems. Hairpin sequences are shown in **Supplemental Table 1**. sgRNAs that targeted Hcac1 were cloned into lentiCRISPR v2 vector. Hairpin and sgRNA sequences are shown in **Supplementary Table 1.**

Statistical analyses.
Data are presented as means ± SEM and individual data points are plotted. Sample size was determined by our experience with inherent variability. No statistical method was used to predetermine sample size. Statistical analyses and the number of samples (*n*) were described in detail for each figure panel. Statistical analyses and the number of samples (*n*) is described in detail for each figure panel. Two-tailed unpaired Student's *t*-test was used for the comparison between two groups. One-way analysis of variance (ANOVA) or two-way ANOVA followed by the Bonferroni's test was used for the multiple comparisons. Statistical analyses were performed using excel and GraphPad Prism. All reported p values were two-sided and differences were considered significant at $p < 0.05$.

Reporting summary. Further information on research design is available in the Nature Research Reporting Summary linked to this article.

Data Availability

The authors declare that the data supporting the findings of this study are available within the paper and its supplementary information files. Source data underlying Figs.1a-n, Figs. 2a-j, Figs. 3a-i, Figs.4a-d, f, g, j, k, Figs. 5a-k, Figs. 6b-g, Figs. 7a-j, Supplementary Figs. 1a-j, Supplementary Figs. 2a-e, Supplementary Figs. 3a-d, Supplementary Figs. 4a-c, Supplementary Figs. 5a-b, Supplementary Fig. 6c, Supplementary Figs. 7a-i, Supplementary Figs. 8a, c, d-f, Supplementary Figs. 10a-e, Supplementary Figs. 11a, b, and Supplementary Fig. 13 provided as a Source Data File. Global profiling data are available in the GEO repository under accession number: GSE153093.

Acknowledgements

Work was funded by AHA Award # 19POST34380834 to DY and R01 DK116008 to SK. We thank Drs. Hei Sook Sul and Jen-Chywan Wally Wang (UC Berkeley) for helpful conversations about manuscript and thank Dr. Shingo Kajimura (UCSF) for allowing us to learn adenoviral injection to inguinal fat pad in his laboratory.

Author Contributions

SK supervised experiments and wrote the manuscript. Experiments were carried out by SDV, DY, JK, HX, PA, and SK. HL analyzed RNA-Seq and 5hmC-Seal analysis. PHJ helped with CLAMS studies. YO helped with adenovirus injections.

Competing Interests

The authors declare no competing interests.

Supplementary Table 2. Oligonucleotide sequences used in this manuscript.

Hairpin	shDnmt1	ACCAAGCTGTGTAGTACTTTG
Hairpin	shDnm3a	CGCTCCGCTGAAGGAATATTT
Hairpin	shDnmt3b	GCACTTTAATCTGGCTACCTT
Hairpin	shTet1	AATAGAGGATTACTAAGCAAG
Hairpin	shTet2	GAGCGTTCCTCAGTATCATTT
Hairpin	shTet3	GCTCCAACGAGAAGCTATTTG
gRNA	gHdac1 (#2)	CACCGAATCCGCATGACTCA
Q-PCR	Cyclophilin_F	GGTGGAGAGCACCAAGACAGA
Q-PCR	Cyclophilin_R	GCCGGAAGTCGACAATGATG
Q-PCR	Tet1-f	CCCAGACTCCTTAACTTGCA
Q-PCR	Tet1-r	CTCGTCCTGGATATTATGTGTAC
Q-PCR	Tet2-f	AGAGCCTCAAGCAACCAAAA
Q-PCR	Tet2-r	ACATCCCTGAGAGCTCTTGC
Q-PCR	Tet3-f	CCGGATTGAGAAGGTCATCTAC
Q-PCR	Tet3-r	AAGATAACAATCACGGCGTTCT
Q-PCR	Ppargc1a_f	AGCCGTGACCACTGACAACGAG
Q-PCR	Ppargc1a_r	GCTGCATGGTTCTGAGTGCTAAG
Q-PCR	Ucp1_f	CACCTTCCCGCTGGACACT
Q-PCR	Ucp1_r	CCCTAGGACACCTTTATACCTAATGG
Q-PCR	Elovl3_f	TCCGCGTTCTCATGTAGGTCT
Q-PCR	Elovl3_r	GGACCTGATGCAACCCTATGA
Q-PCR	Fabp4_f	AAGGTGAAGAGCATCATAACCCT
Q-PCR	Fabp4_r	TCACGCCTTTCATAACACATTCC
Q-PCR	Pparg_f	CAAGAATACCAAAGTGCGATCAA
Q-PCR	Pparg_r	GAGCTGGGTCTTTTCAGAATAATAAG
Q-PCR	Ppara_f	GCCTGTCTGTCGGGATGT
Q-PCR	Ppara_r	GGCTTCGTGGATTCTCTTG
ChIP	Ucp1_promoter_f	CCCACTAGCAGCTCTTTGGA
ChIP	Ucp1_promoter_r	CTGTGGAGCAGCTCAAAGGT
ChIP	Ucp1_enhancer_f	CTCCTCTACAGCGTCACAGAGG
ChIP	Ucp1_enhancer_r	AGTCTGAGGAAAGGGTTGA
ChIP	Ppargc1a_promoter_f	CAAAGCTGGCTTCAGTCACA
ChIP	Ppargc1a_promoter_r	AAAAGTAGGCTGGGCTGTCA
ChIP	Ins_f	GGACCCACAAGTGGAACAAC
ChIP	Ins_r	GTGCAGCACTGATCCACAAT
Bisulfite	Ucp1 (#1)_f	TAAGGGTTGGTTTATGAGTTTAGTTG
Bisulfite	Ucp1 (#1)_r	TTCAAATATCACCTTCAAATTTAAATAACT
Bisulfite	Ucp1 (#2)_f	TTTTGAGAGAAATTATGGGAATTAAAA
Bisulfite	Ucp1_(#2)_r	CATAACCCCAAAACTACAAAAAATAAC
Bisulfite	Ucp1 (#3)_f	AGTTAGGTTGGGTTGTATATTTTTGT
Bisulfite	Ucp1 (#3)_r	TTACTTTTCAAACTTTCTTACACTTTTAAA
Bisulfite	Ucp1 (#4)_f	TTTTTTTGGAGATAGATAAGAAGTTA
Bisulfite	Ucp1_(#4)_r	AAAATATAAAACACCATTTACAAAACAC
Bisulfite	Tet1 (#1)_f	AAAAGAAATTAATATTTGAGGGGAAG

Bisulfite	Tet1 (#1)_r	AATAAACCAACCATCCTAAACTAAAC
Bisulfite	Tet1 (#2)_f	GATTTTTATAATTAGAATTTAGAATAGAG
Bisulfite	Tet1 (#2)_r	ATTCATTAATAAAACACTTACTTAAC
Bisulfite	Tet1 (#3)_f	TTTTTTTGGAGATAGATAAGAAGTTA
Bisulfite	Tet1 (#3)_r	AAAATATAAAACACCATTTACAAAACAC

Supplementary Table 1
Gene list in Figure 4l

RT. WT vs Cold. Up	Cold. WT vs RT. Up	Commonly up in KO at RT and Cold
Abi3	A330041J22Rik	Abi3
Acaa2	A530050N04Rik	Acaa2
Acot11	Abi3	Acot11
Agtr1a	Acaa2	Cidea
Atp1b1	Acacb	Clstn3
Atp7b	Acot11	Cox7a1
Bdnf	Acss1	Cox8b
Cidea	Adcy3	Cpt1b
Clic5	Ankrd9	Dio2
Clstn3	Apold1	Fabp3
Coq10b	Aspg	Fam151a
Cox7a1	Atp2a1	Gk
Cox8b	Calm4	Gm44502
Cpt1b	Cend1	Otop1
Csn1s1	Cidea	Pank1
Csn2	Ckm	Phospho1
Dbp	Cldn1	Ppara
Dcpp3	Clstn3	Ppargc1a
Defb15	Coch	Ppp1r3b
Dio2	Coq8a	Slc27a2
Fabp3	Cox7a1	Ucp1
Fam151a	Cox8b	
Fcgbp	Cpt1b	
Gk	Crct1	
Gm44502	Ctnnbl1	
Gm4841	Cyp2g1	
Gm5148	Dagla	
Gys2	Defb6	
Hsd11b1	Dhrs9	
Muc15	Dio2	
Nr1d2	Dmkn	
Nr4a2	Dpep1	
Nr4a3	Elovl3	
Otop1	Elovl6	
Pank1	Fa2h	
Per2	Fabp3	

Per3
Phospho1
Pnldc1
Ppara
Ppargc1a
Ppp1r3b
Ppp1r3d
Sbp
Slc27a2
Tef
Tnfsf11
Ucp1
Vldlr
Wnk2
Wnk4

Fam151a
Fam69b
Gk
Gm44502
Gm94
Gm9899
Gmpr
Gnao1
Gpd2
Hamp2
Hc
Inmt
Kcnh1
Kcnk3
Krt10
Krtdap
Lce1m
Ldhb
Letmd1
Lor
Lrrc52
Me1
Mmp11
Mrgprg
Mtfp1
Otop1
Pamr1
Pank1
Pdk4
Perm1
Phospho1
Pim1
Ppara
Ppargc1a
Ppif
Ppp1r3b
Psapl1
Pvalb
Pygl
Rorc

Serpina3b
Serpina3j
Slc25a34
Slc27a2
Slc2a5
Slc4a4
Sorcs2
Tnni2
Tnnt3
Ucp1
Ucp3

Supplementary Table 1
Gene list in Supplementary Figure 9b

RT. WT vs Cold down	Cold. WT vs KO down	Commonly down in KO at RT and Cold
Akr1c14	3830417A13Rik	Aoc1
Alox5ap	Agt	C4b
Aoc1	Aldh1l2	Chrdl1
Aqp3	Aoc1	Faim2
Aqp5	Bmper	Padi4
Areg	C2	Vnn1
Arsi	C4b	
Bst1	Cfb	
C4b	Chrdl1	
Ccl6	Creb3l1	
Ccl8	Dclk1	
Ccl9	Faim2	
Cd209f	Fam83e	
Cd209g	Ffar2	
Cfp	Fgf10	
Chrdl1	Irs3	
Chsy3	Mcam	
Cldn11	Padi4	
Clec3b	Prr32	
Cystm1	Prtn3	
Dab2	Serpinh1	
Dscam	Sncg	
Faim2	Spon1	
Fbln1	Timp1	

Fcgr1
Fcgr2b
Fcrls
Gas6
Gm13031
Gm14005
Gng12
Gsr
Hif1a
Il33
Irf4
Itgam
Krt4
Ldb3
Lgi2
Mafb
Matn4
Mcpt4
Mgl2
Mmp9
Mrc1
Ms4a6d
Muc13
Nfam1
Ngfr
Ninj1
Npl
Padi2
Padi4
Pinc
Ptpn5
Sfrp4
Siglec1
Slco2a1
Slpi
Spi1
Sprr1a
Stc2
Syn2
Tcf21
Ttyh2
Vnn1

Tgm2
Thbs2
Thsd4
Tmed3
Tmem176a
Tmem86a
Vnn1
Wfdc17
Wfdc3

Supplementary Table 1
Gene list in Supplementary Figure 9c

	WT.RT_vs_Cold				KO.RT_vs_Cold				RT.WT_vs_KO				Cold.WT_vs_KO			
GeneId	logFC..WT.RT_vs_Cold	logCPM..WT.RT_vs_Cold	PValue..WT.RT_vs_Cold	FDR.WT.RT_vs_Cold	logFC..KO.RT_vs_Cold	logCPM..KO.RT_vs_Cold	PValue..KO.RT_vs_Cold	FDR.KO.RT_vs_Cold	logFC..RT.WT_vs_KO	logCPM..RT.WT_vs_KO	PValue..RT.WT_vs_KO	FDR.RT.WT_vs_KO	logFC.Cold.WT_vs_KO	logCPM..Cold.WT_vs_KO	PValue..Cold.WT_vs_KO	FDR.Cold.WT_vs_KO	Cluster
Apod	-0.108629498	6.59238302	0.582655657	0.954541726	1.035764252	6.59238302	3.39E-06	0.000461389	-0.543619559	6.59238302	1.41E-02	0.413271079	0.600774147	6.59238302	2.48E-03	0.171830909	red
Rcan2	-0.042990323	3.599820475	0.851483073	0.997680032	0.977146414	3.599820475	0.000219668	0.011684579	-0.462551221	3.599820475	0.080220352	0.836876692	0.557584941	3.599820475	0.017672149	0.540450678	red
St3gal5	0.021541019	3.572153343	0.934465195	1	0.931215689	3.572153343	0.000125962	0.007620975	-0.419007713	3.572153343	0.083845486	0.845870221	0.490666349	3.572153343	2.33E-02	0.632583692	red
Ace	0.051509485	7.301925217	0.800094008	0.989314717	0.710066582	7.301925217	0.000995707	0.035376901	-0.316017559	7.301925217	0.141616318	0.992645357	0.3425395	7.301925217	7.67E-02	1	red
Fam25c	0.165203378	4.344488493	0.66453348	0.97513377	1.660163128	4.344488493	1.93E-05	0.001691751	-0.735959739	4.344488493	0.054320648	0.732097757	0.758995891	4.344488493	0.024906296	0.659262104	red
Zfp750	0.174427292	2.662104677	0.564192913	0.947517612	1.028637536	2.662104677	0.001564936	0.047858975	-0.41124793	2.662104677	2.08E-01	1	0.442961031	2.662104677	1.24E-01	1	red
Dapl1	0.604541	-1.188581036	0.460091407	0.914765341	3.259240396	-1.188581036	0.000405527	0.018211169	-1.388311045	-1.188581036	0.160763521	1	1.266503814	-1.188581036	0.072736542	1	red
Ntn4	0.078045357	4.717393443	0.698748702	0.976386163	0.798224403	4.717393443	0.00021161	0.011374868	-0.210104122	4.717393443	3.30E-01	1.00E+00	0.510074255	4.717393443	0.008193833	0.352360031	red
Id2	0.264001479	4.779896333	0.191991381	0.738408831	0.879868442	4.779896333	6.19E-05	0.004281366	-0.182868761	4.779896333	4.05E-01	1	0.432997702	4.779896333	0.027477913	0.68738954	red
Kcnn4	0.415523222	2.951743833	0.161208992	0.697705454	1.088543458	2.951743833	0.000676582	0.026787291	-0.172421197	2.951743833	5.91E-01	1	0.500595697	2.951743833	0.077522789	1	red
Reck	0.386068123	5.763016512	0.04337264	0.401411393	0.950150357	5.763016512	4.90E-06	0.000600532	-0.164504872	5.763016512	0.427403852	1	0.39957697	5.763016512	0.031484941	0.731958842	red
Rassf4	0.293676712	5.34100582	0.116308801	0.619025547	0.832147256	5.34100582	4.29E-05	0.00316872	-0.20860602	5.34100582	3.05E-01	1	0.329864166	5.34100582	0.070050714	1	red
Epsti1	0.233819876	6.453091876	0.166387644	0.705746194	0.629167667	6.453091876	0.000613118	0.02500553	-0.189061366	6.453091876	3.03E-01	1	0.206286325	6.453091876	0.211571846	1	red
Hey1	0.424145713	4.959743294	0.014512186	0.209106904	0.86604804	4.959743294	4.36E-06	0.000557251	-0.2122628	4.959743294	0.260406491	1	0.229639108	4.959743294	0.17349847	1	red
Cldn10	0.560969044	4.45898688	0.01681925	0.231820347	1.079844511	4.45898688	2.25E-05	0.001912749	-0.226148505	4.45898688	0.374655738	1	0.292726139	4.45898688	0.195619443	1	red
Msx2	0.795494123	3.322347333	0.002717414	0.073176444	1.514905773	3.322347333	1.61E-07	3.81E-05	-0.33145887	3.322347333	2.50E-01	1	0.387950599	3.322347333	0.123870545	1	red
Cdk19	0.331489928	7.539643017	0.056436628	0.453570925	0.602806829	7.539643017	0.001395026	0.044110588	-0.128383003	7.539643017	0.495182843	1	0.142933841	7.539643017	0.398746596	1	red
Prom2	1.193112359	7.303735173	1.47E-05	0.001552812	2.171873275	7.303735173	6.22E-13	6.21E-10	-0.500618215	7.303735173	0.084863321	0.847346568	0.478142558	7.303735173	0.065645285	1	red
Adh7	0.918256486	2.140129622	0.008923557	0.157437674	1.631338468	2.140129622	1.87E-05	0.001663136	-0.429150333	2.140129622	2.62E-01	1	0.283928313	2.140129622	0.387808361	1	red
603040881 6Rik	1.816291462	0.415370821	0.000852512	0.031441109	3.826496932	0.415370821	1.14E-09	5.71E-07	-1.331113894	0.415370821	4.51E-02	0.681041299	0.679156217	0.415370821	0.151489999	1	red
Col28a1	0.433126744	3.806931822	0.082501167	0.537546063	0.924274756	3.806931822	0.00064078	0.025883069	-0.271557314	3.806931822	0.317622611	1	0.219589971	3.806931822	0.361461426	1	red
Dpf6	0.426175678	3.716150998	0.052602126	0.436819557	1.013264523	3.716150998	2.26E-05	0.001912749	-0.32078424	3.716150998	1.81E-01	1	0.266303865	3.716150998	0.21037123	1	red
Slc7a8	0.300898852	4.946685521	0.172238746	0.714266342	0.977572101	4.946685521	4.56E-05	0.003305395	-0.371589234	4.946685521	1.20E-01	0.946835239	0.305083801	4.946685521	0.153435069	1	red
Zfp777	0.190997658	4.561099036	0.275455756	0.817343958	0.61028473	4.561099036	0.001310515	0.042008616	-0.232122923	4.561099036	2.23E-01	1.00E+00	0.187163922	4.561099036	0.272400516	1	red
Drd1	0.644391869	0.948295321	0.154368707	0.685958882	2.588432391	0.948295321	4.13E-07	8.48E-05	-1.186402323	0.948295321	0.018815889	0.461913105	0.75765513	0.948295321	0.068401727	1	red
Arhgef10l	0.203943327	4.997584812	0.263686641	0.807177783	0.708945752	4.997584812	0.000343644	0.01622555	-0.252351038	4.997584812	0.202719654	1	0.252651149	4.997584812	0.154911985	1	red
Foxi1	0.472329241	2.584436715	0.217032234	0.763079875	2.14615444	2.584436715	5.37E-07	0.000105658	-0.999030216	2.584436715	1.76E-02	0.447803905	0.674797772	2.584436715	0.063289121	0.993852541	red
Runx1	0.297354695	6.731805583	0.188421799	0.734359705	1.017217784	6.731805583	3.64E-05	0.002749178	-0.45020953	6.731805583	0.065698844	0.780788307	0.269653544	6.731805583	0.219039196	1	red
Lcn2	0.256109881	7.737800922	0.165912742	0.705006144	0.946897534	7.737800922	2.68E-06	0.000382229	-0.407529938	7.737800922	4.20E-02	6.70E-01	0.283257699	7.737800922	0.116448545	1	red
Bmp4	0.269394298	2.300989767	0.373898938	0.883152198	1.071054834	2.300989767	0.000997317	0.035376901	-0.505448776	2.300989767	1.24E-01	0.956226206	0.296211848	2.300989767	0.303847132	1	red
Adamts11	0.158561813	4.953771025	0.490991704	0.929487183	0.889304942	4.953771025	0.000360471	0.016793163	-0.522752823	4.953771025	3.55E-02	0.628189489	0.207990509	4.953771025	0.349045927	1	red
Csn3	0.150930724	7.557973649	0.474281064	0.921496564	1.143601691	7.557973649	6.71E-07	0.000125045	-0.645664474	7.557973649	4.68E-03	0.219530831	0.34700653	7.557973649	0.090096759	1	red
Clic6	0.062991515	4.699448096	0.783681798	0.987952495	1.007920412	4.699448096	3.44E-05	0.00263835	-0.6588512	4.699448096	6.61E-03	0.267790873	0.286078107	4.699448096	0.186665469	1	red
1810010D0 1Rik	0.140318619	2.830844714	0.779992735	0.987750219	2.459296875	2.830844714	4.56E-06	0.000564114	-1.694211522	2.830844714	0.001268888	0.098522137	0.624776932	2.830844714	0.163499204	1	red
Papln	0.075070308	6.582228478	0.714856448	0.978725873	0.735656311	6.582228478	0.000836555	0.0312612	-0.583012877	6.582228478	0.008011331	0.297782883	0.077573286	6.582228478	0.690783319	1	red
Cd163	0.262167102	6.227056219	0.39414502	0.889563201	1.28135235?	6.227056219	0.00013016	0.007740903	-0.830848634	6.227056219	0.012370117	0.182488401	0.1883369	6.227056219	0.520286402	1	red
Sulf1	0.169512068	5.081276831	0.30946396	0.841289301	0.658895397	5.081276831	2.84E-04	0.013934845	-0.439533582	5.081276831	1.54E-02	4.27E-01	0.049850018	5.081276831	0.757051817	1	red
Alox15	0.592229653	3.274833768	0.128121799	0.640425702	1.916626079	3.274833768	8.64E-06	0.000903978	-1.278047451	3.274833768	0.002652601	0.159124298	0.046354666	3.274833768	0.8905699	1	red
Fam3b	1.092836701	1.88675853	0.072798644	0.515060954	3.588994703	1.88675853	5.73E-07	0.000111216	-2.214301856	1.88675853	1.25E-03	0.09783071	0.281912096	1.88675853	0.60537579	1	red
Rnf144b	0.22200944	5.124236763	0.22451287	0.77038838	0.647364879	5.124236763	1.13E-03	3.83E-02	-0.363287952	5.124236763	6.75E-02	7.92E-01	0.062067618	5.124236763	0.725157337	1	red
Cysrt1	0.647293109	1.765860464	0.112801271	0.611858553	2.14546039	1.765860464	2.72E-06	0.000383913	-1.22878985	1.765860464	7.07E-03	0.279062846	0.269391153	1.765860464	0.481090548	1	red
Zmiz1	0.285949049	8.640694867	0.125873262	0.637525066	0.93472613	8.640694867	4.52E-06	0.000563716	-0.505722767	8.640694867	1.26E-02	0.383289531	0.143054329	8.640694867	0.431475949	1	red
Zfp143	0.214463042	3.827112486	0.31227211	0.844621698	0.758735935	3.827112486	0.000987034	0.035371258	-0.385700316	3.827112486	9.48E-02	0.884946568	0.158572689	3.827112486	0.440127118	1	red
Cyb561	0.244311653	5.535540306	0.107149844	0.599010487	0.794593564	5.535540306	1.56E-06	0.000240168	-0.368533205	5.535540306	2.57E-02	5.39E-01	0.18174691	5.535540306	0.220696391	1	red
Scara5	0.497965001	6.411587518	0.068189138	0.500268448	1.470035916	6.411587518	9.08E-07	0.000154731	-0.699680935	6.411587518	1.78E-02	0.448304783	0.27239008	6.411587518	0.299919881	1	red
Cldn4	0.378860817	7.154624181	0.090540117	0.558177622	0.947715297	7.154624181	9.94E-05	0.0063217	-0.422580263	7.154624181	0.080761165	0.836876692	0.146274221	7.154624181	0.498668309	1	red
Stc2	1.083863905	7.31740887	2.36E-05	0.00208639	2.575575524	7.31740887	2.70E-19	1.89E-15	-1.132551069	7.31740887	3.72E-05	0.008765327	0.359160796	7.31740887	0.139665141	1	red
Cfr9	0.415157815	7.113055703	0.040457518	0.386489594	0.989083411	7.113055703	7.39E-06	0.000831143	-0.443338818	7.113055703	0.043125531	0.67446002	0.13058679	7.113055703	0.505453194	1	red
Stat5a	0.368987842	7.602951136	0.081888816	0.536532527	0.89801574	7.602951136	9.92E-05	0.0063217	-0.436984984	7.602951136	5.68E-02	0.746059679	0.092042933	7.602951136	0.651852025	1	red
Enho	0.911628034	4.445085927	8.97E-05	0.006056455	1.80937368	4.445085927	1.42E-12	1.32E-09	-0.724677859	4.445085927	0.00406991	0.203874789	0.173068205	4.445085927	0.434693387	1	red
Cpt1a	0.390321415	7.124552153	0.051655405	0.434844135	0.695833704	7.124552153	0.001383526	0.044045928	-0.251644837	7.124552153	0.246001848	1	0.05386743	7.124552153	0.777997688	1	red
Cptr1	0.618732067	3.624706106	0.008030723	0.146915695	1.031445015	3.624706106	4.76E-05	0.003425797	-0.3209774	3.624706106	0.206353254	1	0.091735002	3.624706106	0.679981263	1	red
Pxylp1	0.595353778	4.803232813	0.003451559	0.085834491	1.103664354	4.803232813	6.18E-07	0.000116808	-0.377193333	4.803232813	8.73E-02	0.851791999	0.131117062	4.803232813	0.503285796	1	red
Adamts15	0.551168963	5.462432794	0.009344882	0.161096467	1.057607686	5.462432794	4.46E-06	0.000561248	-0.378589997	5.462432794	9.84E-02	0.891625163	0.127848636	5.462432794	0.53130487	1	red
Prmt1	0.303739022	6.160411664	0.048404967	0.424142837	0.594698156	6.160411664	0.000378825	0.017358896	-0.257023175	6.160411664	1.24E-01	0.956226206	0.033935958	6.160411664	0.818248367	1	red
H2-M9	0.864382082	2.522791244	0.00703368	0.136911847	1.59636803	2.522791244	5.92E-06	0.000676573	-0.7134494	2.522791244	0.042267026	0.670515276	0.018539024	2.522791244	0.94486982	1	red
Vtcn1	0.939446473	5.136658977	0.002186164	0.062101279	1.875998567	5.136658977	2.44E-08	7.75E-06	-1.054158456	5.136658977	1.42E-03	0.10532897	-0.117605132	5.136658977	0.702684197	1	red
Nbp2	0.204413861	4.983199247	2.12E-01	0.758098043	0.639607698	4.983199247	0.000338	0.016122503	-0.478958572	4.983199247	7.27E-03	0.282156373	-0.043764286	4.983199247	0.794104952	1	red
Akr1c14	0.347356159	4.373696618	0.099717277	0.584339063	1.094363244	4.373696618	2.30E-06	0.000334893	-0.847711089	4.373696618	2.46E-04	0.031790079	-0.100702473	4.373696618	0.636472807	1	red

Myh14	0.210179218	6.118380968	0.213024496	0.75907387	0.621114327	6.118380968	0.000720984	0.028068174	-0.47809807	6.118380968	9.17E-03	0.322895246	-0.067162744	6.118380968	0.69372821	1	red
Aqp5	0.769041214	7.80088837	1.72E-02	0.2336509	1.896364912	7.80088837	9.60E-08	2.40E-05	-1.363748135	7.80088837	9.85E-05	0.016781558	-0.236424115	7.80088837	0.462375081	1	red
Cd200	0.386305358	7.750834621	3.51E-02	0.355195794	0.65974994	7.750834621	0.000914064	0.033796168	-0.427683661	7.750834621	0.01123725	0.597225455	-0.154239017	7.750834621	0.399910344	1	red
Syn2	1.777345693	7.014831259	5.10E-05	3.83E-03	2.584730993	7.014831259	5.56E-08	1.55E-05	-1.677943568	7.014831259	2.76E-04	0.034401024	-0.870557036	7.014831259	0.03997795	0.812110221	red
Fam129b	0.622058418	7.489032598	5.95E-04	0.024809744	0.679350763	7.489032598	0.000511352	0.021656544	-0.256302859	7.489032598	1.89E-01	1	-0.199010499	7.489032598	0.268153507	1	blue
Ngp	2.112559308	-0.76626641	0.00020641	0.010942234	3.158218114	-0.76626641	9.54E-06	0.000980484	-1.573976912	-0.76626641	0.050964427	0.712278826	-0.528036514	-0.76626641	0.323751828	1	blue
Cbln2a	0.727397471	5.655025448	8.07E-05	0.005585307	0.790203008	5.655025448	7.24E-05	0.004849568	-0.23981123	5.655025448	0.227967138	1	-0.177005724	5.655025448	3.32E-01	1	blue
Gb2lb2	0.692891243	3.900078996	0.00098505	0.034677726	0.784135807	3.900078996	5.69E-04	0.023652779	-0.237171127	3.900078996	0.299738622	1	-0.145926711	3.900078996	4.85E-01	1	blue
Mthfd1l	1.239884453	2.780500245	1.46E-05	0.001552812	1.309023667	2.780500245	2.19E-05	0.001879395	-0.361212668	2.780500245	0.245306857	1	-0.292074002	2.780500245	0.292159216	1	blue
Parvb	0.783638711	5.130284373	0.000201603	0.010836924	0.62500825	5.130284373	0.005797158	0.111907568	-0.087119733	5.130284373	0.702172992	1	-0.245750386	5.130284373	0.237955794	1	blue
Man2a1	0.740720719	7.432131169	2.49E-05	0.002117227	0.689815523	7.432131169	0.000262539	0.013246362	-0.189379112	7.432131169	0.314868398	1	-0.240284316	7.432131169	1.66E-01	1	blue
Sgsm1	0.752582301	3.199394697	0.003399491	0.085298535	0.937916814	3.199394697	0.000751222	0.029002995	-0.342960037	3.199394697	0.219765638	1	-0.157625324	3.199394697	5.39E-01	1	blue
Gpr160	0.670086627	4.491463897	0.003094931	0.079144821	0.861691145	4.491463897	0.000441505	0.019349248	-0.317271206	4.491463897	0.195989662	1	-0.125666636	4.491463897	0.578822714	1	blue
Lrp5	0.465327383	7.87439146	0.007551053	0.141465839	0.607281927	7.87439146	0.001284106	0.041639587	-0.224007539	7.87439146	0.233820081	1	-0.082052995	7.87439146	0.63865926	1	blue
Lad1	0.525797576	5.404230021	0.009133695	0.159147836	0.762758298	5.404230021	4.83E-04	0.020649956	-0.329983591	5.404230021	0.130368311	0.975562438	-0.093022785	5.404230021	6.47E-01	1	blue
Cdk18	0.760833455	5.588956451	0.010314218	0.173051033	1.181349819	5.588956451	0.000229181	0.011978651	-0.488141812	5.588956451	0.124432423	0.956226206	-0.067625337	5.588956451	0.825756789	1	blue
Sla	0.695242564	3.24274055	0.010135419	0.171078031	1.002904226	3.24274055	0.000629511	0.025509877	-0.379403897	3.24274055	0.198232799	1	-0.071742101	3.24274055	0.797370332	1	blue
C77080	0.46997306	6.137437638	0.004363467	0.099805943	0.669079772	6.137437638	1.83E-04	0.010003083	-0.205371846	6.137437638	0.250252114	1	-0.006267194	6.137437638	9.76E-01	1	blue
Cd9	0.558244469	8.230203287	0.000168674	0.051136454	0.781493978	8.230203287	4.88E-05	0.003482824	-0.235378252	8.230203287	0.219065602	1	-0.012128758	8.230203287	0.955187036	1	blue
Cyp4b1	0.69611554	6.496385744	0.001388977	0.044992576	0.869747299	6.496385744	2.15E-04	0.011512853	-0.253854153	6.496385744	0.277849216	1	-0.080262303	6.496385744	7.14E-01	1	blue
Ms4a4a	1.268468784	3.425803973	0.000137601	0.00870187	1.626934314	3.425803973	5.91E-06	0.000676573	-0.495508754	3.425803973	0.162601511	1	-0.141043351	3.425803973	0.668687907	1	blue
Id1	0.813859355	5.261985505	1.79E-05	0.001750728	0.910820895	5.261985505	8.45E-06	0.00090111	-0.188354032	5.261985505	0.35710534	1	-0.091392756	5.261985505	0.627877387	1	blue
Myrip	1.024611517	3.699815663	5.13E-05	0.003831278	1.138243604	3.699815663	2.87E-05	0.002304695	-0.252005643	3.699815663	0.356626234	1	-0.138374379	3.699815663	0.579034025	1	blue
Timeg1l	1.038768848	8.021457301	1.24E-06	0.000217262	1.066640464	8.021457301	3.28E-06	0.000454905	-0.216005853	8.021457301	0.341522047	1	-0.188134279	8.021457301	3.70E-01	1	blue
Plekhh1	0.755339538	5.817131215	7.32E-06	0.000947368	0.719575037	5.817131215	7.25E-05	0.004849568	-0.080170445	5.817131215	0.659600358	1	-0.115935163	5.817131215	4.87E-01	1	blue
Fam107a	1.709343976	4.194558541	2.25E-09	9.54E-07	1.785381605	4.194558541	4.25E-09	1.80E-06	-0.239937537	4.194558541	0.426095564	1	-0.163901722	4.194558541	0.549361441	1	blue
Gphbp1	0.795007848	7.542514277	0.000170251	0.010039767	0.854056766	7.542514277	1.72E-04	0.009565959	-0.107261057	7.542514277	0.635437462	1	-0.04821222	7.542514277	0.822578103	1	blue
Pkig	0.551312279	5.244698588	0.000519693	0.02225488	0.682681483	5.244698588	7.24E-05	0.004849568	-0.127344121	5.244698588	0.460828126	1	0.004024819	5.244698588	0.975034494	1	blue
Foxa1	0.996571344	6.985665223	4.53E-05	0.003457768	1.176184119	6.985665223	7.34E-06	0.000813143	-0.190789579	6.985665223	0.462302718	1	-0.011176952	6.985665223	0.971230211	1	blue
Epn2	0.506365994	6.414392354	0.001333669	0.044095063	0.618156512	6.414392354	0.000296527	0.014439958	-0.087103764	6.414392354	0.610413156	1	0.024686621	6.414392354	0.868502147	1	blue
Mthfd2	0.873759819	3.335054493	0.001240012	0.041659638	1.055732843	3.335054493	0.000288689	0.014107398	-0.141425276	3.335054493	0.633425329	1	0.040545772	3.335054493	0.869482856	1	blue
Lpin3	0.694504091	4.242109572	0.000226705	0.011734911	0.77566468	4.242109572	0.00013592	0.007981601	-0.079872055	4.242109572	0.69844175	1	0.001287697	4.242109572	0.990251483	1	blue
Hspb7	1.786455381	1.426913931	5.47E-05	0.004069838	2.055399164	1.426913931	1.62E-05	0.001485077	-0.320225525	1.426913931	0.523648078	1	-0.051294645	1.426913931	0.921353627	1	blue
Btla	1.439206133	2.12675153	0.001112007	0.038091704	1.624285915	2.12675153	0.000553683	0.022338073	-0.192909663	2.12675153	0.687319854	1	-0.00783751	2.12675153	1	1	blue
Jaml	1.696809789	1.398078298	0.000209527	0.011008846	1.874235327	1.398078298	1.14E-04	0.007017402	-0.078097681	1.398078298	0.878460532	1	0.099305974	1.398078298	0.801861759	1	blue
Fgfr3	0.73842259	4.263413093	0.000901689	0.032563333	0.782537733	4.263413093	1.08E-03	0.037238092	-0.028451279	4.263413093	0.908111031	1	0.01566282	4.263413093	0.935891246	1	blue
Rbp7	1.05609521	5.983771762	5.35E-06	0.000740271	1.118141491	5.983771762	6.77E-06	0.000763489	-0.041659931	5.983771762	0.867434166	1	0.020385879	5.983771762	0.919727644	1	blue
Slc38a1	0.925779927	5.693832445	2.08E-07	4.69E-05	0.996518899	5.693832445	1.96E-07	4.55E-05	-0.049778766	5.693832445	0.795647373	1	0.020959721	5.693832445	0.897744151	1	blue
Slc43a3	0.932627044	6.841177894	1.09E-05	0.001241955	0.981802218	6.841177894	1.59E-05	0.00146734	-0.049848789	6.841177894	0.826147355	1	-0.000673827	6.841177894	0.995424324	1	blue
9530014B0 7Rik	1.027381456	3.906150805	0.000141556	0.008817184	1.067224967	3.906150805	0.00021988	0.011684579	-0.034711398	3.906150805	0.907589952	1	0.005130204	3.906150805	0.975684656	1	blue
Tsc22d3	1.025048963	7.140884203	1.74E-05	0.00171012	0.904293295	7.140884203	3.81E-04	0.017414254	0.062637347	7.140884203	0.804606698	1	-0.058118536	7.140884203	0.809367431	1	blue
Bcl2l1	0.761144059	6.352595794	2.28E-05	0.002056111	0.677614809	6.352595794	4.49E-04	0.019549867	0.052269607	6.352595794	0.786695108	1	-0.031259914	6.352595794	0.865249726	1	blue
Eef2k	0.739166459	5.442700054	1.22E-05	0.001364296	0.695700272	5.442700054	0.000129852	0.007740903	0.035696354	5.442700054	0.846064889	1	-0.007770333	5.442700054	0.969485194	1	blue
Smad6	0.807656829	4.460510346	7.20E-05	0.005134623	0.845848159	4.460510346	1.10E-04	0.006861752	0.024920405	4.460510346	0.911123278	1	0.063110521	4.460510346	0.743286091	1	blue
Serinc3	0.64973479	10.47118744	0.000718294	0.027963458	0.666110402	10.47118744	0.001287198	0.041643225	0.032613524	10.47118744	0.874264298	1	0.048989122	10.47118744	0.787557978	1	blue
Traf3ip2	0.644706446	5.006160563	0.00138326	0.044959173	0.657129911	5.006160563	2.47E-03	0.064647751	0.041822454	5.006160563	0.849302732	1	0.054245235	5.006160563	0.776367781	1	blue
Pcdxl	0.708886149	7.837561823	0.000134	0.008551552	0.777727049	7.837561823	0.000100416	0.0063217	0.037335683	7.837561823	0.851287383	1	0.106176469	7.837561823	0.551759386	1	blue
Trim62	0.971451816	4.189021359	0.000168783	0.009995399	1.188347569	4.189021359	1.83E-05	0.001653759	-0.0573611	4.189021359	0.839066256	1	0.159557869	4.189021359	0.513189338	1	blue
Ano1	0.66582106	8.102860229	0.000293472	0.014391437	0.887525204	8.102860229	7.95E-06	0.000860935	-0.088880744	8.102860229	0.652683948	1	0.132823326	8.102860229	0.454068494	1	blue
Prex1	0.677890082	6.159543276	0.000395094	0.017870005	0.832235186	6.159543276	5.53E-05	0.003901387	-0.06630753	6.159543276	0.747493402	1	0.088037297	6.159543276	0.631070916	1	blue
Jade2	0.54881478	5.266674911	0.002118084	0.060660546	0.643301609	5.266674911	8.64E-04	0.032218938	-0.037686101	5.266674911	8.48E-01	1	0.056800313	5.266674911	0.740238481	1	blue
0610039K1 0Rik	0.625035443	6.27843491	0.000109409	0.007281448	0.734482217	6.27843491	2.57E-05	0.002099505	-0.0331429	6.27843491	0.85053656	1	0.076303626	6.27843491	0.624244526	1	blue
Tbc1d8	0.562990795	5.412655912	0.001100272	0.037875373	0.678287465	5.412655912	2.74E-04	1.36E-02	-0.038457792	5.412655912	8.38E-01	1	0.076838472	5.412655912	0.643835541	1	blue
Pdgfra	0.720257488	7.702729003	1.07E-03	0.037054866	0.894398721	7.702729003	1.63E-04	9.14E-03	-0.091796918	7.702729003	6.97E-01	1	0.08234422	7.702729003	0.693635447	1	blue
Ucp2	0.994223124	8.719347437	1.16E-06	0.000207869	1.261972559	8.719347437	9.79E-09	3.51E-06	-0.143275036	8.719347437	0.509043749	1	0.124474335	8.719347437	0.521969097	1	blue
Amd1	0.994689935	6.873066056	1.36E-08	4.76E-06	1.391954758	6.873066056	1.89E-13	2.42E-10	-0.226743405	6.873066056	0.224356415	1	0.17052121	6.873066056	0.308459036	1	blue
Amd2	0.994689929	6.873066056	1.36E-08	4.76E-06	1.39195475	6.873066056	1.90E-13	2.42E-10	-0.226743392	6.873066056	0.224403344	1	0.170521222	6.873066056	0.30850766	1	blue
9130409J2 0Rik	3.633691877	1.981297266	3.23E-08	9.29E-06	5.731203838	1.981297266	5.64E-14	9.84E-11	-1.297162032	1.981297266	0.083943109	0.845870221	0.800412623	1.981297266	0.127935994	1	blue
Acot1	1.205886785	5.875248595	1.42E-05	0.001529395	1.799340142	5.875248595	2.15E-09	1.00E-06	-0.261782996	5.875248595	0.372347246	1	0.331669766	5.875248595	0.204762387	1	blue
Prr15l	0.747639304	3.225279928	0.005779624	0.120922188	1.141296031	3.225279928	0.000100038	0.0063217	-0.191973331	3.225279928	0.516155384	1	0.201681185	3.225279928	0.433383474	1	blue
F3	1.419687011	7.727166625	4.74E-07	9.75E-05	2.278594546	7.727166625	1.23E-13	1.90E-10	-0.376836861	7.727166625	0.200386683	1	0.48207049	7.727166625	0.067251409	1	blue
Erbb3	0.701868021	6.78890901	0.0004618	0.020187667	1.111513818	6.78890901	3.07E-07	6.55E-05	-0.127160678	6.78890901	0.554882959	1	0.282484885	6.78890901	0.143975386	1	blue
Pgf	0.679620726	3.128564667	0.012157716	0.191569999	1.118590638	3.128564667	0.00013349	0.007905338	-0.166553329	3.128564667	0.576059738	1	0.272413935	3.128564667	0.292367441	1	blue
Clrbp	0.530395862	4.952764904	0.003028263	0.078521342	0.946058689	4.952764904	1.07E-06	0.000180917	-0.147347106	4.952764904	0.44760616	1	0.268315073	4.952764904	0.121518797	1	blue
Gm12339	1.081412062	-0.224351867	0.018326512	0.240951394	1.874190423	-0.224351867	1.43E-04	0.008286404	-0.278401718	-0.224351867	0.656907768	1	0.514331146	-0.224351867	0.212954106	1	blue
Ccdc92	0.941406572	4.522393411	0.000156192	0.009449948	1.38829666	4.522393411	2.41E-07	5.36E-05	-0.070572705	4.522393411	0.795376581	1	0.376315643	4.522393411	0.112173623	1	blue
Tbx2	0.5399336	4.354707665	0.012029682	0.190404118	0.73441133	4.354707665	1.55E-03	0.04759797	0.032791581	4.354707665	0.890248802	1	0.227268025	4.354707665	0.273564031	1	blue
Igsf22	0.645833926	5.373131927	0.001604521	0.050053101	0.867101693	5.373131927	8.70E-05	5.66E-03	0.028295778	5.373131927	8.99E-01	1	0.249562817	5.373131927	0.206261185	1	blue
Bex3	0.57854872	5.05985165	0.001295183	0.04309877	0.766950944	5.05985165	7.90E-05	0.005230217	-0.002956467	5.05985165	0.990298915	1	0.185445031	5.05985165	0.286432343	1	blue
Dgke	0.496537693	4.862039232	0.00424558	0.098729172	0.636978701	4.862039232	0.000692514	0.027187022	0.00518059	4.862039232	0.980346623	1	0.145620901	4.862039232	0.387421609	1	blue
Rnf208	0.927684806	2.955234052	0.00062105	0.025604116	1.282774597	2.955234052	1.02E-05	0.001017198	-0.064374074	2.955234052	0.82821698	1	0.290711023	2.955234052	0.254929041	1	blue
Galnt15	1.069569834	5.733849978	1.57E-08	5.00E-06	1.361127225	5.733849978	2.24E-11	1.74E-08	-0.017401078	5.733849978	0.933529324	1	0.274155508	5.733849978	0.128023189	1	blue
Acot4	1.090619856	3.100915954	0.003054407	0.078695583	1.403255774	3.100915954	0.000367164	0.017048125	-0.014033389	3.100915954	0.97719043	1	0.298597283	3.100915954	0.383609117	1	blue
Ccdc160	1.376366978	0.626861344	0.00135125	0.044435459	1.473182592	0.626861344	0.001200993	0.039845004	0.136965239	0.626861344	0.793355156	1	0.233739536	0.626861344	0.543008501	1	blue
Spock2	1.214006164	5.008459561	6.45E-09	2.50E-06	1.261938539	5.008459561	1.53E-08	5.33E-06	0.149303583	5.008459561	0.502236944	1	0.197234272	5.008459561	0.317760217	1	blue
Tmprss2	1.306912053	7.443328782	0.000361864	0.016858051	1.386593368	7.443328782	3.74E-04	0.017246677	0.180993704	7.443328782	0.636635374	1	0.260674656	7.443328782	0.443009178	1	blue
Rdh12	1.414644844	0.551824247	0.001454363	0.046625615	1.447718236	0.551824247	1.80E-03	0.053376774	0.219193509	0.551824247	0.674471731	1	0.252218053	0.551824247	0.527543254	1	blue
Fzd6	0.737725683	5.429315892	0.000135155	0.008586048	0.698317754	5.429315892	7.71E-04	0.029535506	0.135127911	5.429315892	0.515881226	1	0.095719269	5.429315892	0.604775938	1	blue
Pla2g12a	0.90681715	5.637984645	0.000282544	0.014002965	0.863740076	5.637984645	1.23E-03	0.040387032	0.16746133	5.637984645	0.529787115	1	0.124383464	5.637984645	0.598708065	1	blue
Fmo2	0.933919293	6.274333397	2.60E-05	0.002188418	0.907078902	6.274333397	0.000135198	0.007972717	0.188641541	6.274333397	0.425074982	1	0.161800592	6.274333397	0.444315026	1	blue
E030018B1 3Rik	3.464045181	-1.192186001	2.50E-05	0.002117227	2.830144939	-1.192186001	0.000202128	0.01090713	1.168475186	-1.192186001	0.262569411	1	0.533388123	-1.192186001	0.358891106	1	blue
Doc2b	2.025487909	4.173270047	9.59E-19	1.91E-15	1.848847518	4.173270047	7.17E-15	1.43E-11	0.544489981	4.173270047	0.022698887	0.512474439	0.367841776	4.173270047	0.073886315	1	blue
Adgrl5	0.756326259	9.345786667	0.000711696	0.027861808	0.660663506	9.345786667	5.85E-03	0.112480452	0.198353069	9.345786667	0.406243206	1	0.102690264	9.345786667	0.629405073	1	blue
Lncbate1	1.111203802	3.651767409	0.00037831	0.017392296	1.014945315	3.651767409	0.002210222	0.060568758	0.265232528	3.651767409	0.424760762	1	0.168969704	3.651767409	0.561943554	1	blue
Cntfr	1.348822572	4.770386185	5.06E-10	2.44E-07	1.17533991	4.770386185	3.09E-07	6.55E-05	0.26725961	4.770386185	0.244754834	1	0.093774685	4.770386185	0.642900525	1	blue
Vipr1	1.865192981	5.658334984	1.13E-19	3.94E-16	1.706052177	5.658334984	2.44E-15	6.72E-12	0.312816745	5.658334984	0.141518768	0.992645357	0.153673996	5.658334984	0.414320507	1	blue
Timp3	0.964779928	9.688689281	1.49E-05	0.001552812	0.8206474	9.688689281	5.61E-04	0.023459467	0.186689227	9.688689281	0.429035901	1	0.042856651	9.688689281	0.834568293	1	blue
Acot5	4.99615376	2.312573422	1.61E-13	1.61E-10	4.914911385	2.312573422	3.89E-13	4.53E-10	0.550689052	2.312573422	0.476932225	1	0.4692304	2.312573422	0.341469962	1	blue
Lnx1	0.587212079	5.214133977	0.000741044	0.028689287	0.542338226	5.214133977	0.0038743	0.086359187	0.064586598	5.214133977	0.731965938	1	0.01971222	5.214133977	0.903036299	1	blue
Rhpn2	0.84201561	4.691028512	7.93E-05	0.005540888	0.72597817	4.691028512	0.001500221	0.046381353	0.113267491	4.691028512	0.620398178	1	-0.002771064	4.691028512	0.997922404	1	blue
Fkbp5	2.741350376	6.984434929	3.61E-19	1.01E-15	1.96172975	6.984434929	2.45E-10	1.56E-07	0.431172357	6.984434929	0.151956911	0.999246012	-0.348449505	6.984434929	0.209942093	1	blue
E030003E1 8Rik	0.854441344	4.264958251	0.000756522	0.029047101	0.568917148	4.264958251	3.59E-02	3.06E-01	0.147348207	4.264958251	0.59004117	1	-0.138177251	4.264958251	0.583885415	1	blue

Fam117b	0.706367958	5.753259135	1.85E-05	0.001783651	0.479663658	5.753259135	0.006779411	0.122414783	0.154093538	5.753259135	0.386075393	1	-0.072611179	5.753259135	0.658779714	1	blue
Tead1	1.397241814	7.609702097	3.76E-07	7.97E-05	0.997158198	7.609702097	5.69E-04	2.37E-02	0.292594769	7.609702097	0.308245442	1	-0.107489132	7.609702097	0.690675588	1	blue
Rbm3	0.733808345	6.733015213	2.11E-05	0.002008606	0.451102219	6.733015213	0.014794549	0.189493731	0.204571963	6.733015213	0.269222257	1	-0.078134399	6.733015213	0.649165818	1	blue
Mertk	1.029015989	5.358791334	8.45E-10	3.94E-07	0.692586367	5.358791334	1.05E-04	0.006563851	0.250241159	5.358791334	0.162582213	1	-0.086189385	5.358791334	0.630869351	1	blue
Mcf2l	0.83229974	6.388578383	0.000143832	0.008894676	0.633882399	6.388578383	0.006835106	0.123102379	0.165011488	6.388578383	0.480413241	1	-0.033406201	6.388578383	0.883462482	1	blue
Pgm3	0.590573941	4.653485038	0.000761285	0.02914992	0.462073461	4.653485038	1.45E-02	0.188221265	0.128915585	4.653485038	0.49796455	1	0.000414263	4.653485038	0.993461078	1	blue
Rab27a	0.718368643	3.628015463	0.001567823	0.049240227	0.491932192	3.628015463	0.043506771	0.342557397	0.183610962	3.628015463	0.456858875	1	-0.042827555	3.628015463	0.856943214	1	blue
Pkp4	0.656449803	7.60955638	0.000998895	0.034988847	0.454878617	7.60955638	3.38E-02	0.296604626	0.184254245	7.60955638	0.389460298	1	-0.017317067	7.60955638	0.936664876	1	blue
Bdh1	1.1512702	2.954224809	0.000698818	0.02779717	0.864186975	2.954224809	1.60E-02	0.196427164	0.273057185	2.954224809	0.450661204	1	-0.013832208	2.954224809	0.981520631	1	blue
Hif3a	2.58019991	1.987878999	1.77E-11	1.18E-08	1.898632389	1.987878999	8.66E-07	1.51E-04	0.679656229	1.987878999	0.092116638	0.875797372	-0.001958094	1.987878999	1	1	blue
Vwa3a	1.039689419	3.848365904	0.000318916	0.015212199	0.766740901	3.848365904	1.26E-02	0.173063789	0.270758054	3.848365904	0.379427457	1	-0.002193472	3.848365904	0.997654322	1	blue
Arg2	1.332917746	5.95491937	4.80E-10	2.40E-07	1.089840356	5.95491937	1.47E-06	0.000230104	0.496280422	5.95491937	0.027615363	0.560163016	0.253207721	5.95491937	0.208598756	1	blue
Trim24	0.613798861	6.257363855	7.57E-05	0.005315624	0.481248156	6.257363855	3.94E-03	0.087730907	0.249802356	6.257363855	0.13504958	0.984073476	0.11725123	6.257363855	0.435074514	1	blue
Tfap2b	0.979803269	6.429155404	0.000141948	0.008817184	0.724477194	6.429155404	0.008211143	0.137643065	0.47739401	6.429155404	0.080897499	0.836876692	0.222613316	6.429155404	0.362612436	1	blue
Spdef	2.261113551	3.424095102	5.70E-19	1.33E-15	1.702739923	3.424095102	4.46E-11	3.12E-08	0.751215362	3.424095102	0.004548646	0.215497896	0.192826116	3.424095102	0.38815111	1	blue
Mchr1	2.883502982	1.180841908	0.000341136	0.016161749	2.078304758	1.180841908	0.009909756	0.151199508	0.977463862	1.180841908	0.22409868	1	0.172144887	1.180841908	0.783130598	1	blue
Picalm	0.768824764	8.935796305	0.000192816	0.010600388	0.495489458	8.935796305	0.024847809	0.24852317	0.253816156	8.935796305	0.249697144	1	-0.019519214	8.935796305	0.930128978	1	blue
Hacd2	0.977915599	7.660755962	0.000990013	0.03476489	0.706642178	7.660755962	0.025287272	0.251094724	0.304083644	7.660755962	0.334094822	1	0.032810006	7.660755962	0.898503866	1	blue
Acsl1	1.098454525	11.8545152	3.15E-04	0.015184271	0.747139421	11.8545152	2.08E-02	2.24E-01	0.388057345	11.8545152	0.227872521	1	0.036742426	11.8545152	0.889478115	1	blue
Acer2	0.72953022	6.388383381	0.000376462	0.017364469	0.494453544	6.388383381	0.024595767	0.246947158	0.297585942	6.388383381	0.176017921	1	0.062508843	6.388383381	0.747885643	1	blue
Rab11fip4	1.537157873	3.176872231	2.70E-08	8.40E-06	0.98429268	3.176872231	0.000600963	0.024703133	0.658248964	3.176872231	0.023950542	0.527240563	0.105373327	3.176872231	0.674886713	1	blue
Tlll7	1.205549868	4.189772768	8.13E-07	0.000153625	0.681226457	4.189772768	8.25E-03	1.38E-01	0.567931847	4.189772768	0.028729546	0.566324582	0.043604768	4.189772768	0.844653058	1	blue
Cry2	0.698059413	6.102482994	1.09E-05	0.001241955	0.406786363	6.102482994	1.69E-02	2.02E-01	0.283252501	6.102482994	0.097076404	0.888392991	-0.00802099	6.102482994	0.964923332	1	blue
Gramd1b	1.417544479	4.711567254	9.24E-08	2.35E-05	0.814560378	4.711567254	3.42E-03	0.079854772	0.545355622	4.711567254	0.050665479	0.71157815	-0.057631229	4.711567254	0.828998008	1	blue
Lrrn1	1.566323401	1.945104228	4.48E-06	0.000632226	0.719681992	1.945104228	4.04E-02	0.32867894	0.676338939	1.945104228	0.062566578	0.771874186	-0.17032379	1.945104228	0.60582684	1	blue
Atf2	0.952854283	7.119014985	0.000776858	0.029423775	0.416545975	7.119014985	0.166452847	0.627980926	0.385547333	7.119014985	0.200466321	1	-0.150761242	7.119014985	0.592510659	1	blue
Ccdc85a	0.844465458	4.89222276	0.000260985	0.013167964	0.258826256	4.89222276	0.294587729	0.765128804	0.390124727	4.89222276	0.11508933	0.935167722	-0.195515502	4.89222276	0.392347115	1	blue
Hpgd	0.970325176	4.330839936	3.00E-06	0.00047158	0.241566394	4.330839936	0.275541634	0.74699056	0.371677524	4.330839936	0.094851886	0.884946568	-0.357082572	4.330839936	0.079872496	1	blue
Adh1	0.728061415	6.974220274	0.000412052	0.018457822	0.359078623	6.974220274	0.103935757	0.518417611	0.268675727	6.974220274	0.223831906	1	-0.100307275	6.974220274	0.625510121	1	blue
4930523C0 7Rik	0.736666591	6.375915302	2.90E-05	0.002384562	0.436197927	6.375915302	2.09E-02	0.225346693	0.216509725	6.375915302	0.253218217	1	-0.083959245	6.375915302	0.632029343	1	blue
Arxes1	1.760851126	5.26525857	8.16E-08	2.11E-05	1.027076514	5.26525857	0.002531766	0.065519286	0.481440157	5.26525857	0.155505941	1	-0.252336512	5.26525857	0.421832539	1	blue
4930562F0 7Rik	0.806162095	4.461274437	8.04E-05	0.005585307	0.399476353	4.461274437	0.067824736	0.425839405	0.265935769	4.461274437	0.226922817	1	-0.140751203	4.461274437	0.486722652	1	blue
Tmem52	2.476352048	0.166329032	3.26E-06	0.000494542	1.257996319	0.166329032	1.87E-02	2.14E-01	0.703718664	0.166329032	0.254063688	1	-0.514763581	0.166329032	0.279130478	1	blue
Sult1a1	1.024284651	7.632797681	1.07E-06	0.000194915	0.507517797	7.632797681	2.28E-02	2.37E-01	0.261047114	7.632797681	0.240198505	1	-0.255719888	7.632797681	0.213827337	1	blue
Hhipl1	2.113611244	1.606635072	9.43E-09	3.56E-06	1.149638766	1.606635072	0.002199004	0.060498574	0.470240158	1.606635072	0.225812814	1	-0.493762104	1.606635072	0.14457258	1	blue
Map3k6	1.287435331	6.460252583	1.03E-09	4.64E-07	0.808007505	6.460252583	0.000282698	0.013911939	0.147575206	6.460252583	0.506328868	1	-0.33185298	6.460252583	0.104497072	1	blue
Ercc1	0.840560109	5.152430037	4.43E-06	0.000632226	0.531487274	5.152430037	0.006756364	0.122156469	0.115442559	5.152430037	0.557773102	1	-0.193630828	5.152430037	0.282665678	1	blue
Arxes2	1.236206346	6.988556664	0.000313147	0.015143735	0.909743869	6.988556664	0.012039716	0.169112635	0.155903629	6.988556664	0.664042424	1	-0.170559146	6.988556664	0.614956151	1	blue
Arhgap27	0.593845778	5.60393262	0.000259491	0.013140009	0.401428594	5.60393262	2.20E-02	0.233349447	0.077564332	5.60393262	0.659192754	1	-0.114853135	5.60393262	0.477327367	1	blue
Dlg3	0.911285371	5.316144596	1.72E-07	4.08E-05	0.665745686	5.316144596	3.59E-04	0.016766799	0.072303573	5.316144596	0.700495246	1	-0.173236647	5.316144596	0.311306866	1	blue
Hmgcs2	2.24146939	7.089566034	6.43E-08	1.73E-05	2.088628135	7.089566034	1.31E-06	2.10E-04	-0.075307505	7.089566034	0.856893105	1	-0.228149285	7.089566034	0.560417175	1	blue
Arhgef37	1.29507907	2.438323921	2.18E-05	0.002033323	1.126115503	2.438323921	5.04E-04	0.021477797	0.017721178	2.438323921	0.967397572	1	-0.151248704	2.438323921	0.614890737	1	blue
Adam12	0.877406941	6.960743112	1.34E-06	0.00022812	0.717527788	6.960743112	0.000222773	0.011793482	0.035207002	6.960743112	0.856054599	1	-0.124672317	6.960743112	0.486019059	1	blue
Aldh1a1	0.917452432	6.413295798	5.03E-06	0.00070313	0.759955633	6.413295798	0.000408042	0.018219807	0.051680254	6.413295798	0.810405453	1	-0.105816824	6.413295798	0.594528476	1	blue
Abcg2	0.736612966	5.879003949	2.97E-05	0.002413018	0.578880435	5.879003949	0.002262834	0.061159018	0.028454261	5.879003949	0.881603582	1	-0.129278537	5.879003949	0.459173725	1	blue
Asph	0.831581955	7.39324062	3.17E-04	0.015212199	0.618950798	7.39324062	1.22E-02	1.70E-01	0.026461988	7.39324062	0.914828798	1	-0.186169264	7.39324062	0.4150765	1	blue
Arg1	2.599297591	3.184737288	1.99E-04	0.010728997	1.685831854	3.184737288	1.66E-02	0.200276785	0.135037271	3.184737288	0.848350079	1	-0.778417985	3.184737288	0.231775325	1	blue
Gimap3	1.063428819	3.005087274	7.15E-04	2.79E-02	0.729233654	3.005087274	2.96E-02	0.276732073	-0.023909242	3.005087274	0.950697699	1	-0.358106065	3.005087274	0.245829394	1	blue
Slc2a3	0.993676461	3.241694228	1.33E-04	8.51E-03	0.66442156	3.241694228	1.66E-02	2.00E-01	0.008220896	3.241694228	0.981768332	1	-0.321035516	3.241694228	0.207279624	1	blue
Rpp25	2.278147397	-0.250095948	4.13E-06	0.000613971	1.207912568	-0.250095948	0.019524004	0.21742429	0.341661177	-0.250095948	0.588423835	1	-0.72867341	-0.250095948	0.101407825	1	blue
Fam166a	0.771775767	3.611245376	0.000528338	0.022512343	0.297786812	3.611245376	0.213940314	0.693903418	0.171888957	3.611245376	0.476602723	1	-0.302101142	3.611245376	0.169706452	1	blue
Tubb4b	0.768170116	7.747087276	1.37E-05	0.001490146	0.3907997	7.747087276	3.88E-02	0.321259087	0.080042341	7.747087276	0.672188633	1	-0.297328124	7.747087276	0.088266485	1	blue
Acta1	1.43402517	4.939937223	0.000743343	0.028698784	0.86456728	4.939937223	0.052021266	0.376355629	0.023737323	4.939937223	0.958856051	1	-0.545721245	4.939937223	0.187627896	1	blue
Ramp2	0.702589498	5.906020011	8.73E-05	0.005951449	0.454613955	5.906020011	0.018299233	0.212064741	-0.061453976	5.906020011	0.751188386	1	-0.309429557	5.906020011	0.080827951	1	blue
Itgax3	0.6580401	6.249348178	7.55E-05	0.005315624	0.39473008	6.249348178	0.027424771	0.261988107	-0.087201042	6.249348178	0.626631195	1	-0.350511033	6.249348178	0.033500442	0.745544874	blue
Mmp28	1.094307568	5.849210985	1.72E-04	1.01E-02	0.451523702	5.849210985	1.43E-01	5.93E-01	0.041758492	5.849210985	0.892856918	1	-0.601025459	5.849210985	0.036100846	0.776223732	blue
Hsd11b2	1.917871981	1.322557591	3.44E-07	7.50E-05	0.65028404	1.322557591	0.100891488	0.512004154	0.175032262	1.322557591	0.67822458	1	-1.092564683	1.322557591	0.002415982	0.167988845	blue
1700020L2 4Rik	1.023541402	3.887623509	1.86E-04	0.010600388	0.259129067	3.887623509	0.375610062	0.828442549	0.105297158	3.887623509	0.720854792	1	-0.659115283	3.887623509	0.014875005	0.498843884	blue
Snta1	1.03526562	5.022342532	1.83E-04	0.010529899	0.322940749	5.022342532	0.271756433	0.743989796	0.075279219	5.022342532	0.7990293	1	-0.637045716	5.022342532	0.019679916	0.577753327	blue
Prrg3	1.037385269	4.845047341	1.33E-05	0.001458677	0.309956759	4.845047341	0.221293684	0.702201142	0.062612723	4.845047341	0.806684621	1	-0.66481579	4.845047341	0.004687674	0.258952313	blue
Abhd2	0.776396415	6.908758217	1.02E-05	0.001197305	0.274448673	6.908758217	0.145533784	0.596864298	-0.095698467	6.908758217	0.612231282	1	-0.597646111	6.908758217	0.000634225	0.065175918	blue
Prr5	0.75734972	5.323788412	1.59E-03	0.04980942	0.288860176	5.323788412	0.261824677	0.736543853	-0.189601415	5.323788412	0.461729983	1	-0.658090476	5.323788412	0.005932723	0.299640059	blue
Dmrt2	0.940741633	5.309269374	2.68E-04	0.013431649	0.244373989	5.309269374	0.374462263	0.827428394	-0.008292443	5.309269374	0.977323188	1	-0.704659869	5.309269374	0.005938773	0.299640059	blue
Prap1	7.803310191	-2.087893825	6.58E-04	0.026581036	4.434376539	-2.087893825	0.173499692	0.639846002	0	-2.087893825	1	1	-3.38311564	-2.087893825	0.023868007	0.639040746	blue
Bves	1.433830038	0.57218631	0.001156344	0.039321333	0.075472858	0.57218631	0.906951377	0.998463035	0.147108337	0.57218631	0.780483055	1	-1.211239833	0.57218631	0.005385898	0.280832869	blue
Bmper	0.820031452	5.099432266	1.52E-04	0.009306445	-0.044539625	5.099432266	0.848230697	0.983893751	-0.007023704	5.099432266	0.97867452	1	-0.871594107	5.099432266	5.87E-05	0.00976082	blue
Aldh1l2	0.833127391	2.761028558	3.67E-03	8.99E-02	-0.25468257	2.761028558	0.414311295	0.853665733	0.026597756	2.761028558	9.36E-01	1.00E+00	-1.061207162	2.761028558	0.00025176	0.01987248	blue
Sprr2f	8.117505927	-1.779938808	4.99E-04	0.021539862	-1.766546245	-1.779938808	0.354680408	0.812264563	4.993459983	-1.779938808	0.080194858	0.836876692	-4.920393125	-1.779938808	0.003968093	0.233017068	blue
Ldlr	1.016052091	5.593230623	6.81E-07	0.000132197	-0.082622825	5.593230623	0.704709936	0.960193977	6.604783742	5.593230623	5.54E-03	0.243490854	-0.493891781	5.593230623	0.01402656	0.488308544	green
Clca1	1.852552531	5.550276755	6.29E-05	0.00453325	-0.136540547	5.550276755	0.772489798	0.972503068	1.303376697	5.550276755	6.59E-03	0.267790873	-0.685718511	5.550276755	0.122577709	1	green
Zbtb16	1.004343291	6.548549971	1.30E-04	8.40E-03	0.176369804	6.548549971	0.525985422	0.900217029	0.580714704	6.548549971	3.74E-02	6.44E-01	-0.247259231	6.548549971	3.38E-01	1.00E+00	green
Fam90a1a	4.256346294	0.966201982	2.18E-05	0.002033323	0.663652211	0.966201982	0.457654701	0.874323659	2.871424415	0.966201982	4.00E-03	2.03E-01	-0.721666108	0.966201982	3.98E-01	1	green
Hlf	1.159210537	4.589951861	1.42E-07	3.55E-05	0.266468335	4.589951861	0.250681124	0.725724931	0.75792243	4.589951861	0.001226394	0.09733151	-0.134822388	4.589951861	0.531423959	1	green
Slc1a1	1.005737135	3.255130293	1.25E-04	8.24E-03	0.268543444	3.255130293	3.34E-01	0.795715899	0.612735268	3.255130293	2.93E-02	5.74E-01	-0.124463666	3.255130293	0.623270232	1	green
Timp4	1.599184426	6.059068423	3.44E-10	1.85E-07	0.665501909	6.059068423	1.18E-02	1.67E-01	0.826222171	6.059068423	1.87E-03	0.127362287	-0.107461763	6.059068423	6.63E-01	1	green
Elmod1	2.406245051	0.950833131	2.18E-05	0.002033323	0.781485552	0.950833131	1.60E-01	0.620149041	1.455151054	0.950833131	0.031197346	0.39495954	-0.169715658	0.950833131	7.59E-01	1	green
Dbp	2.128361701	5.647384536	7.82E-17	1.21E-13	0.743554083	5.647384536	4.02E-03	8.93E-02	1.474926118	5.647384536	2.23E-08	1.56E-05	0.090114678	5.647384536	6.93E-01	1.00E+00	green
Defb1	3.176162358	4.056296796	2.43E-05	0.002094958	0.705823803	4.056296796	0.324857327	0.790409512	2.375234483	4.056296796	0.001605694	0.114495797	-0.095129588	4.056296796	0.907979067	1	green
Vldlr	0.581999053	6.404520307	0.000470358	0.020352075	-0.105014263	6.404520307	0.557306874	0.907588076	0.636264214	6.404520307	0.000399086	0.044672631	-0.050749528	6.404520307	0.762209753	1	green
Per3	0.712943419	4.720701508	0.000021636	0.011203457	-0.007753704	4.720701508	9.72E-01	1	0.956325054	4.720701508	4.17E-06	0.001388235	0.235625319	4.720701508	2.04E-01	1	green
Ucp1	4.311951949	8.789550622	2.98E-15	4.16E-12	1.517570922	8.789550622	2.41E-03	0.0636901	5.652026585	8.789550622	2.88E-21	2.01E-17	2.857636409	8.789550622	2.06E-10	1.52E-07	green
Atp1b1	0.635062842	5.033336671	0.002394235	0.066261049	0.115990723	5.033336671	6.04E-01	0.925246103	0.789886023	5.033336671	0.000462949	0.049390678	0.27081204	5.033336671	1.79E-01	1	green
Wnk2	0.856611446	4.771147706	1.55E-05	0.001581754	0.209134461	4.771147706	3.20E-01	0.787720626	0.874947373	4.771147706	3.97E-05	0.008958835	0.227467745	4.771147706	2.31E-01	1	green
Slc35f3	0.838419748	4.19440086	0.001487395	0.047245074	0.194894168	4.19440086	0.487341885	0.886860701	0.827005398	4.19440086	0.003469077	0.185343843	0.183476158	4.19440086	4.64E-01	1	green
Hecw2	0.790663299	4.248254429	0.00036825	0.017098568	0.189034088	4.248254429	0.425144386	0.859628985	0.732599653	4.248254429	0.00212231	0.136532201	0.130967375	4.248254429	5.36E-01	1	green
Nr1d2	0.885924594	6.592266291	1.71E-06	0.00028774	0.327181345	6.592266291	0.096831314	0.502530428	0.836251395	6.592266291	2.52E-05	0.006300986	0.277507373	6.592266291	1.18E-01	1.00E+00	green
Hmcn1	1.069436917	5.400113035	8.20E-05	0.005648787	0.5687602	5.400113035	0.047392885	0.357507289	0.995159423	5.400113035	5.91E-04	0.059434824	0.494480251	5.400113035	5.43E-02	9.34E-01	green
Zim1	1.247933662	4.085438773	0.000140958	0.008817184	0.965365938	4.085438773	0.004987724	0.102287048	1.066616002	4.085438773	2.18E-03	0.139031142	0.784040218	4.085438773	1.03E-02	4.05E-01	green
Mrggrg	3.993118823	2.043643367	2.22E-10	1.29E-07	2.787451587	2.043643367	4.80E-07	9.72E-05	3.565532196	2.043643367	2.73E-08	1.82E-05	2.359363228	2.043643367	5.11E-07	1.93E-04	green
Ppargc1a	1.982534947	5.435797876	7.55E-11	4.59E-08	1.773714812	5.435797876	2.07E-08	7.05E-06	1.754274958	5.435797876	3.68E-08	2.23E-05	1.545446915	5.435797876	2.22E-08	1.11E-05	green
Clstn3	1.064770476	6.041001421	1.28E-06	0.000221195	0.984565873	6.041001421	2.57E-05	0.002099505	0.872248158	6.041001421	0.000197947	0.028229657	0.792041809	6.041001421	1.44E-04	0.020316334	green
Dio2	3.251687223	7.214316121	3.16E-21	1.47E-17	2.39748024	7.214316121	2.82E-12	2.46E-09	2.175785787	7.214316121	1.89E-10	2.20E-07	1.321574126	7.214316121	6.28E-06	0.001720873	green

Agtr1a	1.78613458	6.823663073	1.01E-14	1.28E-11	1.061156796	6.823663073	8.82E-06	0.000912587	1.200177633	6.823663073	5.84E-07	0.000282839	0.475198441	6.823663073	2.54E-02	0.667031241	green
Usp2	1.047880391	4.768329828	1.73E-06	0.00028774	0.596314893	4.768329828	0.010090581	0.15213157	0.670113928	4.768329828	0.00415223	0.205785718	0.218545763	4.768329828	2.93E-01	1	green
Pde4c	1.351227457	1.537245209	0.000187769	0.010600388	0.635901299	1.537245209	0.087266143	0.481270409	1.025435112	1.537245209	0.008273823	0.303503793	0.310069874	1.537245209	3.47E-01	1	green
Gm5627	1.900664118	1.012341782	2.46E-05	0.002109815	0.917482479	1.012341782	0.03873415	0.320704074	1.524252488	1.012341782	0.001379506	0.103101487	0.540967895	1.012341782	1.68E-01	1	green
Cpm	1.196917847	3.45537694	3.68E-06	0.000552435	0.486521238	3.45537694	0.071721808	0.438387547	0.895618987	3.45537694	0.001158552	0.093594892	0.185214254	3.45537694	4.44E-01	1	green
Per2	2.064782704	5.563537741	7.39E-24	5.16E-20	0.946938331	5.563537741	5.68E-06	0.000666561	1.270404265	5.563537741	2.10E-09	2.10E-06	0.152556153	5.563537741	4.12E-01	1	green
Plxna2	0.696618996	6.494677677	0.000404515	0.018178471	0.293896068	6.494677677	0.163873002	0.624805269	0.418893276	6.494677677	4.76E-02	0.694640431	0.016169942	6.494677677	9.27E-01	1	green
Tef	1.476517336	7.233668497	4.07E-12	2.84E-09	0.790101395	7.233668497	0.000384084	0.017485204	0.854823149	7.233668497	1.28E-04	0.020511795	0.16840652	7.233668497	3.97E-01	1.00E+00	green
Myzap	0.768756507	4.432975696	0.000388946	0.017706528	0.436775049	4.432975696	0.059482742	0.399327317	0.413771251	4.432975696	7.56E-02	8.18E-01	0.081787823	4.432975696	6.92E-01	1.00E+00	green
Coro2a	0.827407998	7.521081466	2.43E-05	0.002094958	0.874068987	7.521081466	3.28E-05	0.002561752	0.393697096	7.521081466	6.02E-02	7.61E-01	0.440357751	7.521081466	1.94E-02	5.70E-01	purple
Wnt4	0.784124639	5.881931281	0.001248352	0.041739146	0.868194562	5.881931281	0.00087422	0.032494946	0.316077464	5.881931281	2.24E-01	1.00E+00	0.400146464	5.881931281	8.58E-02	1.00E+00	purple
Ciart	2.362758445	2.160857684	1.16E-09	5.07E-07	2.312332835	2.160857684	4.94E-09	1.97E-06	0.867541103	2.160857684	3.24E-02	0.608175827	0.817060862	2.160857684	1.39E-02	0.488308544	purple
Cutal	1.289054787	3.371331092	3.07E-06	0.000476209	1.261300666	3.371331092	1.48E-05	0.001392839	0.476706941	3.371331092	1.03E-01	9.06E-01	0.448944277	3.371331092	8.03E-02	1.00E+00	purple
Rev3l	1.041603752	7.181238286	8.50E-06	0.001052705	1.037035155	7.181238286	3.33E-05	0.002571221	0.324719276	7.181238286	1.90E-01	1.00E+00	0.320150255	7.181238286	1.50E-01	1.00E+00	purple
Nup210	0.685373938	5.540092682	0.000769792	0.029395112	0.697846612	5.540092682	0.001442488	0.045303862	0.230396176	5.540092682	0.29306043	1	0.242867995	5.540092682	0.21605994	1	purple
P2ry14	1.135357851	2.766842375	0.000130352	0.008395362	1.232878239	2.766842375	8.62E-05	0.005641246	0.317565677	2.766842375	3.22E-01	1.00E+00	0.415075705	2.766842375	1.33E-01	1.00E+00	purple
Setx	0.919954055	7.036280574	6.45E-06	0.000858248	1.085964455	7.036280574	7.16E-07	0.000130057	0.261463451	7.036280574	2.29E-01	1.00E+00	0.427473404	7.036280574	2.85E-02	6.97E-01	purple
Rnf103	0.581804773	6.1458953	0.000354	0.016602381	0.665811108	6.1458953	0.000151706	0.008603816	0.17261572	6.1458953	3.26E-01	1.00E+00	0.256621567	6.1458953	1.04E-01	1.00E+00	purple
Penk	0.65869557	5.238105193	0.002206391	0.06229601	0.747870251	5.238105193	0.00124044	0.040600459	0.137026943	5.238105193	5.55E-01	1.00E+00	0.226200717	5.238105193	2.75E-01	1.00E+00	purple
Sox9	0.933093415	6.487667883	0.000444719	0.019726362	1.047910591	6.487667883	0.000233166	0.012069366	0.198613453	6.487667883	0.482387252	1	0.313430064	6.487667883	0.215281857	1	purple
Bmf	0.97100521	4.875736996	2.88E-08	8.57E-06	1.04186115	4.875736996	2.61E-08	7.94E-06	0.207813913	4.875736996	0.269173209	1	0.278668115	4.875736996	0.095035674	1	purple
Pik3ip1	1.289287561	4.20961172	1.55E-08	5.00E-06	1.535313666	4.20961172	2.96E-10	1.79E-07	0.102872295	4.20961172	0.673664811	1	0.348895046	4.20961172	0.102852915	1	purple
Lifr	0.618501836	7.364552415	0.000801655	0.030118099	0.722860275	7.364552415	0.00028228	0.013911939	0.097390004	7.364552415	6.24E-01	1	0.201748261	7.364552415	0.258715847	1	purple
Cldn3	0.660791436	6.275978654	0.000190773	0.010600388	0.820213712	6.275978654	1.77E-05	0.001613007	0.088526489	6.275978654	6.43E-01	1	0.247948337	6.275978654	0.147764778	1	purple
Kcnj31	1.031889361	2.193547139	0.001440683	0.046393969	1.337838714	2.193547139	0.000104904	0.000563851	0.080880443	2.193547139	0.820693992	1	0.38681839	2.193547139	0.197260173	1	purple
Ppp1r1b	1.217769289	2.384261146	0.000710706	0.027861808	1.646155066	2.384261146	1.86E-05	0.001663136	0.092414238	2.384261146	0.822864263	1	0.520787257	2.384261146	0.117333955	1	purple
B4galnt1	0.944127244	6.161515422	1.69E-05	0.001686219	1.276210369	6.161515422	6.75E-08	1.85E-05	0.0789009	6.161515422	0.736253451	1	0.410983332	6.161515422	0.049845827	0.901682314	purple
Tceal9	0.570459844	6.620303944	0.001063529	0.037054886	0.80178076	6.620303944	2.11E-05	0.001818951	0.051457285	6.620303944	0.784722151	1	0.282777891	6.620303944	0.094517883	1	purple
Cyp1b1	0.757259222	5.756235502	0.000259234	0.013140009	1.014522464	5.756235502	5.61E-06	0.000666561	0.101742014	5.756235502	0.648331565	1	0.359004481	5.756235502	0.071630281	1	purple
Slc25a33	0.836046219	4.353422245	0.003059906	0.078695583	1.267566173	4.353422245	3.07E-05	0.002437658	0.0654966	4.353422245	0.831644656	1	0.497014188	4.353422245	0.064395693	1	purple
1700003D0 9Rik	1.316800605	-0.002439808	0.004215143	0.098246499	1.976428455	-0.002439808	4.51E-05	0.003284714	0.037495587	-0.002439808	0.952126885	1	0.697045575	-0.002439808	0.088012738	1	purple
Kcnip3	1.378648895	3.675972929	3.47E-05	0.002747378	2.268615128	3.675972929	3.30E-10	1.85E-07	0.018610211	3.675972929	0.965101772	1	0.908569511	3.675972929	0.003125399	0.199303796	purple
Mrggpre	0.933077231	1.996623469	0.010587745	0.175533	1.324738439	1.996623469	6.96E-04	0.027241824	0.148817785	1.996623469	0.707488281	1	0.540464216	1.996623469	0.113109439	1	purple
Lox	0.598161484	6.774435352	0.00362647	0.089231596	0.795125779	6.774435352	0.000342369	0.016220179	0.125217005	6.774435352	0.571640596	1	0.32218097	6.774435352	0.105317615	1	purple
Adcyap1r1	0.429737764	5.084990331	0.019562026	0.252445862	0.644776236	5.084990331	0.001203105	0.039845004	0.091361546	5.084990331	0.647378981	1	0.306399162	5.084990331	0.086852978	1	purple
Zfp664	0.830175952	8.366031636	6.64E-05	0.004759724	1.200112453	8.366031636	9.50E-08	2.40E-05	0.178568728	8.366031636	0.421378392	1	0.548505058	8.366031636	0.006030876	0.302208908	purple
Stard5	0.468733483	4.390234073	0.013069296	0.199421077	0.652084402	4.390234073	0.001362177	0.043465266	0.161427735	4.390234073	0.431078911	1	0.344776998	4.390234073	0.059359914	0.965078208	purple
Hpdl	1.588182628	1.241813226	0.000153292	0.009355518	2.449632198	1.241813226	2.16E-08	7.20E-06	0.380733695	1.241813226	0.395913419	1	1.242118267	1.241813226	0.000694459	0.070153271	purple
Cyp2d22	0.38487714	5.45947463	0.027142116	0.304444795	0.59937209	5.45947463	1.48E-03	4.60E-02	0.156702358	5.45947463	0.406127204	1	0.371196552	5.45947463	0.02855736	0.696763009	purple
Adcy3	1.004320212	6.541174635	0.000163164	0.00970377	1.743920244	6.541174635	1.74E-09	8.38E-07	0.225419169	6.541174635	0.425293482	1	0.96501827	6.541174635	0.000133907	0.01909671	purple
Cenpo	0.70559601	4.84676238	0.001647684	0.050279548	1.300708147	4.84676238	8.32E-08	2.19E-05	0.139138016	4.84676238	0.56527294	1	0.734248109	4.84676238	0.000621486	0.064339964	purple
Cab39l	0.380719766	6.710905829	0.022581041	0.273951933	0.678451501	6.710905829	1.80E-04	0.009899238	0.062211741	6.710905829	0.731109531	1	0.3599432	6.710905829	0.027073322	0.685465124	purple
Sec14l4	0.621248347	1.170932261	0.001841175	0.054633245	1.274829126	1.170932261	4.42E-09	1.81E-06	0.052630899	1.170932261	0.806234209	1	0.56148228	4.018524456	0.023780012	0.637906804	purple
Dpep1	0.621248347	1.170932261	0.001841175	0.054633245	1.274829126	1.170932261	4.42E-09	1.81E-06	0.052630899	1.170932261	0.806234209	1	0.706211328	1.170932261	0.000242983	0.031270596	purple
Herpud1	0.324832352	6.644343507	0.045645863	0.413365976	0.736049728	6.644343507	3.09E-05	0.002437658	0.028518044	6.644343507	0.871838229	1	0.439735124	6.644343507	0.005558695	0.286572758	purple
Tmem37	0.312426937	1.610296088	0.359518011	0.875369987	1.194482297	1.610296088	9.42E-04	0.034102749	-0.033814735	1.610296088	0.932250767	1	0.848226096	1.610296088	0.007866059	0.349003314	purple
Ctnnbl1	0.202933088	5.664924001	0.282171458	0.821629834	1.018323042	5.664924001	7.17E-07	0.000130057	-0.077096135	5.664924001	0.707404369	1	0.73829313	5.664924001	5.49E-05	0.009244813	purple
Setdb2	0.303502235	3.643238724	0.204706337	0.751812939	0.993801032	3.643238724	1.20E-04	0.007292034	-0.041942238	3.643238724	0.875568769	1	0.648353749	3.643238724	0.004841626	0.263294013	purple
Setdb2- pps1c	0.301964527	3.78475548	0.186514735	0.730995496	0.887827859	3.78475548	0.000319493	0.015291874	0.015540998	3.78475548	0.953428334	1	0.601401752	3.78475548	0.006331402	0.30702712	purple
Inmt	1.040794509	6.141049989	3.59E-07	7.71E-05	1.945213502	6.141049989	2.67E-18	1.25E-14	0.426854983	6.141049989	0.049833646	0.709014016	1.331272245	6.141049989	6.19E-12	5.41E-09	purple
Elovl3	1.316951643	2.403575347	0.005187665	0.111542773	2.675270648	2.403575347	1.44E-07	3.49E-05	0.723452694	2.403575347	0.144159449	0.994029995	2.081727412	2.403575347	1.28E-06	0.000424439	purple
Bbs9	0.323911685	4.491351099	0.146819264	0.675986263	0.798213091	4.491351099	0.000922544	0.033841126	0.210501736	4.491351099	0.382988327	1	0.684801016	4.491351099	0.001472751	0.121077447	purple
Hccs	0.346707231	4.846496156	0.079466897	0.529953489	0.702549794	4.846496156	9.94E-04	0.035376901	0.084236065	4.846496156	0.18393415	1	0.640072908	4.846496156	0.000820041	0.078216873	purple
Cited1	1.292056572	6.726855209	0.001628993	0.050252623	1.694044408	6.726855209	0.000115448	0.007058465	0.83893387	6.726855209	0.051752528	0.715274536	1.240920204	6.726855209	0.001183105	0.103487941	purple
Ankrd9	1.522982286	3.977521496	4.26E-06	0.000620047	1.810631352	3.977521496	2.06E-07	4.71E-05	1.172880951	3.977521496	0.000765741	0.069493449	1.460515879	3.977521496	1.52E-06	0.000492605	purple
Gk	1.58801393	5.905133288	1.42E-08	4.82E-06	1.947533109	5.905133288	6.36E-11	4.23E-08	1.475250312	5.905133288	6.08E-07	0.000283224	1.834764542	5.905133288	1.61E-12	1.50E-09	purple
Slc4a4	0.731593336	5.659593766	1.93E-04	1.06E-02	0.93213481	5.659593766	1.02E-05	0.001017198	0.697828139	5.659593766	0.000973532	0.082963926	0.896367737	5.659593766	1.95E-06	6.20E-04	purple
Ppif	0.57605741	4.797562573	5.13E-03	0.110805494	0.921523494	4.797562573	3.12E-05	0.002450372	0.523518501	4.797562573	0.018330606	0.458076995	0.868981762	4.797562573	1.07E-05	0.002781713	purple
Lrrc52	1.762604553	-1.31541922	0.073319329	0.515060954	3.232378347	-1.31541922	5.49E-06	0.000661923	1.73324033	-1.31541922	0.094404665	0.883132257	3.20116385	-1.31541922	1.37E-07	5.81E-05	purple
Gmpr	0.396410929	3.302938604	2.40E-01	0.784039429	2.151352508	3.302938604	5.54E-09	2.15E-06	0.29817562	3.302938604	0.411774349	1	2.053104227	3.302938604	1.33E-10	1.03E-07	purple
Cend1	0.421714655	-0.02492599	3.91E-01	0.887695628	1.852359983	-0.02492599	5.95E-05	0.004160542	0.427890975	-0.02492599	0.406397268	1	1.858406803	-0.02492599	3.91E-06	0.001137958	purple
Mrnp11	0.053982636	3.301820608	0.886437376	1	1.043283672	3.301820608	0.004029715	0.08939571	0.270766951	3.301820608	0.456598955	1	1.260060926	3.301820608	9.04E-05	0.01404172	purple
Dhrs9	0.046108713	2.087416357	0.914743135	1	1.433609639	2.087416357	0.0003738	0.017246677	0.575875426	2.087416357	0.157307121	1	1.963347329	2.087416357	4.52E-08	2.18E-05	purple
Slc25a34	-0.417462478	1.849186457	0.337796058	0.85956143	1.169976747	1.849186457	0.017100857	0.20397708	-0.042055954	1.849186457	0.932806163	1	1.541366645	1.849186457	0.000384553	0.043575463	yellow
2310050C0 9Rik	-5.794351339	-1.929092343	0.007231776	0.138558137	5.330516317	-1.929092343	0.004828611	0.10042361	-2.63813539	-1.929092343	0.171000922	1	8.473441346	-1.929092343	2.51E-05	0.005307817	yellow
Awat1	-5.323645551	-2.202390551	0.007170551	0.138038053	8.23511128	-2.202390551	6.84E-05	0.004628206	-5.356447184	-2.202390551	0.03292348	0.60864888	8.204879445	-2.202390551	1.00E-06	0.000359976	yellow
Coch	-1.356107798	0.281665635	0.038879701	0.3786339	3.501929062	0.281665635	1.94E-05	0.001691751	-2.4588584	0.281665635	0.002439642	0.150199913	2.399251744	0.281665635	0.000299486	0.037371556	yellow
Nbl1	-0.23816484	5.919537583	0.155606715	0.68952424	0.826755127	5.919537583	9.63E-06	0.000982322	-0.563691198	5.919537583	0.002492084	0.152093273	0.501228798	5.919537583	0.002739709	0.18380356	yellow
Serpina3j	-1.266276175	0.437321864	9.60E-02	0.574767387	3.912042709	0.437321864	3.95E-05	0.002967507	-2.213768698	0.437321864	0.014340158	0.415805081	2.964597334	0.437321864	0.00011217	0.016501962	yellow
Fa2h	-1.017084897	1.452829135	0.123314418	0.631528879	2.587868571	1.452829135	0.000993772	0.035376901	-1.199558618	1.452829135	0.116587709	0.940779341	2.405384544	1.452829135	0.000326374	0.040012316	yellow
Lce1a2	-5.794998343	-2.436261812	0.004958885	0.108919069	7.801706449	-2.436261812	0.001104974	0.037943768	-5.828029497	-2.436261812	0.026601068	0.549152925	7.771510258	-2.436261812	4.95E-05	0.008875233	yellow
Sdr16c6	-6.299900766	-2.14787901	0.002860027	0.07556093	8.111616558	-2.14787901	0.001191598	0.039835152	-6.331107815	-2.14787901	0.01676538	0.439308492	8.081393817	-2.14787901	5.44E-05	0.009244813	yellow
Gm94	-6.778785664	-1.546906642	0.001840476	0.054633245	8.863536164	-1.546906642	0.000895708	0.033205337	-6.812111423	-1.546906642	0.013226607	0.104989444	8.833268412	-1.546906642	3.20E-05	0.006306695	yellow
Serpina3b	-2.473527938	0.885715834	0.008276685	0.149450842	4.980985466	0.885715834	4.37E-05	0.003197945	-3.122019243	0.885715834	0.005801965	0.24804562	4.332564288	0.885715834	1.12E-05	0.002850493	yellow
Lor	-2.389286944	0.678325548	0.008609371	0.154064748	4.518967916	0.678325548	9.32E-05	0.006022318	-2.981886028	0.678325548	0.007205089	0.28049672	3.926427881	0.678325548	2.87E-05	0.005935889	yellow
Calm4	-4.651982286	-1.245186888	0.002252095	0.063076724	9.1304615	-1.245186888	1.43E-04	0.008286404	-7.322585073	-1.245186888	0.002887989	0.16817725	6.47543838	-1.245186888	2.99E-05	0.006061516	yellow
Krt10	-1.508562462	2.705129684	0.02093764	0.263287053	2.513373311	2.705129684	1.21E-03	0.039899767	-1.537034083	2.705129684	0.041194782	0.664824796	2.484898968	2.705129684	0.00018384	0.024945108	yellow
Krtdap	-3.027264383	0.482229258	0.007303674	0.139448298	4.671525949	0.482229258	0.0009745	0.035139157	-2.918862263	0.482229258	0.027996828	0.563809316	4.779907898	0.482229258	4.70E-05	0.008644648	yellow
Lce1m	-8.049628567	-0.503882042	0.000531914	0.022595817	9.95457059	-0.503882042	7.96E-04	0.003166529	-8.083131232	-0.503882042	0.006216485	0.258376689	9.924267923	-0.503882042	2.50E-05	0.005307817	yellow
Cyp2g1	-8.574935601	-0.292260674	0.000306832	0.014889886	10.08047626	-0.292260674	9.21E-04	0.033841126	-8.608476518	-0.292260674	0.004304853	0.207634596	10.05017101	-0.292260674	3.04E-05	0.00607066	yellow
Crct1	-7.358586001	-1.633763257	0.000672943	0.026948562	8.536012083	-1.633763257	0.001607722	0.048953205	-7.392011713	-1.633763257	0.006887646	0.276162238	8.505761101	-1.633763257	7.45E-05	0.01170174	yellow
Hamp2	-6.15069011	-2.488952939	2.36E-03	0.065329896	5.303878854	-2.488952939	5.77E-03	0.111761879	-5.901813511	-2.488952939	0.048124135	0.69697711	7.541351738	-2.488952939	9.68E-05	0.014706612	yellow
Psapl1	-2.416637443	0.171833608	0.009571305	0.164334842	3.343717987	0.171833608	2.75E-03	0.069040116	-2.068632711	0.171833608	0.054157533	0.73130984	3.6916733	0.171833608	9.88E-05	0.014840599	yellow
Rnase2b	-6.158255644	-2.338810684	1.09E-03	0.037793345	6.635965597	-2.338810684	3.49E-03	0.080707258	-5.009584835	-2.338810684	0.061357153	0.779378476	7.771541056	-2.338810684	1.07E-05	0.002781713	yellow
Dmkn	-2.182662497	1.898978278	0.010372337	0.173609322	3.12514811	1.898978278	2.34E-03	0.062527393	-1.726164455	1.898978278	0.078699481	0.829490156	3.581627246	1.898978278	5.12E-05	0.008935676	yellow
Spink5	-2.945771851	0.196011606	4.78E-03	1.06E-01	2.739134472	0.196011606	2.22E-02	2.34E-01	-1.836579972	0.196011606	0.119358663	0.946835239	3.848216355	0.196011606	0.000278866	0.035112051	yellow
Lce1a1	-4.541348911	-2.418568698	1.38E-03	0.044959173	3.039643097	-2.418568698	1.96E-02	2.18E-01	-2.022111802	-2.418568698	0.134910309	0.983974457	5.555482801	-2.418568698	5.10E-05	0.008936576	yellow
Defb6	-7.939927477	-1.190066988	0.000691753	0.027623678	4.360326483	-1.190066988	3.23E-02	0.289603338	-3.415169998	-1.190066988	0.101456556	0.901434724	8.87097783	-1.190066988	0.000154598	0.021392746	yellow
Cyp26b1	-0.929659331	3.58954082	0.000720425	0.027968495	0.811394894	3.58954082	0.008411176	0.138953415	-0.793167629	3.58954082	0.010024521	0.340055107	0.948426475	3.58954082	0.000561161	0.058968362	yellow
Mafb	-0.761999625	6.156003759	0.001105917	0.037976173	0.436041343	6.156003759	9.45E-02	0.498074045	-0.96402004	6.156003759	0.000237831	0.031357795	0.234021394	6.156003759	0.316722981	1	yellow
Il33	-2.277792588	4.437293273	5.81E-06	0.000788775	1.30309815	4.437293273	0.02123273	0.227742623	-2.160945947	4.437293273	0.000191893	0.027648483	1.419946304	4.437293273	0.004241066	0.244930341	yellow
Nuak2	-0.73203141	3.325934643	0.001537898	0.04851842	0.175510542	3.325934643	4.99E-01	0.890090934	-0.552093749	3.325934643	0.031967361	0.604471554	0.355449563	3.325934643	0.126736189	1	yellow

Adrb2	-0.73094708	3.954353775	0.0008949	0.032498532	0.158617771	3.954353775	0.519715207	0.898174816	-0.486178069	3.954353775	0.047196947	0.692882916	0.403387383	3.954353775	0.068177817	1	yellow
Chil1	-1.12320778	4.345506428	0.001092994	0.037811095	0.402341579	4.345506428	0.295259667	0.765358313	-0.535394815	4.345506428	0.16388465	1	0.990153967	4.345506428	0.004003491	0.234112097	yellow
Tmem132c	-1.260047674	2.776117532	5.72E-05	0.004185854	0.191467457	2.776117532	0.586825478	0.919099782	-0.515255267	2.776117532	0.13879472	0.990196533	0.936258508	2.776117532	0.00288177	0.189641677	yellow
Aspg	-2.282092526	4.194521625	1.44E-12	1.06E-09	-0.900980146	4.194521625	1.07E-02	0.156648581	0.903413653	4.194521625	0.010492992	0.34669045	2.284517927	4.194521625	1.42E-12	1.42E-09	royalblue
A33004112 2Rik	-1.257119042	5.530070629	2.88E-04	0.014240943	-0.56758781	5.530070629	1.43E-01	0.592754364	0.595548439	5.530070629	0.124415558	0.956226206	1.285078347	5.530070629	0.000210857	0.027801341	royalblue
Me1	-1.219404243	10.62586096	0.00095579	0.033990115	-0.542131807	10.62586096	1.90E-01	0.661557439	0.646588245	10.62586096	0.118480975	0.945142756	1.323860639	10.62586096	0.00033837	0.040767691	royalblue
Sorcs2	-0.991711004	4.126960226	8.66E-05	0.005933737	-0.724327254	4.126960226	0.009704436	0.150487956	0.702423807	4.126960226	0.012108277	0.379428874	0.969804711	4.126960226	0.0001247	0.017967041	royalblue
Slc2a5	-2.04260938	4.249812902	2.37E-05	0.00208639	-1.188271126	4.249812902	0.027736624	0.264064748	1.346040678	4.249812902	0.012998977	0.391208682	2.200370336	4.249812902	5.53E-06	0.001544725	royalblue
Pygl	-0.872403081	8.096352134	0.000416617	0.01860268	-0.479860021	8.096352134	0.081801974	0.465541383	0.612003335	8.096352134	0.026665115	0.549663193	1.004546211	8.096352134	4.81E-05	0.008722537	royalblue
Pdk4	-0.715150669	8.515306032	5.87E-04	0.024565329	-0.230199632	8.515306032	3.20E-01	0.787640039	0.411205913	8.515306032	0.075762605	0.817704713	0.896156837	8.515306032	1.62E-05	0.003783626	royalblue
Adcy10	-1.536128352	1.987654346	1.92E-04	0.010600388	-0.581208879	1.987654346	1.92E-01	0.662606457	1.066381587	1.987654346	0.017802601	0.448304783	2.021269276	1.987654346	9.08E-07	0.000333845	royalblue
Gpd2	-0.634755852	7.670563161	0.00640689	0.129772028	-0.347269572	7.670563161	0.179968762	0.6467584	0.727564945	7.670563161	0.00514686	0.235844335	1.015050935	7.670563161	1.27E-05	0.003001013	royalblue
Apold1	-0.573535562	7.052820663	0.002893156	0.07629197	-0.267153606	7.052820663	0.210717502	0.687438797	0.732720092	7.052820663	0.000634394	0.062002007	1.039101582	7.052820663	6.23E-08	2.81E-05	royalblue
Adprhl1	-2.202218723	-0.901186619	1.20E-02	0.190158556	-0.334253868	-0.901186619	0.670084635	0.951254734	2.079579028	-0.901186619	0.014752927	0.419932609	3.946694221	-0.901186619	2.18E-06	0.000675596	royalblue
Otop1	-0.491609819	3.974809309	2.81E-01	0.821408556	-0.577841468	3.974809309	0.25529048	0.729851304	2.091584708	3.974809309	7.39E-05	0.013772289	2.00534065	3.974809309	1.20E-05	0.002951736	royalblue
Acot11	-0.368704185	4.251496329	3.13E-01	0.844786178	-0.256155914	4.251496329	0.524383625	0.900170012	2.518993281	4.251496329	3.55E-09	3.10E-06	2.63152609	4.251496329	1.17E-12	1.26E-09	royalblue
Fam151a	-0.475972696	2.443826775	2.86E-01	0.823769409	-0.185897063	2.443826775	0.6978793	0.955882348	2.416175936	2.443826775	1.91E-06	0.000797648	2.706198354	2.443826775	1.08E-09	6.59E-07	royalblue
Dcpp3	-1.980876233	-1.5562302	0.127098347	0.63968133	-0.245606192	-1.5562302	0.682153701	0.952820984	3.519379088	-1.5562302	5.66E-07	0.000282839	5.251161091	-1.5562302	1.85E-11	1.52E-08	royalblue
Cpdlb	-0.28928321	5.746735495	2.07E-01	0.753949176	-0.010348918	5.746735495	9.68E-01	1	1.046538191	5.746735495	4.35E-05	0.009384939	1.3254707	5.746735495	6.03E-09	3.24E-06	royalblue
Cidea	-0.097251067	5.986852101	0.689350678	0.97543435	0.280271529	5.986852101	0.300545638	0.770624892	2.129799683	5.986852101	4.54E-14	9.06E-11	2.507318234	5.986852101	4.14E-24	9.65E-21	royalblue
Letmd1	-0.127861161	6.222308186	0.511362703	0.934711632	0.085498934	6.222308186	0.692826441	0.955447289	0.616907903	6.222308186	0.004467841	0.213044717	0.830267229	6.222308186	1.97E-05	0.004300966	royalblue
Gnao1	-0.250625174	3.434116951	0.276980844	0.818930459	0.196042178	3.434116951	0.437087254	0.863970822	0.550385415	3.434116951	0.027922343	0.579250129	0.997047175	3.434116951	1.15E-05	0.002861715	royalblue
Pim1	-0.231502722	6.042434314	0.254409486	0.797836601	0.059071063	6.042434314	7.94E-01	0.976199887	0.431643507	6.042434314	0.055727828	0.742471039	0.722216637	6.042434314	0.000365708	0.042950711	royalblue
Mtfp1	-0.376855756	3.089599219	0.174805337	0.719187341	0.207293322	3.089599219	4.98E-01	0.889724687	0.544428964	3.089599219	0.076301912	0.818134822	1.128570524	3.089599219	4.08E-05	0.007700671	royalblue
Gm9899	-0.641662406	3.896457329	0.022649869	0.274106207	0.425307368	3.896457329	0.17028881	0.634485847	0.703854957	3.896457329	0.024125605	0.52932411	1.770818102	3.896457329	2.54E-10	1.77E-07	royalblue
Pvalb	-1.624705605	0.280747195	0.068466628	0.501694422	0.357783774	0.280747195	0.713997787	0.961722539	1.360446743	0.280747195	0.168055548	1	3.342723504	0.280747195	0.000220105	0.028749356	royalblue
Atp2a1	-1.328473241	1.318057273	0.002945789	0.076810355	0.217378569	1.318057273	6.51E-01	0.942302597	0.69856003	1.318057273	0.151228804	0.999246012	2.244363116	1.318057273	4.14E-07	0.000160712	royalblue
Ckm	-1.650232504	1.253371109	0.017807714	0.237247232	0.339324435	1.253371109	6.57E-01	0.945507563	1.056395075	1.253371109	0.1725831	1	3.045868803	1.253371109	1.68E-05	0.003803256	royalblue
Ucp3	-0.551562936	5.052887525	0.003924999	0.093292153	0.055722694	5.052887525	7.93E-01	0.976199887	0.425521964	5.052887525	0.044071427	0.679711223	1.032806042	5.052887525	5.64E-08	2.63E-05	royalblue
Kcnh1	-0.884099701	4.357395023	0.002155606	0.061483175	-0.003102401	4.357395023	9.94E-01	1	0.742926335	4.357395023	0.020589472	0.483627674	1.623919306	4.357395023	1.68E-08	8.68E-06	royalblue
Tnnt3	-1.365226097	1.107875076	0.010278167	0.172861206	0.520316974	1.107875076	3.66E-01	0.82073697	0.591495873	1.107875076	0.309808698	1	2.47697788	1.107875076	3.12E-06	0.000927604	royalblue
Tnni2	-0.990455147	-0.438529831	0.062208858	0.476415264	0.387333417	-0.438529831	4.78E-01	0.882522979	0.414507557	-0.438529831	0.482774674	1	1.792177061	-0.438529831	0.000371333	0.043247899	royalblue
Fam69b	-0.461431028	3.166520478	0.077086497	0.52413909	0.08496775	3.166520478	5.14E-01	0.894229	0.301630386	3.166520478	0.296352299	1	0.951553152	3.166520478	0.000243882	0.031270596	royalblue
Acacb	-0.429035816	8.353633843	0.086886502	0.548432133	0.378185889	8.353633843	0.175383931	0.641834466	0.295704593	8.353633843	0.289165412	1	1.102926137	8.353633843	1.04E-05	0.002781713	royalblue
Kcnk3	-0.435779831	6.662795487	0.079051707	0.528372382	0.593253815	6.662795487	0.031830997	0.286827864	0.502706056	6.662795487	0.068874007	0.795523236	1.53173889	6.662795487	6.44E-10	4.29E-07	royalblue
Pamr1	-0.246043608	4.855085314	0.393984776	0.889563201	0.861156352	4.855085314	0.007754156	0.133633206	0.422529335	4.855085314	0.190803306	1	1.529726467	4.855085314	1.20E-07	5.22E-05	royalblue
Abi3	-0.066395634	5.852880377	0.697465024	0.975980943	0.852408628	5.852880377	5.42E-06	0.00065829	0.869119253	5.852880377	4.00E-06	0.001362649	1.78792141	5.852880377	2.56E-26	7.17E-23	royalblue
Phospho1	-0.1343002	5.640943926	0.455215821	0.913501714	0.972694992	5.640943926	8.73E-07	0.000150677	1.125593689	5.640943926	1.73E-08	1.27E-05	2.232585606	5.640943926	7.83E-36	5.47E-32	royalblue
Perm1	-0.125559782	2.262536387	0.6967799	0.976014878	0.763772629	2.262536387	2.28E-02	0.236750324	0.925736952	2.262536387	0.006915912	0.276162238	1.815043349	2.262536387	2.47E-09	1.38E-06	royalblue
Hc	-0.104555078	5.530403666	0.737123023	0.981536925	0.395420179	5.530403666	0.268922609	0.74085702	0.636309181	5.530403666	0.076326786	0.818134822	1.136282834	5.530403666	0.000386617	0.043575463	royalblue
Pank1 A530050N04 4Rik	-0.022068755	4.739562782	0.907632539	1	0.613658868	4.739562782	4.76E-03	0.100263094	1.193639047	4.739562782	6.76E-08	3.78E-05	1.829361352	4.739562782	1.21E-20	2.12E-17	royalblue
	1.156883735	0.639816728	0.498960173	0.932175597	1.979492105	0.639816728	1.35E-05	0.001281951	5.988632528	0.639816728	4.00E-15	9.32E-12	6.806831526	0.639816728	6.08E-35	2.83E-31	royalblue
Dagla	0.12793813	4.196815496	0.525356544	0.938266133	0.869844278	4.196815496	4.31E-05	0.00316872	0.713201075	4.196815496	0.000907432	0.078771833	1.455101685	4.196815496	2.43E-14	2.83E-11	royalblue
Slc27a2	0.833785755	3.229791259	0.006714714	0.133302339	1.895757658	3.229791259	3.08E-10	1.79E-07	2.601784263	3.229791259	1.54E-15	5.39E-12	3.664686727	3.229791259	3.24E-39	4.53E-35	royalblue
Cldn1	0.353060772	3.499178984	0.240777251	0.78435695	0.709409434	3.499178984	0.026145129	0.255153509	0.796537704	3.499178984	0.011640528	0.402194133	1.152877788	3.499178984	5.43E-05	0.009244813	royalblue
Ldhb	0.438268791	6.283421373	0.025731213	0.296349735	0.381942705	6.283421373	0.071173198	0.43743035	0.743301164	6.283421373	0.000480212	0.050844272	0.68697414	6.283421373	0.000307498	0.038031772	royalblue
Fabp3	1.649205304	2.486591348	0.007315176	0.139477362	1.426686496	2.486591348	0.010919367	0.158773827	4.607004825	2.486591348	5.37E-12	7.50E-09	4.384146026	2.486591348	4.85E-16	6.16E-13	royalblue
Acss1	0.129226847	4.513668016	0.52596481	0.938266133	0.227405615	4.513668016	0.294769221	0.765202649	0.600555807	4.513668016	0.00601094	0.254083859	0.698732052	4.513668016	0.000358319	0.042802318	royalblue
Ppara	0.145557457	5.176667183	0.515295526	0.936858884	0.247312906	5.176667183	0.298657406	0.769765915	1.198400063	5.176667183	7.09E-07	0.000319836	1.300152333	5.176667183	1.27E-09	7.37E-07	royalblue
Gm44502	0.221703812	6.238748628	0.228560175	0.773020276	0.287289243	6.238748628	0.145691319	0.596927386	1.600815752	6.238748628	2.78E-15	7.77E-12	1.666399023	6.238748628	8.81E-21	1.76E-17	royalblue
Cox7a1	0.15156033	3.106297835	0.605018471	0.961467803	0.247837601	3.106297835	0.390763971	0.838396877	2.191484315	3.106297835	9.39E-13	1.46E-09	2.287732058	3.106297835	8.63E-18	1.21E-14	royalblue
Acaa2	0.165856503	7.189805404	0.335142476	0.858883664	0.130598465	7.189805404	4.83E-01	0.884299667	0.721128851	7.189805404	0.000114666	0.018965291	0.685870385	7.189805404	4.24E-05	0.007893084	royalblue
Ppp1r3b	0.37576778	5.353351514	0.048905421	0.425171207	0.219918957	5.353351514	0.278218699	0.750074179	1.787109551	5.353351514	1.61E-17	7.51E-14	1.631256332	5.353351514	5.91E-19	9.18E-16	royalblue
Cpt1b	0.942238284	5.387950268	0.000204372	0.010942234	0.496792911	5.387950268	5.84E-02	0.395362461	3.332175146	5.387950268	1.18E-30	1.65E-26	2.886716335	5.387950268	9.69E-33	3.39E-29	royalblue
Hsd11b1	0.376785234	6.259639053	0.085831279	0.545075371	0.11886881	6.259639053	0.615059738	0.928502365	0.870799276	6.259639053	0.000253543	0.031964298	0.612881916	6.259639053	0.003931403	0.231836632	royalblue
Nr4a3	0.492119494	6.886749523	0.027798312	0.308229671	0.014115945	6.886749523	9.53E-01	1	1.02871201	6.886749523	2.30E-05	0.005839258	0.550707792	6.886749523	0.010930211	0.420828182	royalblue
Coq10b	0.27743915	6.188785492	0.090950314	0.559037814	-0.022064126	6.188785492	9.02E-01	0.997031331	0.724293667	6.188785492	4.86E-05	0.00998344	0.424789666	6.188785492	0.007977379	0.349504208	royalblue
Sbp	0.658855129	1.319840146	0.492477561	0.930368531	-0.415206267	1.319840146	0.656709584	0.945507563	3.664981385	1.319840146	0.000423995	0.046381842	2.590706364	1.319840146	0.002185895	0.160789842	royalblue
Gys2	0.292309719	4.952167384	0.395593517	0.889930544	-0.222971192	4.952167384	0.54269308	0.904681263	1.382706723	4.952167384	0.000209949	0.029051924	0.867422472	4.952167384	0.008236913	0.353126047	royalblue
Nr4a2	0.248740362	5.853623534	0.30577194	0.837935027	-0.215567236	5.853623534	4.09E-01	0.849836988	1.016162064	5.853623534	0.000115344	0.018965291	0.551853274	5.853623534	0.018727424	0.559261714	royalblue
Gm5148	0.484067329	2.364143918	0.123706215	0.632145542	-0.442237018	2.364143918	1.76E-01	6.43E-01	1.445360428	2.364143918	1.69E-05	0.004646006	0.519037756	2.364143918	0.079819144	1	lightgreen
Clic5	0.152535707	5.662526399	0.451907513	0.913501714	-0.410719812	5.662526399	0.059867676	0.400346125	0.860208754	5.662526399	8.95E-05	0.015442991	0.296952327	5.662526399	0.131754723	1	lightgreen
Cyn1s1	0.443217905	1.59340209	0.460792888	0.915038563	-1.460958841	1.59340209	1.59E-02	0.196111641	3.064660193	1.59340209	2.25E-06	0.000872703	1.160399411	1.59340209	0.031877922	0.733837288	lightgreen
Pnldc1	0.279002982	1.782950037	0.43757327	0.908732183	-0.760837746	1.782950037	3.90E-02	0.322005228	1.348538436	1.782950037	0.000316363	0.036845692	0.308677765	1.782950037	0.355627924	1	lightgreen
Tnfsf11	0.957359352	0.401056271	0.376076358	0.884817534	-2.627814473	0.401056271	0.010996292	0.159359628	4.29980646	0.401056271	0.000131635	0.02098527	0.714284652	0.401056271	0.40233657	1	lightgreen
Bdnf	0.429207257	4.155867806	0.054650741	0.445363704	-0.556035349	4.155867806	2.02E-02	2.22E-01	1.092593643	4.155867806	6.25E-06	0.001986106	0.107348032	4.155867806	0.618126061	1	lightgreen
Wnk4	0.594721784	2.861576326	0.046978526	0.41987895	-0.440107431	2.861576326	1.66E-01	0.627233726	1.1971702	2.861576326	0.000207095	0.028943588	0.162331602	2.861576326	0.568036083	1	lightgreen
Csn2	2.971016679	0.035740291	0.000278336	0.01384349	-1.41176907	0.035740291	0.038704192	0.320645987	4.978883795	0.035740291	4.67E-09	3.84E-06	0.595117135	0.035740291	0.331140929	1	lightgreen
Defb15	2.06313401	-2.386333859	0.045098365	0.410348141	-2.199581646	-2.386333859	0.004821588	0.10042361	3.582984864	-2.386333859	0.000104995	0.017679668	-0.681563897	-2.386333859	0.45136269	1	lightgreen
Fcgbp	0.326509018	6.663183916	0.34449672	0.864240918	-1.322640492	6.663183916	0.000429086	0.01865317	1.513813523	6.663183916	5.95E-05	0.011882753	-0.135336437	6.663183916	0.70050342	1	lightgreen
Atp7b	0.039253765	0.856377626	1	1	-3.745261218	0.856377626	5.96E-13	6.21E-10	3.900651099	0.856377626	9.63E-14	1.68E-10	0.116026863	0.856377626	0.857216099	1	lightgreen
Entpd8	1.542325885	-0.82659896	0.317351878	0.846885321	-4.797700208	-0.82659896	0.000597215	0.024621483	5.585745661	-0.82659896	0.00015503	0.023050036	-0.755482219	-0.82659896	0.638498775	1	lightgreen
Calca	0.220416357	1.603758299	0.835135454	0.994187369	-3.398801094	1.603758299	7.76E-04	0.029626726	3.209511908	1.603758299	0.001373933	0.103101487	-0.409727725	1.603758299	0.672448517	1	lightgreen
Ppp1r3d	0.176353574	3.243076303	0.502770212	0.933318504	-1.355691633	3.243076303	1.64E-06	0.000249252	1.148886836	3.243076303	4.31E-05	0.009384939	-0.383159489	3.243076303	0.14263453	1	lightgreen
Gm4847	0.045343401	0.39777344	1	1	-6.113654613	0.39777344	2.56E-05	0.002099505	3.002351521	0.39777344	0.014272225	0.414695662	-3.155662777	0.39777344	0.016052488	0.514563239	lightgreen
Il1a	-0.343717644	1.581689886	0.479285448	0.924567759	-2.145412503	1.581689886	0.000151321	0.008603816	1.632698095	1.581689886	0.00326584	0.177600705	-0.16900016	1.581689886	0.761596301	1	lightgreen
Rasef	-0.328868077	5.213830757	0.16922153	0.709710104	-1.188423828	5.213830757	9.75E-06	0.000987831	0.826356725	5.213830757	0.001946253	0.129527749	-0.033199227	5.213830757	0.901517151	1	lightgreen
Il12b	-0.54795453	0.308394811	0.337751791	0.85956143	-2.256251544	0.308394811	0.000463363	0.019926014	1.7945975594	0.308394811	0.004611464	0.217735883	0.086277809	0.308394811	0.911147304	1	lightgreen
Sc5d	-0.115604283	6.498008096	0.538404209	0.94090594	-0.70728118	6.498008096	0.000747172	0.028926523	0.650615648	6.498008096	0.001907872	0.127580947	0.058938561	6.498008096	0.751308701	1	lightgreen
Muc15	-0.207339539	5.170642329	0.509681051	0.934141884	-1.161973227	5.170642329	0.001142747	0.038670775	1.315099458	5.170642329	0.00024407	0.031790079	0.360464358	5.170642329	0.254478406	1	lightgreen
Gm4841	-0.799535061	1.474439892	0.045698701	0.413388376	-1.705943976	1.474439892	0.00012736	0.00767234	1.609558256	1.474439892	0.000281477	0.034813489	0.703125351	1.474439892	0.082189267	1	lightgreen
Mir7116	-1.465155389	0.022203241	0.01222525	0.192019475	-1.991528172	0.022203241	0.001473531	0.046039414	1.563440976	0.022203241	0.011274531	0.363337878	1.03698843	0.022203241	0.080762088	1	orange
Igp1	-0.872827283	7.979361033	0.000191994	0.010600388	-1.102543859	7.979361033	2.85E-05	0.002303482	0.855846022	7.979361033	0.00109893	0.089742492	0.626129306	7.979361033	0.007532802	0.338515871	orange
Slc25a35	-0.724672529	5.861236418	0.000359515	0.016804611	-0.758768853	5.861236418	8.02E-04	0.030291008	0.508696588	5.861236418	0.024112504	0.52932411	0.474599706	5.861236418	0.019763405	0.577852195	orange
Ppp1r9a	-0.53148292	5.006422573	0.001717669	0.051961348	-0.667063963	5.006422573	0.000388809	0.017585738	0.356372451	5.006422573	0.057002695	0.746059679	0.220791185	5.006422573	0.194842762	1	orange
Rnf150	-0.571685017	4.480421577	0.00137737	0.044959173	-0.715912844	4.480421577	0.000301869	0.014649038	0.380427403	4.480421577	0.053551521	0.727343113	0.236199239	4.480421577	0.188841473	1	orange
Hspa4l	-0.469893335	4.484511816	0.010054391	0.170327473	-0.636194714	4.484511816	0.001645134	0.049767086	0.345008987	4.484511816	0.08642649	0.849375486	0.178707334	4.484511816	0.329856093	1	orange
Adap1	-0.680845788	4.184863696	0.011725827	0.188367998	-0.965989101	4.184863696	0.001387335	0.044066796	0.556349298	4.184863696	0.063733328	0.77496143	0.271205403	4.184863696	0.316828497	1	orange
Cxcl9	-0.390900805	6.373669034	0.057172263	0.45557183	-0.757509217	6.373669034	0.000939887	0.034102749	0.554009303	6.373669034	0.015252968	0.426259774	0.187400725	6.373669034	0.361291757	1	orange
Mir6935	-0.694302189	1.723946894	0.071199197	0.509252803	-1.371336578	1.723946894	0.001506664	0.046381353	0.911697789	1.723946894	0.033031823	0.609337417	0.23465877	1.723946894	0.548523075	1	orange
Rhoq	-0.326156821	7.217831862	0.074114664	0.516364178	-0.757403529	7.217831862	0.000195149	0.010612473	0.48562889	7.217831862	0.016533782	0.439241368	0.054382141	7.217831862	0.762188183	1	orange
Hvcn1	-0.354258989	4.794303331	0.055287285	0.448608979	-0.752088966	4.794303331	2.43E-04	0.012463372	0.447569544	4.794303331	0.028216539	0.564152758	0.049739418	4.794303331	0.785963075	1	orange

Pigf	-0.353216476	4.639523102	0.051458136	0.434024692	-0.735852136	4.639523102	0.000249595	0.01273117	0.441141419	4.639523102	0.027379018	0.557797606	0.058505577	4.639523102	0.746155676	1	orange
Zfp667	-0.560713191	3.799779915	0.005902156	0.122735018	-1.117576751	3.799779915	8.22E-07	0.000145358	0.618719872	3.799779915	0.00577291	0.24804562	0.061856191	3.799779915	0.761342718	1	orange
Palm2	-0.57134873	2.774626089	0.035356118	0.357048393	-1.031307825	2.774626089	0.000660288	0.026366243	0.573936841	2.774626089	0.054631185	0.732627562	0.113977153	2.774626089	0.678502794	1	orange
Tmem179	-0.558965823	5.965973401	0.007806078	0.144500326	-0.99052897	5.965973401	2.51E-05	0.002099505	0.586772427	5.965973401	0.011981225	0.378845246	0.155209162	5.965973401	0.459909137	1	orange
Myo5c	-0.7863444777	3.966273098	0.002655801	0.071793962	-1.114909745	3.966273098	0.000146325	0.00845058	0.51743741	3.966273098	0.074810892	0.813663053	0.188872363	3.966273098	0.471415561	1	orange
Snhg11	-0.919016947	5.103249215	0.007457875	0.140662966	-1.303494881	5.103249215	0.000819413	0.03078525	0.560356046	5.103249215	0.144852754	0.994029995	0.175878201	5.103249215	0.604048145	1	orange
Ssbp3	-0.407537738	5.836069193	0.009234981	0.16025376	-0.620473732	5.836069193	0.000353276	0.016624199	0.281159254	5.836069193	0.104183903	0.907211355	0.068223261	5.836069193	0.662032072	1	orange
Mob3b	-0.447892072	3.969163962	0.027756986	0.308229671	-0.760908036	3.969163962	0.000759124	0.029147023	0.358094515	3.969163962	0.110937219	0.921880751	0.045078612	3.969163962	0.823127278	1	orange
Nwat1	-0.529793435	6.869479887	0.035008396	0.355195794	-0.912875549	6.869479887	0.001194435	0.039835152	0.398962519	6.869479887	0.153981822	1	0.015880444	6.869479887	0.941462947	1	orange
Sox2ip	-0.461745481	4.805006289	0.015908104	0.22255422	-0.864540524	4.805006289	5.08E-05	0.003607063	0.386382517	4.805006289	0.068145915	0.79192982	-0.016412356	4.805006289	0.942745965	1	orange
Scd2	-0.781105085	8.109843498	0.017865963	0.233752372	-1.419896191	8.109843498	0.000155658	0.008772065	0.589731565	8.109843498	0.110519412	0.920939068	-0.049059488	8.109843498	0.896422375	1	orange
P2rx5	-1.062834767	2.880286578	0.000648568	0.02642919	-1.985519147	2.880286578	2.68E-08	7.97E-06	0.818043255	2.880286578	0.017533177	0.447803905	-0.108637072	2.880286578	0.75142543	1	orange
Mettl24	-0.633187847	1.332498869	0.065006201	0.485583463	-1.247340448	1.332498869	0.001197107	0.039835152	0.519698285	1.332498869	0.16985187	1	-0.094448846	1.332498869	0.803846842	1	orange
Scnn1g	-2.003851461	1.220678968	2.30E-05	0.002058739	-3.359141801	1.220678968	3.15E-09	1.42E-06	1.097082057	1.220678968	0.031963597	0.604771554	-0.258154805	1.220678968	0.636200751	1	orange
Mir5114	-0.969978095	3.204860557	0.01106503	0.18065989	-1.606616144	3.204860557	0.000230556	0.011978651	0.566621317	3.204860557	0.183218096	1	-0.070014113	3.204860557	0.8745492	1	orange
Ptch2	-1.034472066	3.678179143	0.003015244	0.035472641	-1.601307658	3.678179143	8.43E-06	0.00090111	0.388329907	3.678179143	0.26758478	1	-0.178502728	3.678179143	0.59295623	1	orange
Piger3	-0.993146098	5.644269522	1.12E-05	0.001258001	-1.366365435	5.644269522	9.24E-08	2.39E-05	0.300925939	5.644269522	0.231130818	1	-0.072292837	5.644269522	0.762804468	1	orange
Acp6	-0.489637577	4.895307338	0.003139081	0.080058024	-0.67040226	4.895307338	0.000272301	0.013543364	0.158814141	4.895307338	0.38602694	1	-0.021950188	4.895307338	0.904257009	1	orange
Tlnrb	-0.669917768	4.446811916	0.000206052	0.010942234	-0.895472029	4.446811916	8.65E-06	0.000903978	0.222066545	4.446811916	0.269147933	1	-0.00528709	4.446811916	0.986509046	1	orange
Gbp7	-0.457904515	5.759103308	0.013070242	0.199421077	-0.674189966	5.759103308	0.001022491	0.036088689	0.202955569	5.759103308	0.320427511	1	-0.01332973	5.759103308	0.951158193	1	orange
A530016L2 4Rik	-0.702238455	7.580158747	0.002078308	0.059889562	-1.0714495	7.580158747	2.94E-05	0.002348845	0.366432653	7.580158747	0.148947808	0.995387977	-0.002778329	7.580158747	0.999155672	1	orange
Dhcr7	-0.458623782	4.515825698	0.019747333	0.253899471	-0.714359178	4.515825698	0.001087907	0.037542199	0.245659429	4.515825698	0.25863291	1	-0.010075658	4.515825698	0.968737684	1	orange
Rb1	-0.399098568	6.396382164	0.013780459	0.204237212	-0.590198756	6.396382164	0.001034118	0.036405126	0.210679531	6.396382164	0.239888737	1	0.019579394	6.396382164	0.899932071	1	orange
Trps1	-0.545990343	7.387082765	0.006241603	0.127533108	-0.846600336	7.387082765	0.000148185	0.00848783	0.339192441	7.387082765	0.12616178	0.960892121	0.038582477	7.387082765	0.841533808	1	orange
Tle28	-0.459165051	6.488178468	0.007449915	0.140662966	-0.663351878	6.488178468	0.000508444	0.021598835	0.258697514	6.488178468	0.173464623	1	0.05451072	6.488178468	0.748042031	1	orange
Kcnb1	-0.892706175	5.431611756	7.57E-06	0.000962194	-1.247255716	5.431611756	2.74E-08	7.97E-06	0.443883163	5.431611756	0.044781018	0.680286059	0.089333862	5.431611756	0.654747751	1	orange
Ccbl2a	-0.680553423	4.695990531	0.001209889	0.040745561	-0.856052502	4.695990531	0.000267678	0.013408856	0.222258663	4.695990531	0.340413139	1	0.046759991	4.695990531	0.821402869	1	orange
Igtp	-0.670373849	5.433590422	0.000635473	0.026045092	-0.873345725	5.433590422	6.79E-05	0.00463165	0.273077815	5.433590422	0.209291883	1	0.070106119	5.433590422	0.719097819	1	orange
Mxipl	-1.03148438	6.801061989	0.000332403	0.015801578	-1.277558618	6.801061989	8.64E-05	0.005641246	0.379357133	6.801061989	0.236895584	1	0.133283008	6.801061989	0.638588478	1	orange
Sema6d	-0.614565563	5.687837295	0.000875388	0.032027281	-0.62050477	5.687837295	0.0025362	0.065519286	0.184632452	5.687837295	0.367322124	1	0.178693272	5.687837295	0.334668979	1	orange
Tbc1d32	-0.591500442	4.153392303	0.001284544	0.042846734	-0.545944329	4.153392303	0.007360496	0.129722935	0.136282095	4.153392303	0.501992866	1	0.181838303	4.153392303	0.326212062	1	orange
Rybp	-0.639841447	5.436805808	0.0005725	0.024027816	-0.535200483	5.436805808	0.009607662	0.150206382	0.080761357	5.436805808	0.695717387	1	0.185402413	5.436805808	0.319956288	1	orange
Cxadr	-0.879892619	6.191492394	1.38E-05	0.001490146	-0.72270654	6.191492394	0.001393159	0.044110588	0.087371621	6.191492394	0.698110965	1	0.244557784	6.191492394	0.228714812	1	orange
Cdon	-0.745959547	6.152157737	0.000181507	0.010516358	-0.684982553	6.152157737	0.002067559	0.058118807	0.110654598	6.152157737	0.617365135	1	0.171631687	6.152157737	0.390027274	1	orange
Tspan18	-0.827130995	6.399945745	1.54E-05	0.001579378	-0.754602441	6.399945745	0.00041346	0.018344482	0.128349896	6.399945745	0.545733599	1	0.200878529	6.399945745	0.295701712	1	orange
Mapkapk3	-0.937737005	4.565284086	8.99E-06	0.001091972	-0.852567263	4.565284086	0.000305581	0.014777865	0.118435192	4.565284086	0.614158795	1	0.203605336	4.565284086	0.339012737	1	orange
Gbp5	-0.85523878	4.427991697	0.000292389	0.014388834	-0.905662384	4.427991697	0.000613688	0.02500553	0.196158809	4.427991697	0.454332859	1	0.145735651	4.427991697	0.537956656	1	orange
Rdh10	-0.685188021	4.368808025	0.000173101	0.010122417	-0.739385584	4.368808025	0.000271159	0.013534716	0.154027213	4.368808025	0.445408626	1	0.099830068	4.368808025	0.58734793	1	orange
Ndbp2l1	-0.671119694	4.94532962	0.000977825	0.034597687	-0.700540921	4.94532962	0.002023438	0.057301809	0.135060256	4.94532962	0.54961514	1	0.1056393	4.94532962	0.603525418	1	orange
Cntnap1	-1.193910129	4.241899136	1.55E-07	3.80E-05	-1.231000312	4.241899136	1.54E-06	0.000239423	0.187490101	4.241899136	0.457157446	1	0.150400933	4.241899136	0.513422745	1	orange
Sfxn5	-0.837619268	4.622528233	0.000305646	0.014884004	-0.893653754	4.622528233	0.000581752	0.024126307	0.102047001	4.622528233	0.69270286	1	0.046013221	4.622528233	0.840103181	1	orange
Syne1	-0.66081935	6.307088667	1.04E-05	0.001210173	-0.666939013	6.307088667	6.46E-05	0.004450547	0.049646995	6.307088667	0.765359477	1	0.043527504	6.307088667	0.769808792	1	orange
Tbc1d31	-0.84206528	4.040143096	5.79E-05	0.004216646	-0.836806086	4.040143096	0.000354992	0.016648873	0.005050155	4.040143096	0.984612541	1	0.010310665	4.040143096	0.956610407	1	orange
Meis2	-0.700058396	3.874778263	0.000446017	0.019726362	-0.714505701	3.874778263	0.001317333	0.042130548	0.007279492	3.874778263	0.976497516	1	-0.007166536	3.874778263	0.983658995	1	orange
Ccdc69	-1.086583828	4.017663834	3.26E-08	9.29E-06	-1.163196229	4.017663834	1.45E-07	3.49E-05	0.01959087	4.017663834	0.930223988	1	-0.057019449	4.017663834	0.788924974	1	orange
Vgll4	-0.775667814	5.362427678	4.90E-07	9.79E-05	-0.829593099	5.362427678	1.46E-06	0.000230104	0.03601213	5.362427678	0.833859637	1	-0.017912644	5.362427678	0.917061196	1	orange
A430046D1 3Rik	-1.497843719	2.531415326	1.81E-07	4.21E-05	-1.58109032	2.531415326	1.26E-06	0.000204986	0.053942502	2.531415326	0.867070135	1	-0.029296099	2.531415326	0.935281287	1	orange
Fgf11	-0.932015504	3.550254773	5.12E-05	0.003831278	-1.109193482	3.550254773	1.83E-05	0.001653759	0.14328301	3.550254773	0.574311133	1	-0.033892817	3.550254773	0.894215403	1	orange
Irgm2	-0.736867934	5.830855292	0.000207449	0.010942234	-0.938663314	5.830855292	2.45E-05	0.00206418	0.176302632	5.830855292	0.423816956	1	-0.025492434	5.830855292	0.908042021	1	orange
Banp	-1.276646412	3.582021071	4.59E-07	9.58E-05	-1.671369997	3.582021071	7.74E-09	2.85E-06	0.236346268	3.582021071	0.998451686	1	-0.158373342	3.582021071	0.559344574	1	orange
Wscd2	-1.113493448	3.016627167	9.76E-06	0.001165596	-1.673893706	3.016627167	7.98E-07	0.000142988	0.185113649	3.016627167	0.573698368	1	-0.175280293	3.016627167	0.579128729	1	orange
Sox6	-1.065430531	4.946596431	1.04E-08	3.83E-06	-1.235162681	4.946596431	3.89E-09	1.70E-06	0.106115793	4.946596431	0.607175237	1	-0.063615307	4.946596431	0.746986402	1	orange
Adrb3	-2.214191886	7.772984615	2.65E-32	3.70E-28	-2.546636798	7.772984615	1.51E-31	2.11E-27	0.127484004	7.772984615	0.535519077	1	-0.20496042	7.772984615	0.284120379	1	orange
Gbp6	-1.245335944	5.164081029	1.09E-13	1.18E-10	-1.547304272	5.164081029	4.28E-16	1.49E-12	0.124485607	5.164081029	0.502050571	1	-0.177481366	5.164081029	0.309209162	1	orange
Anggt1	-0.943601391	4.487877528	1.85E-06	0.000304474	-1.227894426	4.487877528	3.60E-08	1.03E-05	0.125116107	4.487877528	0.568609194	1	-0.159175359	4.487877528	0.440476112	1	orange
Tln2	-0.694995751	6.276381903	1.68E-05	0.001684372	-0.920739596	6.276381903	3.47E-07	7.23E-05	0.072523494	6.276381903	0.68586613	1	-0.153220002	6.276381903	0.356365189	1	orange
Six5	-0.673544782	4.179913996	0.000351583	0.01660044	-0.805695325	4.179913996	0.000128975	0.007736271	0.036454815	4.179913996	0.863100292	1	-0.095694452	4.179913996	0.628691302	1	orange
Prag1	-0.698582311	6.953212756	0.000160739	0.009641558	-0.799320756	6.953212756	0.000111986	0.006925286	-0.00088615	6.953212756	0.99705859	1	-0.101624393	6.953212756	0.596050295	1	orange
Slc45a3	-0.755288378	4.885028188	0.000852617	0.031441109	-0.890098156	4.885028188	0.000456836	0.019705984	-0.044922074	4.885028188	0.859487875	1	-0.179730742	4.885028188	0.445806028	1	orange
Plekhm1	-0.541342951	5.949697631	0.00065133	0.026462186	-0.612168749	5.949697631	0.000530747	0.022342528	-0.044407526	5.949697631	0.801261599	1	-0.115232967	5.949697631	0.480540564	1	orange
Strip2	-1.115529458	3.814169989	5.54E-06	0.000758602	-1.149722335	3.814169989	3.33E-05	0.002571221	-0.108262385	3.814169989	0.691472389	1	-0.142452204	3.814169989	0.584211418	1	orange
Tgm1	-1.609761787	4.750428461	1.29E-14	1.50E-11	-1.585634878	4.750428461	2.47E-11	1.82E-08	-0.190507595	4.750428461	0.41020394	1	-0.16637826	4.750428461	0.447154351	1	orange
Med12l	-1.183309431	4.167770506	2.11E-07	4.69E-05	-1.189343919	4.167770506	3.75E-06	0.000503294	-0.063078621	4.167770506	0.810027059	1	-0.067110949	4.167770506	0.785329239	1	orange
Tssc1	-0.625695763	3.852730019	0.001454548	0.046625615	-0.619233189	3.852730019	0.004698952	0.099503864	-0.041644272	3.852730019	0.849919964	1	-0.035180355	3.852730019	0.87158472	1	orange
Abca2	-0.654351623	6.528256623	0.000179909	0.010476722	-0.631258845	6.528256623	0.001185673	0.039738534	-0.059332113	6.528256623	0.759742265	1	-0.036237112	6.528256623	0.845058543	1	orange
Tbc1d4	-0.79062076	5.785735208	7.92E-07	0.00015169	-0.738770436	5.785735208	3.62E-05	0.002748981	-0.082647852	5.785735208	0.641617903	1	-0.030797077	5.785735208	0.857789862	1	orange
Pomt1	-0.684795803	5.326331966	0.000139267	0.008767544	-0.622024355	5.326331966	0.001905833	0.055376124	-0.078098699	5.326331966	0.695737373	1	-0.01532704	5.326331966	0.941055719	1	orange
Tmem94	-0.750340032	5.717633305	6.41E-07	0.000126168	-0.520693163	5.717633305	0.001917023	0.055470642	-0.151577281	5.717633305	0.363975174	1	0.078069931	5.717633305	0.606083349	1	orange
Rgs2	-1.368153619	6.716138857	2.43E-13	2.13E-10	-0.881382566	6.716138857	2.55E-05	0.002099505	-0.293528646	6.716138857	0.157454974	1	0.193242679	6.716138857	0.303291411	1	orange
Ddhd1	-0.907871802	5.185387903	1.68E-07	4.06E-05	-0.596861408	5.185387903	0.002058932	0.05801538	-0.194263284	5.185387903	0.312447312	1	0.116747672	5.185387903	0.504357897	1	orange
1190005I0 6Rik	-1.212162516	2.943547153	2.26E-05	0.002049444	-0.708372127	2.943547153	0.027004465	0.259927279	-0.326316892	2.943547153	0.303375511	1	0.177476947	2.943547153	0.540323244	1	orange
Rnf125	-0.699034433	4.752253022	5.11E-05	0.003831278	-0.518689838	4.752253022	0.006961232	0.124430753	-0.128113256	4.752253022	0.50249987	1	0.052232002	4.752253022	0.762308049	1	orange
Relb	-0.816394099	4.246687777	3.25E-05	0.002595765	-0.629095578	4.246687777	0.004167352	0.09172112	-0.176151613	4.246687777	0.418611606	1	0.011148192	4.246687777	0.950938145	1	orange
Cables1	-0.855429535	4.824234624	2.25E-05	0.002049444	-0.659362366	4.824234624	0.003435665	0.079952888	-0.163010931	4.824234624	0.467183606	1	0.033057075	4.824234624	0.867739596	1	orange
9530053E0 2Rik	-0.800957506	3.728880714	0.000462225	0.020187667	-0.623642733	3.728880714	0.014657067	0.188451851	-0.113360093	3.728880714	0.655566503	1	0.063956144	3.728880714	0.779751424	1	orange
Trim68	-0.846493088	4.356160415	4.19E-06	0.000616568	-0.7007038	4.356160415	0.000651714	0.026173436	-0.129903658	4.356160415	0.52375245	1	0.015886799	4.356160415	0.928963253	1	orange
Lrig1	-0.761855022	6.467814333	4.85E-07	9.79E-05	-0.616549831	6.467814333	0.000258827	0.013106377	-0.132391053	6.467814333	0.430512583	1	0.012914386	6.467814333	0.928225212	1	orange
Vegfa	-0.769665659	8.135130387	0.00089649	0.032498532	-0.606434905	8.135130387	0.019135615	0.215233848	-0.155737437	8.135130387	0.545962954	1	0.007493397	8.135130387	0.966041164	1	orange
Ptx3	-0.991250365	6.060459833	0.000210882	0.011038524	-0.842550895	6.060459833	0.005017375	0.102287048	-0.192976622	6.060459833	0.517268343	1	-0.044276656	6.060459833	0.881625446	1	orange
Cachd1	-0.713520147	5.521571332	0.000185578	0.010600388	-0.646039488	5.521571332	0.002420298	0.063822801	-0.06779545	5.521571332	0.748921091	1	-0.000309352	5.521571332	0.995399718	1	orange
Nudt6	-0.934713041	3.819579223	2.63E-05	0.002200348	-0.808946823	3.819579223	0.001160484	0.039176151	-0.097165448	3.819579223	0.693758676	1	0.028602533	3.819579223	0.895977611	1	orange
Pag1	-0.600974832	4.356394469	0.000932637	0.033507808	-0.547765627	4.356394469	0.006715785	0.121895851	-0.030730198	4.356394469	0.880119864	1	0.02247974	4.356394469	0.89858718	1	orange
Kcnk2	-1.186145755	3.813618402	2.24E-05	0.002049444	-0.964796839	3.813618402	0.002160364	0.059552755	-0.126945548	3.813618402	0.683727598	1	0.094405349	3.813618402	0.735064539	1	orange
Irs2	-0.731877196	7.934721427	0.000194055	0.010600388	-0.613861493	7.934721427	0.005078079	0.102708014	-0.04710401	7.934721427	0.829140402	1	0.070911758	7.934721427	0.714863958	1	orange
Fgf2	-1.967073406	1.72458226	2.82E-08	8.55E-06	-1.688162756	1.72458226	2.70E-05	0.002191277	-0.11493879	1.72458226	0.766810601	1	0.163986256	1.72458226	0.662048196	1	orange
Nfkb2	-0.775090121	5.441027062	2.36E-05	0.00208639	-0.650980772	5.441027062	0.001459049	0.045721231	-0.025936197	5.441027062	0.898830457	1	0.098173493	5.441027062	0.592661751	1	orange
Fam13a	-1.53970795	7.958372205	3.20E-10	1.79E-07	-1.348329046	7.958372205	1.12E-06	0.000186296	0.003249886	7.958372205	0.990535902	1	0.194628905	7.958372205	0.425082894	1	orange
Mir3058	-3.16855069	-2.584259636	0.000449832	0.019769989	-2.519034845	-2.584259636	0.010709917	0.156648581	-0.092299168	-2.584259636	0.942856736	1	0.557563356	-2.584259636	0.826521764	1	orange
Gbp11	-2.339827976	2.164718801	2.44E-13	2.13E-10	-1.942524575	2.164718801	8.01E-08	2.15E-05	-0.038387623	2.164718801	0.914379346	1	0.358924813	2.164718801	0.277089017	1	orange
Atp1b2	-0.653103952	4.684044138	0.000514723	0.022134662	-0.572419356	4.684044138	0.006224112	0.11646666	0.010331254	4.684044138	0.961863689	1	0.091016293	4.684044138	0.629561733	1	orange
A830010M 20Rik	-0.9872205	3.183361532	3.10E-05	0.002506953	-0.863515356	3.183361532	0.001129739	0.038323378	0.028077622	3.183361532	0.917955004	1	0.151784521	3.183361532	0.529024019	1	orange
Hist2h2be	-0.769566398	3.436620329	0.000949363	0.033847699	-0.667936205	3.436620329	0.010072385	0.152123343	0.045031274	3.436620329	0.864162671	1	0.146662416	3.436620329	0.532806411	1	orange

Dock4	-0.662356839	4.647291355	0.000447862	0.019745502	-0.55515112	4.647291355	0.008171764	0.13729361	0.008208387	4.647291355	0.970416295	1	0.115414513	4.647291355	0.543171503	1	orange
Exd1	-1.069920231	2.200853998	0.000465267	0.020257227	-0.802883486	2.200853998	0.018979239	0.214478284	-0.060879905	2.200853998	0.860236216	1	0.206160376	2.200853998	0.508502382	1	orange
Rims4	-1.40854062	0.676488733	0.001466427	0.046767604	-1.030132424	0.676488733	0.038787831	0.320958397	-0.116287225	0.676488733	0.813609869	1	0.262134723	0.676488733	0.57836856	1	orange
Hps4	-0.742724705	3.939927796	0.000194927	0.010600388	-0.552577604	3.939927796	0.012825592	0.173692314	-0.061042436	3.939927796	0.783093769	1	0.129105506	3.939927796	0.521529424	1	orange
Pelt3	-1.077657623	2.120872624	0.000231242	0.011925598	-0.809764277	2.120872624	0.013913582	0.182587997	-0.091318919	2.120872624	0.783666333	1	0.176578785	2.120872624	0.550174449	1	orange
Mfsd2a	-2.253776893	5.546515477	4.37E-10	2.26E-07	-1.677373021	5.546515477	4.08E-05	0.003030799	-0.216030049	5.546515477	0.587594474	1	0.360374643	5.546515477	0.312010387	1	orange
Ano8	-0.64309615	4.514170041	0.000198398	0.010728997	-0.510776298	4.514170041	0.007866158	0.134639363	-0.041828098	4.514170041	0.828137709	1	0.090492293	4.514170041	0.602822779	1	orange
Uck1	-0.681086945	7.148670482	0.000940454	0.033702021	-0.535808578	7.148670482	0.019540618	0.217436047	-0.046849796	7.148670482	0.837917904	1	0.098428661	7.148670482	0.630409543	1	orange
Limch1	-0.855038029	4.991831987	1.31E-05	0.001451015	-0.66509173	4.991831987	0.002387796	0.063380503	-0.090044546	4.991831987	0.680178933	1	0.099902321	4.991831987	0.611489946	1	orange
Abcd4	-0.681246581	3.879952358	0.000663599	0.026727537	-0.466455381	3.879952358	0.036293998	0.307302421	-0.084861925	3.879952358	0.703314356	1	0.129930088	3.879952358	0.51927666	1	orange
Arid5b	-0.873971361	6.597068664	2.00E-06	0.000325598	-0.584417438	6.597068664	0.00438325	0.095124697	-0.121690339	6.597068664	0.55143261	1	0.167863738	6.597068664	0.362892437	1	orange
Cish	-1.666381143	5.105952965	4.95E-08	1.36E-05	-1.051346549	5.105952965	0.00220503	0.060545173	-0.296491276	5.105952965	0.38264051	1	0.318544097	5.105952965	0.296387785	1	orange
Ksr1	-0.754074578	5.026602629	0.000192678	0.010600388	-0.484759205	5.026602629	0.031402633	0.284619452	-0.088678635	5.026602629	0.693786064	1	0.180637068	5.026602629	0.374285504	1	orange
Baiap2l2	-2.056362028	1.24111884	9.08E-07	0.000169117	-1.221953815	1.24111884	0.008936901	0.144369474	-0.098304548	1.24111884	0.833076526	1	0.736103383	1.24111884	0.090266345	1	orange
Saa2	-1.966880393	-1.416332942	0.001169757	0.039584811	-0.993129409	-1.416332942	0.126399323	0.566068691	0.055198621	-1.416332942	0.965108926	1	1.028873868	-1.416332942	0.130549982	1	orange
Ric8b	-0.676624837	5.091267977	2.79E-05	0.002309255	-0.411426763	5.091267977	0.021557874	0.230170238	0.067078905	5.091267977	0.707892457	1	0.332276887	5.091267977	0.040833906	0.821143416	orange
Ptpn14	-0.826403514	6.515269748	1.04E-06	0.000191482	-0.582739245	6.515269748	0.001985467	0.056746199	0.125307591	6.515269748	0.504797626	1	0.368971824	6.515269748	0.030000411	0.712887181	orange
Srgap3	-1.18870684	4.027515467	6.24E-06	0.000383903	-0.874459071	4.027515467	0.002967646	0.072839404	0.186523078	4.027515467	0.523641702	1	0.500770548	4.027515467	0.05869212	0.962015487	orange
Ikzf2	-1.043714274	2.848292838	0.000871667	0.031974853	-0.852665512	2.848292838	0.014954656	0.190262765	0.230996288	2.848292838	0.507683258	1	0.422044881	2.848292838	0.180296973	1	orange
Cxcp1	-0.756743439	3.939873557	0.00153179	0.048435066	-0.622037117	3.939873557	0.019155386	0.215233848	0.223376777	3.939873557	0.998406219	1	0.358082675	3.939873557	0.136164871	1	orange
Klhl24	-0.598953285	6.482179126	0.000610632	0.025324032	-0.530906034	6.482179126	0.0062877	0.117169187	0.206965087	6.482179126	0.285514683	1	0.275012281	6.482179126	0.116683209	1	orange
4930480K2 3Rik	-1.177874942	1.533950808	0.000317958	0.015212199	-0.986855852	1.533950808	0.006279033	0.117163911	0.343252936	1.533950808	0.336276035	1	0.534268313	1.533950808	0.108677963	1	orange
Pak6	-1.053065514	3.660929124	9.36E-05	0.006288961	-1.054803192	3.660929124	0.000478295	0.020505074	0.36802685	3.660929124	0.217638968	1	0.366288941	3.660929124	0.177798639	1	orange
Adamts4	-0.896925654	6.62545231	0.000146053	0.008992255	-0.900201364	6.62545231	0.000676362	0.026787291	0.332560554	6.62545231	0.206039288	1	0.329284806	6.62545231	0.16419583	1	orange
Atat1	-0.72893855	4.065151302	0.000251925	0.012849992	-0.750741949	4.065151302	0.000683742	0.026994278	0.33021957	4.065151302	0.132995205	0.982421237	0.308415772	4.065151302	0.124716416	1	orange
Ank	-0.883359173	5.962246699	4.34E-06	0.000625835	-0.79138274	5.962246699	0.00022621	0.011885403	0.350338267	5.962246699	0.100667205	0.899993457	0.442314516	5.962246699	0.022014206	0.621556641	orange
Sec31b	-0.776111555	3.278482587	0.001556984	0.049009939	-0.650551622	3.278482587	0.016812913	0.20221796	0.303215752	3.278482587	0.263174561	1	0.428774446	3.278482587	0.08252675	1	orange
Ddo	-0.995802137	3.846101285	2.79E-05	0.002309255	-0.78256336	3.846101285	0.00303381	0.073997431	0.394204741	3.846101285	0.133194456	0.982854129	0.607442125	3.846101285	0.011100374	0.426205566	orange
Acss2os	-1.328292409	4.761805379	0.001246428	0.041739146	-0.977431391	4.761805379	0.034931168	0.301170882	0.50687865	4.761805379	0.270785251	1	0.857738474	4.761805379	0.036918088	0.784121507	orange
Mapk1ip1	-0.640342957	3.982250057	0.000842878	0.031413503	-0.4841445	3.982250057	0.022577382	0.235654588	0.194124437	3.982250057	0.359538088	1	0.350322385	3.982250057	0.069622855	1	orange
Coq8a	-1.267060955	5.964180488	8.33E-13	6.47E-10	-0.91947312	5.964180488	3.40E-06	0.000461389	0.285331018	5.964180488	0.146149768	0.994029995	0.632918631	5.964180488	0.000374723	0.043282012	orange
Atp1a3	-1.55669325	5.100076104	5.60E-05	0.004141367	-0.96802435	5.100076104	0.02576422	0.253075701	0.285182327	5.100076104	0.507733948	1	0.873850504	5.100076104	0.023401274	0.633191108	orange
Acaca	-1.191773412	10.79327996	7.36E-05	0.005218393	-0.764526504	10.79327996	0.023350484	0.24013713	0.349394775	10.79327996	0.297849565	1	0.776641669	10.79327996	0.00975495	0.396323192	orange
Fasn	-1.173653235	13.49489746	0.000207477	0.010942234	-0.730542661	13.49489746	0.039513809	0.324357628	0.41367731	13.49489746	0.242011976	1	0.856787881	13.49489746	0.006737913	0.313896921	orange
Grk3	-0.826176217	5.224991488	2.20E-05	0.002038088	-0.521031016	5.224991488	0.016010525	0.196785932	0.309828583	5.224991488	0.151226379	0.999246012	0.614973207	5.224991488	0.001628966	0.130093848	orange
Elovl6	-1.795651745	9.196748276	2.02E-07	4.62E-05	-0.871090394	9.196748276	0.02422061	0.244409562	0.400659823	9.196748276	0.297117934	1	1.32522108	9.196748276	0.000116593	0.016974008	orange
Rorc	-1.092135708	4.64136973	3.12E-09	1.25E-06	-0.305816063	4.64136973	0.13475673	0.578238515	-0.012166086	4.64136973	0.953257245	1	0.774152863	4.64136973	2.89E-05	0.005935889	orange
Nwl2	-1.199340609	1.362695796	0.000700548	0.02779717	-0.183713707	1.362695796	0.646506331	0.940363476	-0.069521213	1.362695796	0.860628179	1	0.946096518	1.362695796	0.008030985	0.350318033	orange
Mir23b	-5.356854426	-3.737631899	0.000846605	0.031441109	-0.291789184	-3.737631899	1	1	-1.341134155	-3.737631899	0.268212815	1	3.711698709	-3.737631899	0.142983931	1	orange
Gm15441	-0.635384134	8.64046549	0.000755903	0.029047101	-0.133836303	8.64046549	0.522939404	0.900170012	-0.155521989	8.64046549	0.457923829	1	0.346025843	8.64046549	0.067110432	1	orange
Txnip	-0.603484247	10.68356812	0.001469017	0.046767604	-0.147019919	10.68356812	0.485326767	0.885297579	-0.120215672	10.68356812	0.568287977	1	0.336248656	10.68356812	0.076810955	1	orange
Bcas1	-1.169242269	1.988719041	0.000617209	0.025521036	-0.410046502	1.988719041	0.282888522	0.755019189	-0.21161149	1.988719041	0.578663146	1	0.547584522	1.988719041	0.111663507	1	orange
Apol10b	-0.91758102	3.105428406	0.000841166	0.031413503	-0.41350359	3.105428406	0.17763197	0.6437745	-0.113467576	3.105428406	0.712522248	1	0.390610199	3.105428406	0.158188472	1	orange
Hs3st3b1	-1.11425527	3.717919476	4.24E-05	0.003277589	-0.417864594	3.717919476	0.169901385	0.633887281	-0.312839796	3.717919476	0.301353045	1	0.383551769	3.717919476	0.161727717	1	orange
Nr3c2	-0.826471534	4.166840058	0.000656256	0.026581036	-0.432018806	4.166840058	0.110571934	0.532696776	-0.144315483	4.166840058	0.592916446	1	0.250137786	4.166840058	0.304600582	1	orange
Cbed2	-0.876948798	6.376686549	1.47E-08	4.89E-06	-0.563042454	6.376686549	0.001107885	0.037950499	-0.259347705	6.376686549	0.131323708	0.978347623	0.054558938	6.376686549	0.723824983	1	brown
Gfod2	-0.890122478	3.531486466	3.73E-05	0.002929871	-0.519433384	3.531486466	0.031705081	0.28624691	-0.363413001	3.531486466	0.128788783	0.972421414	0.007278722	3.531486466	0.970986703	1	brown
Igflbp5	-1.186385781	9.79314182	2.63E-09	1.08E-06	-0.650161238	9.79314182	0.00349947	0.080707258	-0.475878603	9.79314182	0.032208086	0.605841474	0.060345981	9.79314182	0.758211702	1	brown
If47	-0.907076909	4.48636319	0.000387169	0.017683244	-0.541413007	4.48636319	0.058292313	0.395098623	-0.327830536	4.48636319	0.249732387	1	0.037834621	4.48636319	0.876888272	1	brown
4930412C1 8Rik	-1.19174569	1.641816586	0.000191064	0.010600388	-0.550193511	1.641816586	0.127164823	0.56726957	-0.427017292	1.641816586	0.227348405	1	0.214543233	1.641816586	0.513440503	1	brown
Arntl	-1.079691075	4.275934798	4.14E-08	1.16E-05	-0.396121068	4.275934798	0.071914915	0.438517827	-0.48265821	4.275934798	0.0271641	0.555043565	0.200913114	4.275934798	0.313881051	1	brown
Gm13889	-1.050130392	3.827244875	3.23E-06	0.000494542	-0.399710891	3.827244875	0.113015133	0.537179221	-0.44283191	3.827244875	0.077150487	0.822467745	0.207589256	3.827244875	0.363361461	1	brown
Syt3	-1.293319154	1.775560341	0.00012627	0.008246505	-0.375977053	1.775560341	0.325577308	0.790959397	-0.519541059	1.775560341	0.164764407	1	0.397806559	1.775560341	0.251529595	1	brown
St3gal4	-0.723861926	5.185874374	3.99E-05	0.003118561	-0.204345674	5.185874374	0.297921557	0.768645316	-0.32465847	5.185874374	0.096791387	0.888392991	0.194858196	5.185874374	0.271679922	1	brown
Nmnat3	-0.740014638	4.069389513	0.00011416	0.007561636	-0.237687452	4.069389513	0.267371532	0.740071375	-0.37944152	4.069389513	0.074402062	0.812856567	0.122886899	4.069389513	0.525452618	1	brown
Thbs1	-0.938095728	9.077791328	0.000385978	0.017683244	-0.339592636	9.077791328	0.249474598	0.725182207	-0.487388616	9.077791328	0.098700054	0.892836214	0.111114527	9.077791328	0.669530024	1	brown
Syt2	-1.093555014	3.366107839	3.48E-05	0.002747378	-0.435677103	3.366107839	0.141693638	0.591573599	-0.600601934	3.366107839	0.041483254	0.666634647	0.05727959	3.366107839	0.825883027	1	brown
B230311B0 6Rik	-1.480562403	0.007987519	0.001164085	0.03948849	-0.54706989	0.007987519	0.3120534	0.781307473	-0.905979401	0.007987519	0.074204339	0.812758499	0.027569295	0.007987519	0.954187463	1	brown
5930412G1 2Rik	-1.079093155	2.115294763	0.00157661	0.049405162	-0.137252637	2.115294763	0.730222383	0.965045279	-0.729335856	2.115294763	0.056923112	0.746059679	0.212511888	2.115294763	0.537098694	1	brown
Adm	-0.602958972	4.535425075	0.0008515	0.031441109	-0.06014219	4.535425075	0.769959996	0.970758052	-0.406828338	4.535425075	0.042960496	0.67446002	0.13673472	4.535425075	0.451820893	1	brown
Pinc	-3.779720452	-0.621354285	3.40E-11	2.16E-08	0.114486002	-0.621354285	0.913063154	0.998835231	-2.105816956	-0.621354285	0.000427209	0.046381842	1.78833287	-0.621354285	0.003822536	0.227921322	brown
Lalba	-2.406830958	1.547101455	2.44E-06	0.000387896	0.146349243	1.547101455	0.807408079	0.976199887	-1.78229871	1.547101455	0.002047022	0.1339501	1.778936862	1.547101455	0.129625448	1	brown
Cyf2rb	-0.660679812	6.146721353	0.000162011	0.009676361	-0.064793711	6.146721353	0.739855222	0.965045279	-0.528169704	6.146721353	0.006725622	0.271668487	0.067716766	6.146721353	0.697667492	1	brown
Syt15	-1.010601828	3.129374267	0.000234394	0.011999621	-0.115079498	3.129374267	0.712545852	0.96143872	-0.806900948	3.129374267	0.008764152	0.314351894	0.088625839	3.129374267	0.748488668	1	brown
Cyf2rb2	-0.765084399	5.224045738	0.000182095	0.010516358	-0.105660306	5.224045738	0.643597857	0.939498978	-0.630786602	5.224045738	0.005654473	0.245803133	0.028638372	5.224045738	0.884697152	1	brown
Slc27a6	-1.358890382	1.433418997	0.000549509	0.023202217	-0.17677737	1.433418997	0.707706299	0.961245088	-1.166418299	1.433418997	0.008686781	0.313711747	0.014816671	1.433418997	0.969073959	1	brown
Cd12	-1.784654553	1.484999424	1.50E-05	0.001552812	-0.547177108	1.484999424	0.244105302	0.72206739	-1.416239155	1.484999424	0.002449944	0.150199913	-0.178728951	1.484999424	0.701319014	1	brown
Thbd	-0.7601640l4	7.0946841	6.90E-06	0.000909632	-0.356514234	7.0946841	0.058139294	0.394416599	-0.477942316	7.0946841	0.011006671	0.36012661	-0.07429228	7.0946841	0.671687527	1	brown
Gulp1	-0.693209495	5.300684157	0.000468597	0.020338865	-0.289380863	5.300684157	0.190446542	0.662262313	-0.432560812	5.300684157	0.049578534	0.708496518	-0.028731432	5.300684157	0.895550957	1	brown
St3gal2	-0.775471428	5.839737123	1.96E-05	0.001877839	-0.369797648	5.839737123	0.667729607	0.425586838	-0.454182424	5.839737123	0.024604637	0.530027096	-0.048508067	5.839737123	0.800518131	1	brown
Socs2	-0.744589848	4.639219076	0.000520703	0.02225488	-0.370272948	4.639219076	0.122610075	0.558129292	-0.442845143	4.639219076	0.063507205	0.77496143	-0.068526908	4.639219076	0.76417	1	brown
Sirpa	-0.663243408	5.603544865	0.000270675	0.013510561	-0.410020942	5.603544865	0.04333841	0.342395489	-0.383256639	5.603544865	0.058154529	0.752562678	-0.130033482	5.603544865	0.489671669	1	brown
Ccl2	-1.146075039	4.930533346	0.000401585	0.018105014	-0.740736974	4.930533346	0.041849886	0.333954643	-0.565787634	4.930533346	0.118464988	0.945142756	-0.160447853	4.930533346	0.641073107	1	brown
Irf4	-2.100292277	7.110242922	9.46E-18	1.65E-14	-1.292260503	7.110242922	2.58E-06	0.000371945	-1.174709012	7.110242922	1.76E-05	0.004740051	-0.366676385	7.110242922	0.145046191	1	brown
Ccl7	-1.166443973	4.115208665	0.0007741	0.029389871	-0.77422615	4.115208665	0.047768307	0.35887623	-0.724589178	4.115208665	0.062629173	0.771874186	-0.33236739	4.115208665	0.363249911	1	brown
Lrrn4	-1.171232299	1.288872807	0.000785993	0.029609255	-0.803208939	1.288872807	0.044070101	0.34505531	-0.722936643	1.288872807	0.062332302	0.771874186	-0.354884027	1.288872807	0.347255967	1	brown
Oasl1	-1.538990009	3.503562359	7.18E-06	0.000937525	-0.95782578	3.503562359	0.013679472	0.181217344	-0.968048365	3.503562359	0.01192471	0.377938143	-0.386876111	3.503562359	0.28591526	1	brown
Serpina3k	-1.711192255	1.834559805	0.000947665	0.033847699	-0.853619147	1.834559805	0.147813486	0.599715571	-1.262928592	1.834559805	0.031493577	0.601303591	-0.405325904	1.834559805	0.468508762	1	brown
Cmah	-0.916512518	4.532624702	0.000547584	0.023191222	-0.659795671	4.532624702	0.026791121	0.258764824	-0.659797635	4.532624702	0.02613458	0.545191024	-0.403077988	4.532624702	0.14505402	1	brown
Gfra2	-0.969219797	4.35697012	0.000607513	0.02526965	-0.581251076	4.35697012	0.067622031	0.425139681	-0.895559606	4.35697012	0.004803894	0.22454591	-0.50758702	4.35697012	0.08610077	1	brown
Plppr3	-0.658924494	5.776090002	0.000708409	0.027861808	-0.397779682	5.776090002	0.06704582	0.423295188	-0.646895854	5.776090002	0.002862037	0.167363302	-0.385750024	5.776090002	0.054778411	0.935725048	brown
Prtn3	-1.229556262	3.266739602	0.004647458	0.103924598	-1.498038236	3.266739602	0.00293653	0.072510512	-1.427950644	3.266739602	0.004012422	0.203122991	-1.696407338	3.266739602	0.000403459	0.045109948	brown
AW551984	-1.325991072	2.795901179	0.000304455	0.014877857	-1.150536094	2.795901179	0.006065999	0.114410803	-0.766556244	2.795901179	0.061983359	0.770026154	-0.591087076	2.795901179	0.129375903	1	brown
Npas2	-1.180750654	3.382433944	7.48E-06	0.000958492	-0.976668064	3.382433944	0.00111745	0.038091405	-0.686195612	3.382433944	0.019635571	0.4711954	-0.482105252	3.382433944	0.084382815	1	brown
Rgs16	-0.750053033	5.931507322	0.000648627	0.02642919	-0.625033593	5.931507322	0.011041753	0.159557034	-0.399158122	5.931507322	0.10311584	0.906449992	-0.274137936	5.931507322	0.228191508	1	brown
Spon2	-1.067539922	5.633705632	8.51E-06	0.001052705	-1.006766958	5.633705632	0.00019468	0.010612473	-0.566593224	5.633705632	0.034293237	0.618332787	-0.505818717	5.633705632	0.042565846	0.848645178	brown
Xbp1	-0.726099028	7.979722648	3.13E-05	0.002511027	-0.701235871	7.979722648	0.00031655	0.015255525	-0.368470325	7.979722648	0.057389369	0.746809887	-0.343606975	7.979722648	0.055314319	0.938195297	brown
Sh3pxd2a	-0.928687941	8.975523899	2.41E-06	0.000387303	-0.994503087	8.975523899	6.95E-06	0.000777344	-0.421996466	8.975523899	0.054446206	0.732627562	-0.487811477	8.975523899	0.016521909	0.5236059	brown
Ifnb1	-3.071606689	-1.527334171	8.26E-06	0.001039402	-7.258851241	-1.527334171	4.39E-06	0.000557251	-1.247289436	-1.527334171	0.090931535	0.868666527	-5.404518287	-1.527334171	0.006205708	0.304425461	brown
Cpne2	-0.747600655	4.929698354	0.000125839	0.008246505	-0.863377072	4.929698354	7.97E-05	0.00525301 8	-0.27725628	4.929698354	0.199892667	1	-0.393031003	4.929698354	0.051696626	0.908820182	brown
Srgap1	-0.610841366	4.179620075	0.001458315	0.046639376	-0.648661985	4.179620075	0.002508518	0.065408669	-0.204801376	4.179620075	0.335493211	1	-0.242620037	4.179620075	0.22271874	1	brown
Ccl4	-1.352197344	3.364187985	0.00021204	0.011057752	-1.30880937	3.364187985	0.00168867	0.050863891	-0.50466182	3.364187985	0.216086788	1	-0.461265646	3.364187985	0.234612722	1	brown

Steap3	-0.714855145	5.591406783	0.00026733	0.013431649	-0.707020602	5.591406783	0.001261057	0.041178814	-0.246755999	5.591406783	0.257285505	1	-0.238920645	5.591406783	0.237825693	1	brown
Ifit1	-0.92665295	4.690128965	0.00023239	0.011940767	-0.742434113	4.690128965	0.008520827	0.139609704	-0.306543198	4.690128965	0.274427976	1	-0.122322866	4.690128965	0.644656832	1	brown
Nfil3	-1.073431605	6.030533908	1.21E-06	0.000214098	-0.745334308	6.030533908	0.002626105	0.066975252	-0.4185298	6.030533908	0.089249272	0.862619516	-0.090431852	6.030533908	0.697041443	1	brown
Hcar1	-1.447263243	6.241284203	6.74E-08	1.78E-05	-1.253715092	6.241284203	3.54E-05	0.002704425	-0.522346845	6.241284203	0.080603316	0.836876692	-0.328797689	6.241284203	0.237506264	1	brown
Itsn1	-0.685848329	6.186717131	1.49E-05	0.001552812	-0.635899845	6.186717131	0.000319468	0.015291874	-0.236749847	6.186717131	0.177867819	1	-0.186800887	6.186717131	0.251257589	1	brown
Ar	-0.681372312	5.438873059	1.01E-05	0.00119424	-0.634293607	5.438873059	0.000230069	0.011978651	-0.214662095	5.438873059	0.209138044	1	-0.167582633	5.438873059	0.291831121	1	brown
Stxbp4	-1.569199961	2.58840176	1.08E-05	0.001241955	-1.332551615	2.58840176	0.001040539	0.036520641	-0.515770219	2.58840176	0.19320776	1	-0.27910906	2.58840176	0.470993048	1	brown
Hs1bp3	-0.627857654	4.310634719	0.000706855	0.027861808	-0.554929881	4.310634719	0.007308238	0.129291059	-0.187438452	4.310634719	0.36184946	1	-0.114509296	4.310634719	0.554116198	1	brown
Tppp	-1.289660716	4.968984562	3.83E-13	3.15E-10	-1.117828387	4.968984562	2.44E-08	7.75E-06	-0.394127706	4.968984562	0.045386546	0.682801253	-0.222293489	4.968984562	0.229103371	1	brown
Prkag2	-0.693271643	5.540929019	0.000127109	0.00826265	-0.61430589	5.540929019	0.002334895	0.062394835	-0.17170932	5.540929019	0.392113901	1	-0.092742976	5.540929019	0.621656682	1	brown
Irs1	-0.893616105	7.008049318	4.31E-05	0.003313484	-0.788231516	7.008049318	0.001275807	0.041466688	-0.22404485	7.008049318	0.356857609	1	-0.118659983	7.008049318	0.601753316	1	brown
Ldb2	-0.588982462	4.663370782	0.000984892	0.034677726	-0.57843796	4.663370782	0.003685805	0.083541409	-0.134756982	4.663370782	0.49662308	1	-0.12421146	4.663370782	0.502490331	1	brown
Tmprss13	-0.769389372	4.793743504	8.88E-06	0.001088992	-0.776907645	4.793743504	6.12E-05	0.004253036	-0.15540596	4.793743504	0.418585308	1	-0.162923008	4.793743504	0.365036935	1	brown
Pm20d2	-1.067521454	3.424284715	8.87E-05	0.006018955	-1.088134476	3.424284715	0.000419775	0.018565751	-0.290938705	3.424284715	0.336018275	1	-0.311546411	3.424284715	0.276599854	1	brown
Slc5a3	-0.85470978	6.025793453	0.001390726	0.044992576	-1.064137225	6.025793453	0.0004124	0.018344482	-0.100016143	6.025793453	0.737102562	1	-0.309442877	6.025793453	0.265016864	1	cyan
Steap4	-0.98020291	8.463136341	4.03E-05	0.003127965	-1.224233411	8.463136341	5.66E-06	0.000666561	-0.097654758	8.463136341	0.713345855	1	-0.341685106	8.463136341	0.166336685	1	cyan
C1rl	-0.701894005	3.831040096	0.001497751	0.047466141	-0.911008998	3.831040096	0.000238387	0.012248862	-0.045592393	3.831040096	0.854070591	1	-0.254704832	3.831040096	0.268550729	1	cyan
Napepld	-0.689647641	4.108989061	0.004569007	0.102934021	-0.903479077	4.108989061	0.000927863	0.033858505	-0.029149521	4.108989061	0.915503885	1	-0.242978938	4.108989061	0.337392313	1	cyan
Cxcl1	-0.695566726	7.314174234	0.005153359	0.111147144	-0.891173086	7.314174234	0.001402418	0.044177329	-0.098027037	7.314174234	0.723264629	1	-0.293633147	7.314174234	0.253846977	1	cyan
Igf1	-0.792079007	7.61866596	0.000439871	0.019578451	-1.039974681	7.61866596	4.07E-05	0.003030799	-0.189786263	7.61866596	0.449097309	1	-0.437681656	7.61866596	0.0603209886	0.967905971	cyan
Ablim2	-0.899128332	2.909407527	0.000866881	0.031882973	-1.249352103	2.909407527	4.86E-05	0.003482824	-0.186927013	2.909407527	0.533316112	1	-0.537141701	2.909407527	0.059928007	0.965078208	cyan
Myb	-1.081372451	4.505107257	0.001334589	0.044095063	-1.689211727	4.505107257	1.26E-05	0.001218188	-0.09944833	4.505107257	0.79233637	1	-0.707283491	4.505107257	0.0463687	0.874164634	cyan
Cpeb1	-0.595856867	3.696546683	0.013842137	0.204558206	-0.890064306	3.696546683	0.001042626	0.036520641	-0.024093847	3.696546683	0.930364028	1	-0.31829844	3.696546683	0.206397971	1	cyan
Blcap	-0.460882163	6.310896759	0.012486022	0.194198129	-0.703317464	6.310896759	0.000611856	0.02500553	-0.003777466	6.310896759	0.98574302	1	-0.247012424	6.310896759	0.191577342	1	cyan
Slc22a3	-0.856556664	4.97860417	0.000783645	0.02960062	-1.456784132	4.97860417	5.03E-07	0.000100426	0.033254399	4.97860417	0.907578309	1	-0.566970944	4.97860417	0.033039931	0.743584658	cyan
Zfp185	-0.519034598	4.879988551	0.005930152	0.122872372	-0.945390314	4.879988551	7.53E-06	0.000822444	0.096588203	4.879988551	0.644937543	1	-0.329766391	4.879988551	0.090272529	1	cyan
Plag1	-0.480832983	5.290763887	0.009330698	0.161096467	-0.936840254	5.290763887	5.95E-06	0.000676573	0.110880706	5.290763887	0.588777462	1	-0.345125734	5.290763887	0.070151365	1	cyan
Mmab	-0.414635348	4.691837278	0.070155955	0.505697475	-0.835757175	4.691837278	0.001093042	0.037626495	0.110080512	4.691837278	0.665458281	1	-0.311040239	4.691837278	0.188406408	1	cyan
Khdc7a	-0.486855235	7.438230923	0.051679744	0.434844135	-0.925504453	7.438230923	0.000975529	0.035139157	0.135381978	7.438230923	0.626749124	1	-0.303267071	7.438230923	0.241033178	1	cyan
Mvk	-0.444462441	4.0881636	0.062770875	0.476871702	-0.87403115	4.0881636	0.001069075	0.037167654	0.130764125	4.0881636	0.622220714	1	-0.298802956	4.0881636	0.227181462	1	cyan
Adamts9	-0.273743096	6.166977706	0.093174801	0.566424978	-0.634801923	6.166977706	0.000454845	0.019705984	0.140061733	6.166977706	0.437164417	1	-0.220996862	6.166977706	0.185122249	1	cyan
Morc4	-0.468269168	4.79024127	0.007957546	0.146335078	-0.90627809	4.79024127	4.19E-06	0.000551793	0.170827692	4.79024127	0.380830065	1	-0.267180304	4.79024127	0.141500045	1	cyan
Unc5a	-0.741390854	5.31849252	2.96E-05	0.002413018	-1.370024308	5.31849252	8.51E-12	7.00E-09	0.208559228	5.31849252	0.288765335	1	-0.42007304	5.31849252	0.02227448	0.625116719	cyan
Glrp10	-1.455988444	2.739788442	1.58E-05	0.00159568	-2.464349597	2.739788442	6.57E-10	3.40E-07	0.206445424	2.739788442	0.580622763	1	-0.801895326	2.739788442	0.028228187	0.693510036	cyan
Trhde	-0.831276187	3.238662089	0.009725255	0.166241583	-1.39469895	3.238662089	0.000140771	0.008231871	0.085843861	3.238662089	0.812026861	1	-0.477572807	3.238662089	0.15748689	1	cyan
Cxcl10	-0.972231431	6.784214391	0.000826309	0.030961122	-1.445075983	6.784214391	1.25E-05	0.001218188	0.072929339	6.784214391	0.822218675	1	-0.399914697	6.784214391	0.186263116	1	cyan
Trmt1l	-0.387986321	4.831765766	0.020596316	0.26116258	-0.588865899	4.831765766	0.001564911	0.047858975	0.037060805	4.831765766	0.842209868	1	-0.163818109	4.831765766	0.342415458	1	cyan
Kctd21	-0.884295587	3.768831629	5.68E-05	0.004176837	-1.18319229	3.768831629	1.87E-06	0.000280613	0.01824103	3.768831629	0.942066619	1	-0.280652452	3.768831629	0.223417505	1	cyan
Fbxo45	-0.604443956	5.179256774	0.000154911	0.009413199	-0.777381297	5.179256774	1.29E-05	0.001236006	0.024084917	5.179256774	0.893132047	1	-0.148851742	5.179256774	0.36629954	1	cyan
Rasl2	-0.708746003	4.588594603	0.000392265	0.017799662	-1.181337799	4.588594603	3.29E-06	0.000454905	0.073443451	4.588594603	0.770314848	1	-0.309146594	4.588594603	0.186313018	1	cyan
B3galt2	-0.800525268	7.662657083	0.001793894	0.053917134	-1.165267264	7.662657083	5.64E-05	0.003957778	0.094593976	7.662657083	0.740479087	1	-0.270147829	7.662657083	0.309226141	1	cyan
Dach1	-0.593835747	3.776833438	0.014450198	0.208847955	-0.890469287	3.776833438	0.001062035	0.037014951	0.09489692	3.776833438	0.725663123	1	-0.201734669	3.776833438	0.427122317	1	cyan
Gm4951	-1.19933001	4.255873887	2.40E-05	0.002094958	-1.816492593	4.255873887	2.56E-08	7.94E-06	0.170126582	4.255873887	0.590318072	1	-0.447032208	4.255873887	0.133708432	1	cyan
Nrip1	-0.417638331	6.860399972	0.027077055	0.304203315	-0.693561878	6.860399972	0.000984194	0.035360149	0.11173377	6.860399972	0.593988185	1	-0.16418962	6.860399972	0.397968658	1	cyan
Zeb2	-0.39119775	7.524327573	0.031808906	0.332258053	-0.688665919	7.524327573	0.000687778	0.027077124	0.13090387	7.524327573	0.51688983	1	-0.166564206	7.524327573	0.373004299	1	cyan
Micall3	-0.381414261	6.660872102	0.029057353	0.315299357	-0.62886189	6.660872102	0.001214068	0.039899767	0.112929864	6.660872102	0.55967211	1	-0.134517615	6.660872102	0.453562474	1	cyan
Hykk	-0.691081454	2.852855754	0.007289384	0.139365844	-1.128727582	2.852855754	9.97E-05	0.0063217	0.176653105	2.852855754	0.535434937	1	-0.260988425	2.852855754	0.338171048	1	cyan
Aox1	-0.423592662	5.745520266	0.017585432	0.235415709	-0.664689926	5.745520266	0.000811029	0.03055241	0.138186081	5.745520266	0.484403045	1	-0.102910922	5.745520266	0.576513047	1	cyan
Srf	-0.393516748	6.545497507	0.020792783	0.262058515	-0.635114838	6.545497507	0.000792533	0.030166529	0.13204412	6.545497507	0.483812772	1	-0.109553824	6.545497507	0.531705103	1	cyan
Nlrx1	-0.3949552	4.281665259	0.038562158	-0.673841196	4.281665259	0.00162392	0.049231911	0.148618723	4.281665259	0.485186073	1	-0.130266519	4.281665259	0.514033116	1	cyan
Caprin2	-0.481927541	3.063085597	0.070147804	0.505697475	-0.976082713	3.063085597	0.00107643	0.037238092	0.280346225	3.063085597	0.342356995	1	-0.21380648	3.063085597	0.447459802	1	cyan
Tra2a	-0.341099415	5.799573537	0.044852114	0.409116592	-0.662574034	5.799573537	0.000945553	0.019705984	0.189754755	5.799573537	0.331123762	1	-0.131719645	5.799573537	0.451352548	1	cyan
Ccr10	-0.794372408	0.491421989	0.025769337	0.296349735	-1.453367311	0.491421989	0.000342293	0.016220179	0.379749328	0.491421989	0.325355758	1	-0.279219087	0.491421989	0.497471154	1	cyan
Hoxc6	-0.535512876	4.222381912	0.008668573	0.154727945	-0.997856049	4.222381912	1.19E-05	0.00118296	0.293120227	4.222381912	0.193279118	1	-0.169221924	4.222381912	0.423619053	1	cyan
Efna5	-0.350053342	4.247581332	0.074183331	0.516585071	-0.822767434	4.247581332	0.00015811	0.008874495	0.420997265	4.247581332	0.051687895	0.715274536	-0.051716688	4.247581332	0.804977708	1	cyan
Hsph1	-0.594796213	5.788931896	0.005477559	0.116521108	-1.409570039	5.788931896	5.75E-09	2.17E-06	0.616771004	5.788931896	0.009600531	0.331452611	-0.198002484	5.788931896	0.371143888	1	cyan
Glb2	-0.252387193	6.511745738	0.219731189	0.765683478	-0.811516183	6.511745738	0.000406546	0.018211169	0.405528091	6.511745738	0.076590748	0.817704713	-0.153600831	6.511745738	0.468811914	1	cyan
Gnptab	-0.166833277	6.362024217	0.342785305	0.863177667	-0.629942984	6.362024217	0.001272972	0.041466688	0.308796061	6.362024217	0.113012421	0.928722145	-0.15431358	6.362024217	0.392406849	1	cyan
Slc16a5	-1.486137879	1.54565587	0.001199939	0.040508089	-3.482932024	1.54565587	6.52E-10	3.40E-07	1.123691881	1.54565587	0.02676784	0.550157848	-0.873037136	1.54565587	0.095203645	1	cyan
Abcd2	-0.415574495	8.321498391	0.095176744	0.573017654	-0.992500237	8.321498391	0.000386998	0.01756068	0.351866968	8.321498391	0.20449533	1	-0.225058718	8.321498391	0.38245824	1	cyan
Unc119	-0.361841735	4.957295904	0.10166579	0.589718853	-0.900508656	4.957295904	0.000265712	0.013358216	0.291600837	4.957295904	0.233911128	1	-0.247065491	4.957295904	0.278529153	1	cyan
Smtb1	-0.31524821	5.417668277	0.143913981	0.671342389	-0.834471794	5.417668277	0.000529365	0.022342528	0.303552768	5.417668277	0.204483113	1	-0.215670478	5.417668277	0.332082937	1	cyan
Prpla3	-0.52822955	7.752685298	0.105540189	0.596453572	-1.397060944	7.752685298	0.000169038	0.009412245	0.472810676	7.752685298	0.195612	1	-0.396020563	7.752685298	0.245044588	1	cyan
Cldn8	-0.623107851	4.409060495	0.001362703	0.044602187	-1.747477339	4.409060495	2.89E-15	6.72E-12	0.611813284	4.409060495	0.004435937	0.212317292	-0.512553981	4.409060495	0.011522321	0.434398616	cyan
Mknk2	-0.300444678	9.444750595	0.149580381	0.679962827	-0.793982865	9.444750595	0.000649788	0.026171275	0.26543824	9.444750595	0.251658519	1	-0.228099925	9.444750595	0.287325899	1	cyan
Zfp467	-0.225657879	4.804509838	0.200456576	0.749423702	-0.634761966	4.804509838	0.001173604	0.03946393	0.192151907	4.804509838	0.323539266	1	-0.216951685	4.804509838	0.230103595	1	cyan
Dmpk	-0.320257592	6.248253207	0.156726734	0.691243258	-0.934233098	6.248253207	0.000225406	0.011885403	0.274709684	6.248253207	0.274192651	1	-0.339265513	6.248253207	0.145675073	1	cyan
Sfpq	-0.145487549	7.339392446	0.396338437	0.890020106	-0.601773024	7.339392446	0.00162285	0.049231911	0.24609341	7.339392446	0.196020637	1	-0.210192006	7.339392446	0.232019705	1	cyan
Serpina1c	-0.657646668	-0.623565762	0.226986649	0.771865062	-2.754000115	-0.623565762	2.05E-05	0.001179052	0.832636612	-0.623565762	0.146671622	0.994029995	-1.263475074	-0.623565762	0.044160047	0.858387787	cyan
Cdsn	-0.207113514	5.68933344	0.493575452	0.930813487	-1.140083378	5.68933344	0.000917081	0.033818261	0.42939961	5.68933344	0.206777794	1	-0.503569702	5.68933344	0.112598815	1	cyan
Esrrb	-0.193399859	2.921335333	0.772291005	0.981189896	-2.826909521	2.921335333	6.79E-05	0.00463165	1.054094794	2.921335333	0.114294559	0.933150299	-1.579394136	2.921335333	0.014911044	0.498843884	cyan
Mir6392	-0.154735294	0.165952071	0.743352995	0.982603121	-2.633240362	0.165952071	3.88E-06	0.000516465	0.851586438	0.165952071	0.100893369	0.900794776	-1.626776479	0.165952071	0.002654037	0.179192371	cyan
Parp3	-0.304925167	6.160294502	0.147054715	0.676064703	-0.892558446	6.160294502	0.000147819	0.00848783	0.093731302	6.160294502	0.688062046	1	-0.49390146	6.160294502	0.022859698	0.628715895	cyan
Dclk1	-0.458693167	4.596638046	0.048687307	0.424752689	-1.36325766	4.596638046	2.31E-07	5.22E-05	0.037738425	4.596638046	0.88519321	1	-0.86682296	4.596638046	0.000383748	0.043575463	cyan
Slc2a13	-0.438509626	4.151513304	0.140038009	0.664574266	-1.143671529	4.151513304	0.000666053	0.026520674	-0.023926832	4.151513304	0.943274952	1	-0.728995214	4.151513304	0.019378008	0.570162176	cyan
Tshr	-0.626089173	6.302974488	0.014040854	0.204766082	-1.403974445	6.302974488	1.21E-06	0.000199416	-0.087710223	6.302974488	0.753716164	1	-0.865594425	6.302974488	0.00119644	0.103859953	cyan
Rbm14	-0.27321298	4.903956848	0.093074536	0.566061668	-0.66109674	4.903956848	0.000258644	0.013106377	0.025418606	4.903956848	0.88895805	1	-0.362464215	4.903956848	0.030071027	0.712887181	cyan
Slc18b1	-0.376743982	5.021003054	0.084030241	0.539791925	-0.837792284	5.021003054	0.000587619	0.024297523	0.050283777	5.021003054	0.835903501	1	-0.41076463	5.021003054	0.068020809	1	cyan
Hoxc8	-0.362211326	5.367955282	0.072616115	0.514592937	-0.722971049	5.367955282	0.00130796	0.042008616	0.042540306	5.367955282	0.849935504	1	-0.318218744	5.367955282	0.125257652	1	cyan
Rgs7bp	-0.580934416	2.884841897	0.063907776	0.480977428	-1.14275987	2.884841897	0.001299105	0.041910457	0.013903506	2.884841897	0.971363358	1	-0.547914721	2.884841897	0.096051431	1	cyan
Apcdd1	-0.572878611	6.703558939	0.010105312	0.170982853	-0.987020744	6.703558939	7.74E-05	0.005150196	-0.092343113	6.703558939	0.708787753	1	-0.507075757	6.703558939	0.027599856	0.687550018	cyan
Ephb2	-0.848049728	3.907302519	0.003835427	0.091944986	-1.30296513	3.907302519	9.35E-05	0.006022318	-0.184057221	3.907302519	0.573266335	1	-0.638967633	3.907302519	0.038091425	0.794575765	cyan
Lhfpl2	-0.455209617	5.996942478	0.022659267	0.274106207	-0.760012461	5.996942478	0.000655449	0.02624802	-0.102083196	5.996942478	0.645098129	1	-0.40688542	5.996942478	0.048034353	0.884490277	cyan
Fam20c	-0.703526453	3.348807939	0.002533336	0.068883094	-1.177484616	3.348807939	8.67E-06	0.000903978	-0.196383971	3.348807939	0.447534292	1	-0.670335135	3.348807939	0.006366786	0.30702712	cyan
Rtp4	-0.405201454	5.296288953	0.025961753	0.296924269	-0.65815673	5.296288953	0.001174656	0.03946393	-0.120904335	5.296288953	0.549439109	1	-0.373858691	5.296288953	0.045947244	0.874164634	cyan
Idh1	-0.707270376	7.961231696	0.00648504	0.130597857	-0.998953804	7.961231696	0.000629716	0.025509877	-0.270982396	7.961231696	0.349271244	1	-0.56266557	7.961231696	0.037085312	0.784121507	cyan
Dtx2	-0.758039033	5.2408423	1.85E-05	0.001783651	-0.859080346	5.2408423	1.55E-05	0.00143999	-0.402513517	5.2408423	0.040570113	0.661619478	-0.50355318	5.2408423	0.006092689	0.303004374	cyan
Phkg1	-1.090425922	3.472813964	0.005703442	0.120409828	-1.485369435	3.472813964	0.001061267	0.037014951	-0.690571382	3.472813964	0.118822329	0.946501935	-1.085502413	3.472813964	0.010487921	0.406036508	cyan
Trabd2b	-0.875841622	6.195963414	0.002821159	0.075245257	-1.51644741	6.195963414	5.82E-06	0.000676573	-0.347292674	6.195963414	0.288699196	1	-0.98788693	6.195963414	0.001420434	0.117467379	cyan
Cmklr1	-0.560996948	6.852962702	0.009187507	0.159707212	-1.113054462	6.852962702	4.36E-06	0.000557251	-0.167604346	6.852962702	0.483546366	1	-0.719661265	6.852962702	0.001312615	0.112546638	cyan
Igfals	-0.889737669	4.903258112	0.00497586	0.108919069	-1.672152154	4.903258112	4.25E-06	0.000555396	-0.315090071	4.903258112	0.379131157	1	-1.097500347	4.903258112	0.001123865	0.100686796	cyan
Ffar2	-0.598681365	4.829452698	0.00683179	0.134860315	-1.081708478	4.829452698	1.48E-05	0.001392839	-0.343799145	4.829452698	0.162115973	1	-0.826823375	4.829452698	0.000363376	0.042950711	cyan

Mcam	-0.539167949	7.890879587	0.009032817	0.15819881	-1.013276253	7.890879587	1.23E-05	0.001210891	-0.324702596	7.890879587	0.157181396	1	-0.798810576	7.890879587	0.000203759	0.027121311	cyan
Tenm4	-0.728837038	7.430054636	0.03912539	0.380791405	-1.425073817	7.430054636	0.00040506	0.018211169	-0.35241304	7.430054636	0.372965583	1	-1.048649178	7.430054636	0.00516908	0.273341102	cyan
Serpina3c	-0.470897679	6.650315254	0.117680028	0.622755045	-1.078277209	6.650315254	0.001505391	0.046381353	-0.155172946	6.650315254	0.644116596	1	-0.762551795	6.650315254	0.015625393	0.50904544	cyan
Peg10	-0.267730781	3.893054777	0.181524208	0.728300217	-0.749934482	3.893054777	0.000834931	0.0312612	-0.088436756	3.893054777	0.691626232	1	-0.570637466	3.893054777	0.006113855	0.303004374	cyan
Irs3	-0.127886354	4.635216326	0.60530965	0.96149007	-1.413725178	4.635216326	5.87E-07	0.000112399	0.239865418	4.635216326	0.386876573	1	-1.045970459	4.635216326	7.05E-05	0.011330343	cyan
Serpina3n	-0.131557939	7.68672432	0.670560717	0.973876581	-1.182494955	7.68672432	0.000925469	0.033858505	-0.064745436	7.68672432	0.8541904B3	1	-1.11568205	7.68672432	0.000855734	0.080319634	cyan
Sgms2	-0.06643689	5.783369542	0.782762078	0.987952495	-0.936190191	5.783369542	0.000757848	0.029147023	-0.001496532	5.783369542	0.996484398	1	-0.871248786	5.783369542	0.000774757	0.076253534	cyan
Sncg	0.281533027	7.679267496	0.357849641	0.873590669	-1.023945657	7.679267496	0.002025407	0.057301809	0.089752657	7.679267496	0.784695865	1	-1.215725689	7.679267496	0.000102628	0.015258823	cyan
Pyr32	1.064190869	0.929111753	0.079406966	0.529953489	-1.084198716	0.929111753	0.112426707	0.536821202	-0.460636174	0.929111753	0.479905519	1	-2.608917261	0.929111753	6.54E-05	0.010630753	firebrick1
Timp1	0.423590599	3.274513317	0.260756957	0.805555578	-0.47982719	3.274513317	0.240395382	0.720200554	-0.546804817	3.274513317	0.177135114	1	-1.450212445	3.274513317	0.000193009	0.025937381	firebrick1
Fam83e	0.356579147	2.160952793	0.449684531	0.912511115	-1.075733015	2.160952793	0.039568824	0.324357628	-1.216053376	2.160952793	0.017282202	0.445638474	-2.64830305	2.160952793	3.05E-07	0.000125553	firebrick1
Creb3l1	0.08235482	5.3306639	0.678948305	0.973876581	-0.478847283	5.3306639	0.025409345	0.251502131	-0.378555099	5.3306639	0.076071952	0.818134822	-0.939755591	5.3306639	2.80E-06	0.000849798	firebrick1
Spon1	-0.075600221	7.5358696	0.776741352	0.987066641	-0.610504974	7.5358696	0.047333461	0.357507289	-0.72320192	7.5358696	0.018881872	0.461913105	-1.258106107	7.5358696	1.71E-05	0.003803256	firebrick1
Agt	0.06164286	4.910788222	0.826174714	0.993897116	-0.811859501	4.910788222	0.005627304	0.109996092	-0.54195502	4.910788222	0.062359319	0.771874186	-1.41545373	4.910788222	3.80E-07	0.000151715	firebrick1
3830417A1 3Rik	0.105994432	0.837694188	0.870240614	1	-1.382885782	0.837694188	0.02760013	0.263303353	-0.77058486	0.837694188	0.194428047	1	-2.259340338	0.837694188	0.000146936	0.020535843	firebrick1
Fgf10	0.039297288	6.27743709	0.813469785	0.992237189	-0.427674129	6.27743709	0.015741253	0.19566743	-0.150194003	6.27743709	0.395302238	1	-0.617165827	6.27743709	0.000173489	0.023771338	firebrick1
Cfb	-0.115174903	7.317063723	0.593491171	0.95880622	-0.683294157	7.317063723	0.004889993	0.101376359	-0.318202951	7.317063723	0.18812539	1	-0.886321787	7.317063723	9.54E-05	0.014658159	firebrick1
Serpinh1	-0.183624079	9.119820877	0.346391208	0.866251564	-0.634095457	9.119820877	0.003555326	0.081860357	-0.276092949	9.119820877	0.202796282	1	-0.726564226	9.119820877	0.000333196	0.040517746	firebrick1
Tsyh2	-0.341436666	6.115326008	0.061294981	0.473815629	-0.573696169	6.115326008	0.004821415	0.10042361	-0.598432392	6.115326008	0.003188367	0.176364499	-0.83069079	6.115326008	1.23E-05	0.00295713	firebrick1
C2	-0.230859588	6.19835561	0.185627906	0.730456392	-0.498956288	6.19835561	0.010223779	0.15251593	-0.510505246	6.19835561	0.008400237	0.306129109	-0.778601035	6.19835561	1.71E-05	0.003803256	firebrick1
C4b	-0.264366688	8.982150868	0.156915229	0.691376808	-0.731506398	8.982150868	0.000443813	0.019383518	-0.74828335	8.982150868	0.000325202	0.037254236	-1.215422845	8.982150868	6.94E-10	4.41E-07	firebrick1
Chrdl1	-0.289334016	5.945803862	0.063272794	0.47800331	-0.370003339	5.945803862	0.033111612	0.293926096	-0.705980766	5.945803862	4.64E-05	0.009682532	-0.786648887	5.945803862	1.16E-06	0.000405646	firebrick1
Gas6	-1.515651368	8.666581017	0.000370262	0.017135018	-0.500421971	8.666581017	0.293923568	0.765012213	-1.801369159	8.666581017	0.000236673	0.031357795	-0.786139399	8.666581017	0.079942195	1	firebrick1
Efhd1	-0.942398546	3.912798826	0.000670159	0.026914212	-0.288065495	3.912798826	0.355568554	0.812794589	-1.002934293	3.912798826	0.001298086	0.100232328	-0.348596615	3.912798826	0.229076898	1	firebrick1
Ldb3	-2.135048925	3.528305598	9.53E-06	0.001148677	-0.401991226	3.528305598	0.46204131	0.877383718	-2.459592694	3.528305598	1.32E-05	0.003761765	-0.726517926	3.528305598	0.154335	1	firebrick1
Lgi2	-1.16338824	2.886391564	0.002273022	0.063555518	-0.267198133	2.886391564	0.543875861	0.905060463	-1.601202525	2.886391564	0.000253866	0.031964298	-0.704996102	2.886391564	0.081971	1	firebrick1
Cd209g	-1.417734235	3.058817124	0.000109185	0.007281448	-0.144481775	3.058817124	0.72994669	0.965045279	-1.720715953	3.058817124	4.42E-05	0.009384939	-0.447450139	3.058817124	0.251593984	1	firebrick1
Ivl	-4.200360847	-0.978687181	1.72E-05	0.001708203	1.565861032	-0.978687181	0.285413102	0.756852872	-5.486450848	-0.978687181	1.87E-05	0.004924492	0.281045452	-0.978687181	0.850866969	1	firebrick1
Dab2	-0.764236601	6.309940035	0.000187387	0.010600388	0.037286002	6.309940035	0.870916255	0.988639654	-0.901084939	6.309940035	8.49E-05	0.01540585	-0.099561733	6.309940035	0.64022988	1	firebrick1
Ngfr	-1.86595823	3.82443267	5.85E-05	0.004234773	0.293803325	3.82443267	0.575118167	0.914616378	-2.44864968	3.82443267	7.51E-06	0.002282734	-0.284878116	3.82443267	0.565855984	1	firebrick1
Arsi	-1.222267311	2.644622585	0.001730217	0.052227904	0.185883296	2.644622585	0.682008694	0.952820984	-1.663751506	2.644622585	0.000203887	0.028783008	-0.255586274	2.644622585	0.540514148	1	firebrick1
Chsy3	-1.010990275	2.089708637	0.004751895	0.105416649	0.312349504	2.089708637	0.448837192	0.868423605	-1.448212634	2.089708637	0.000413163	0.045828357	-0.124855857	2.089708637	0.758720706	1	firebrick1
Cldn11	-1.812953211	0.082820914	0.00557761	0.118289341	0.446543952	0.082820914	0.618678693	0.929258879	-3.002952381	0.082820914	0.000175938	0.025883311	-0.743243085	0.082820914	0.308038647	1	firebrick1
Hif1a	-0.582153085	7.897680488	0.004350517	0.099676769	0.06919138	7.897680488	0.760673163	0.968583101	-0.873066677	7.897680488	0.00013266	0.02098527	-0.221722001	7.897680488	0.291295246	1	firebrick1
Sprr1a	-1.351369007	2.94260577	0.000353761	0.016602381	0.329426328	2.94260577	0.447494365	0.869239922	-2.109977768	2.94260577	1.76E-06	0.000767591	-0.429166138	2.94260577	0.286261942	1	firebrick1
Gsr	-0.521862224	6.406781314	0.007023971	0.136911847	0.279566642	6.406781314	0.194962101	0.667601274	-1.028805985	6.406781314	2.17E-06	0.000864821	-0.227376469	6.406781314	0.253367533	1	firebrick1
Mrc1	-0.436612215	6.894775325	0.101433693	0.589454178	0.32803339	6.894775325	0.27034355	0.742594625	-1.087644184	6.894775325	0.000293004	0.035573925	-0.322998065	6.894775325	0.242228823	1	firebrick1
Gm14005	-0.785642145	2.363416587	0.02763947	0.308047179	0.750684986	2.363416587	0.072426925	0.44029522	-2.31424186	2.363416587	4.39E-08	2.56E-05	-0.777884471	2.363416587	0.040261937	0.814861989	firebrick1
Mgl2	-0.333659808	5.637249091	0.228482335	0.773020276	0.311371794	5.637249091	0.315934783	0.785073719	-1.130553228	5.637249091	0.003004339	0.03604613	-0.485520218	5.637249091	0.092017363	1	firebrick1
Areg	-0.396601574	8.008953601	0.225939719	0.771815654	0.469824741	8.008953601	0.201122076	0.674853955	-1.439902293	8.008953601	0.000117401	0.019079065	-0.573475632	8.008953601	0.094498889	1	firebrick1
Thsd4	-0.293793243	5.773376075	0.249789364	0.794011058	0.300261558	5.773376075	0.293163588	0.764413118	-1.18859181	5.773376075	3.76E-05	0.008765327	-0.594535583	5.773376075	0.025124468	0.66252748	firebrick1
Siglec1	-0.583887758	5.675613489	0.045613251	0.413365976	0.069986903	5.675613489	0.831721104	0.980677001	-1.384942475	5.675613489	3.01E-05	0.007374637	-0.731065866	5.675613489	0.016821808	0.527550793	firebrick1
Wfdc17	-0.737419667	2.638940486	0.051970475	0.435078428	0.081903654	2.638940486	0.856229639	0.984992665	-1.569628381	2.638940486	0.000323633	0.037254236	-0.750287053	2.638940486	0.063697495	0.998022638	firebrick1
Sfrp4	-0.743758294	4.027944069	0.022451723	0.273332127	0.128989531	4.027944069	0.728428748	0.965045279	-1.409626606	4.027944069	0.000146274	0.022465104	-0.536873206	4.027944069	0.116168774	1	firebrick1
Cd209f	-1.031620784	4.494775155	0.001634469	0.050252623	0.05674995	4.494775155	0.880696438	0.990473438	-1.772960862	4.494775155	2.54E-06	0.0009583	-0.684584732	4.494775155	0.046827559	0.874949149	firebrick1
Fcgr1	-0.972470036	3.003002523	0.008219482	0.14895629	-0.079591055	3.003002523	0.854434111	0.984607393	-1.55764938	3.003002523	0.000225752	0.030632082	-0.664756602	3.003002523	0.087754348	1	firebrick1
Npl	-0.80837096	2.415136742	0.012155313	0.191569999	-0.071160492	2.415136742	0.86029913	0.986263689	-1.378014503	2.415136742	0.000179501	0.026132408	-0.640785549	2.415136742	0.062047622	0.979861648	firebrick1
Bst1	-0.484426706	2.103957866	0.152952593	0.683983455	-0.004699776	2.103957866	1	1	-1.432064325	2.103957866	0.000236481	0.031357795	-0.952310362	2.103957866	0.008738408	0.369985586	firebrick1
Ccl8	-0.481789919	4.040652834	0.109336056	0.604462311	0.114887395	4.040652834	0.738679744	0.965045279	-1.408776064	4.040652834	3.95E-05	0.008958835	-0.812092415	4.040652834	0.01035029	0.404698347	firebrick1
Tmed3	-0.441604626	7.50068509	0.109935092	0.605717291	0.151031575	7.50068509	0.624542675	0.931608926	-1.466417224	7.50068509	3.07E-06	0.001071415	-0.873780415	7.50068509	0.002570053	0.176823703	firebrick1
Tcf21	-0.897636317	-0.640277544	0.28765791	0.824970472	1.576613091	-0.640277544	0.43940259	0.865305943	-6.148430213	-0.640277544	7.22E-06	0.002243028	-3.671029552	-0.640277544	0.001363224	0.114862431	firebrick1
Rnase1	-0.393776259	-1.192340747	0.454152188	0.913501714	-1.211636258	-1.192340747	0.267312126	0.740071375	-3.006132343	-1.192340747	2.10E-05	0.005422402	-3.821955711	-1.192340747	1.25E-06	0.000424439	firebrick1
Vrm1	-0.120962563	3.123880895	0.687378612	0.974759724	-0.210391396	3.123880895	0.551986536	0.907049956	-1.224538549	3.123880895	0.000428109	0.046181842	-1.313952772	3.123880895	6.50E-05	0.010630753	firebrick1
Pad4	-0.318888633	3.802089597	0.560699276	0.946944793	0.145239522	3.802089597	0.831885058	0.980677001	-1.148547478	3.802089597	5.13E-06	0.001667822	-2.684386379	3.802089597	3.86E-05	0.007388841	firebrick1
Muc13	-0.065159007	4.817661121	0.896040214	1	0.460560857	4.817661121	0.485338478	0.885297579	-2.724055014	4.817661121	8.95E-05	0.015442991	-2.201963688	4.817661121	0.000734623	0.072816296	firebrick1
Upk3b	0.842594239	-0.525561475	0.453994862	0.913501714	0	-0.525561475	1	1	-8.389166747	-0.525561475	4.97E-05	0.010060595	-9.183459255	-0.525561475	5.27E-06	0.00150266	firebrick1
Aoc1	-0.086140421	4.821036587	0.880826855	1	2.501946478	4.821036587	0.004457223	0.096281531	-6.05834159	4.821036587	2.86E-09	2.67E-06	-3.470183005	4.821036587	7.30E-05	0.011599423	darkgreen
Ms4a6d	-0.036717769	3.348371754	0.89770714	1	0.729990736	3.348371754	0.038116833	0.316907112	-1.339745054	3.348371754	0.000151316	0.022812507	-0.573028565	3.348371754	0.076470564	1	darkgreen
Krt4	0.147921623	1.746538842	0.817211532	0.992918622	1.666780548	1.746538842	0.012401475	0.171606939	-2.961256183	1.746538842	1.70E-05	0.004646006	-1.442311188	1.746538842	0.018500519	0.554856774	darkgreen
Wfdc3	0.191486819	2.318550889	0.719750559	0.980142426	1.423872467	2.318550889	0.012796244	0.173692314	-2.805459257	2.318550889	1.94E-06	0.000797648	-1.573018296	2.318550889	0.002998054	0.193091276	darkgreen
Faim2	0.762081593	4.193802732	0.033543188	0.345213255	1.100025393	4.193802732	0.004932506	0.101701826	-1.85608405	4.193802732	2.97E-06	0.001070258	-1.518126674	4.193802732	3.81E-05	0.007388841	darkgreen
Slco2a1	0.273913782	7.196662291	0.190754088	0.737272992	0.686659284	7.196662291	0.002545457	0.06554194	-0.932332497	7.196662291	4.43E-05	0.009384939	-0.519586622	7.196662291	0.013450854	0.479564123	darkgreen
Greb1	0.36223352	2.008932254	0.632585788	0.969614941	2.5000041	2.008932254	0.002830983	0.070653258	-3.423758012	2.008932254	7.38E-05	0.013772289	-1.285890022	2.008932254	0.085207477	1	darkgreen
Gng12	0.098171432	8.312034352	0.579032882	0.953302094	0.43673505	8.312034352	0.022296168	0.234494547	-0.730959137	8.312034352	0.000137139	0.02129612	-0.392395386	8.312034352	0.026160109	0.680844858	darkgreen
Tmem176a	0.064241324	6.834487605	0.75330096	0.983951948	0.44949169	6.834487605	0.039092435	0.322333848	-0.765531655	6.834487605	0.000459041	0.049150387	-0.380280905	6.834487605	0.058666146	0.962015487	darkgreen
Tmem86a	0.146162463	5.704651744	0.685045723	0.974473184	1.466720838	5.704651744	0.000152057	0.008603816	-2.10766784	5.704651744	9.10E-08	4.89E-05	-0.787106644	5.704651744	0.027012182	0.685465124	darkgreen
Tgm2	0.01262139	10.88713806	0.973285771	1	1.171208983	10.88713806	0.000115655	0.007058465	-1.781767431	10.88713806	7.93E-09	6.15E-06	-0.623179779	10.88713806	0.026042599	0.680320318	darkgreen
Ptprr5	-0.235956815	4.230415661	0.705737548	0.976863224	4.103681985	4.230415661	2.07E-06	0.000305062	-5.637865185	4.230415661	1.07E-09	1.15E-06	-1.298156189	4.230415661	0.074419426	1	darkgreen
Fbln1	0.143915463	5.870305998	0.454000037	0.913501714	0.768753438	5.870305998	0.00023658	0.012200885	-0.838541057	5.870305998	6.13E-05	0.012075656	-0.213702433	5.870305998	0.265194089	1	darkgreen
Ccl9	0.237840072	6.104432277	0.229432481	0.773780974	1.032461712	6.104432277	1.90E-06	0.000282562	-1.083473301	6.104432277	5.87E-07	0.000282839	-0.288850895	6.104432277	0.144437826	1	darkgreen
Ms4a6c	0.260763736	4.307117619	0.294755649	0.82920792	0.898251365	4.307117619	0.000939043	0.034102749	-0.907500429	4.307117619	0.000803084	0.073452215	-0.27001065	4.307117619	0.278150526	1	darkgreen
Ccl6	0.366847287	7.004637986	0.156143983	0.691028594	1.463337241	7.004637986	2.69E-07	5.87E-05	-1.32452912	7.004637986	2.99E-06	0.001070258	-0.228038657	7.004637986	0.378559992	1	darkgreen
Ninj1	0.049447597	5.327904469	0.781634129	0.987815684	0.644289137	5.327904469	0.000701049	0.027368342	-0.685574694	5.327904469	0.000310704	0.036490767	-0.090732475	5.327904469	0.605824221	1	darkgreen
Fcgr2b	0.015907523	4.974415883	0.950173218	1	0.844991536	4.974415883	0.000378581	0.011735896	-0.941265071	4.974415883	7.61E-05	0.013995466	-0.112179788	4.974415883	0.61019141	1	darkgreen
Alox5ap	-0.047317666	4.212379709	0.851088043	0.997576004	0.942049416	4.212379709	0.001497897	0.046381353	-1.09668701	4.212379709	0.000223694	0.030632082	-0.107317351	4.212379709	0.669040334	1	darkgreen
Thbs2	-0.116075446	7.509686801	0.537374786	0.940321774	0.792033458	7.509686801	0.000175775	0.009709993	-0.838091879	7.509686801	7.27E-05	0.013772289	0.070017184	7.509686801	0.707594879	1	darkgreen
Mcpt4	-0.355850975	4.116096427	0.203468716	0.751702402	0.864343357	4.116096427	0.006123861	0.115346467	-1.128874528	4.116096427	0.00035749	0.040620217	0.091322285	4.116096427	0.739716345	1	darkgreen
Slpi	-0.442712874	3.731087085	0.040207194	0.385415463	1.067389147	3.731087085	1.26E-05	0.001218188	-1.357610601	3.731087085	3.18E-08	2.02E-05	0.152495351	3.731087085	0.481163298	1	darkgreen
Matn4	-0.594291137	1.414156086	0.069217501	0.503115788	0.869232935	1.414156086	0.021107454	0.226634864	-1.359508586	1.414156086	0.000292223	0.035573925	0.104036121	1.414156086	0.756918236	1	darkgreen
Dscam	-1.164402953	2.357968295	0.055932769	0.451044994	1.695222336	2.357968295	0.017445552	0.206626299	-2.589229735	2.357968295	0.000399548	0.044672631	0.270419827	2.357968295	0.648934735	1	darkgreen
Mmp9	-0.757380069	3.600051917	0.01469097	0.211018493	0.775307338	3.600051917	0.027349474	0.261773795	-1.386235032	3.600051917	8.87E-05	0.015442991	0.146456862	3.600051917	0.634555222	1	darkgreen
Clec3b	-0.390876516	6.729961858	0.053938011	0.441874348	0.569218735	6.729961858	0.01179628	0.166362066	-0.943714819	6.729961858	3.24E-05	0.007812573	0.016380794	6.729961858	0.929290544	1	darkgreen
Cyslm1	-0.256440791	3.932157711	0.188896484	0.73476684	0.416057914	3.932157711	0.057316121	0.392287027	-0.789965797	3.932157711	0.000296682	0.035573925	-0.117464664	3.932157711	0.562548133	1	darkgreen
Nfam1	-0.42304073	3.408923677	0.132211096	0.65130045	0.500768998	3.408923677	0.114956193	0.540654648	-1.166634641	3.408923677	0.00025059	0.031964298	-0.242819246	3.408923677	0.409142553	1	darkgreen
Fcrls	-0.283048288	4.602875016	0.200887366	0.749441765	0.391680082	4.602875016	0.141469965	0.5394234	-0.975355687	4.602875016	8.67E-05	0.015442991	-0.300625117	4.602875016	0.188209176	1	darkgreen
Itgam	-0.192638206	5.109687116	0.479542932	0.924624379	0.560162727	5.109687116	0.068525004	0.428120455	-1.229005759	5.109687116	7.37E-05	0.013772289	-0.476202741	5.109687116	0.094224904	1	darkgreen
Cfp	-0.13919803	5.621597244	0.599021995	0.960083876	0.579291207	5.621597244	0.053314878	0.379478602	-1.143986146	5.621597244	0.0001518	0.022812507	-0.425495589	5.621597244	0.125025226	1	darkgreen
Gm13031	-0.335201552	2.070189347	0.369061462	0.880194409	1.040788616	2.070189347	0.017899307	0.209630678	-1.961563591	2.070189347	9.28E-06	0.002758403	-0.58544468	2.070189347	0.142100715	1	darkgreen
Spi1	-0.1770576	3.787691061	0.495308868	0.931687313	0.55394869	3.787691061	0.05987238	0.400346125	-1.066066032	3.787691061	0.000297807	0.035573925	-0.335055572	3.787691061	0.215705241	1	darkgreen
Pad2	-0.351820167	5.687445826	0.218911486	0.764384385	1.39749848	5.687445826	1.88E-05	0.001663136	-2.235978296	5.687445826	2.30E-11	2.93E-08	-0.486657004	5.687445826	0.102403218	1	darkgreen
Aqp3	-0.416575482	0.973379448	0.31895265	0.847629252	1.431905002	0.973379448	0.003850706	0.086107947	-1.178865286	0.973379448	1.22E-05	0.003547466	-0.330320801	0.973379448	0.46124331	1	darkgreen

References

1 Ikeda, K. *et al.* (2018) The common and distinct features of brown and beige adipocytes. *Trends Endocrinol. Metab.* 29, 191–200

2 Kajimura, S. *et al.* (2015) Brown and Beige Fat: Physiological Roles beyond Heat Generation. *Cell Metab.* 22, 546–559

3 Sanchez-Gurmaches, J. *et al.* (2012) PTEN loss in the Myf5 lineage redistributes body fat and reveals subsets of white adipocytes that arise from Myf5 precursors. *Cell Metab.* 16, 348–362

4 Seale, P. *et al.* (2008) PRDM16 controls a brown fat/skeletal muscle switch. *Nature* 454, 961–967

5 Chu, D.-T. and Gawronska-Kozak, B. (2017) Brown and brite adipocytes: Same function, but different origin and response. *Biochimie* 138, 102–105

6 Chu, D.-T. and Tao, Y. (2017) Human thermogenic adipocytes: a reflection on types of adipocyte, developmental origin, and potential application. *J. Physiol. Biochem.* 73, 1–4

7 Chu, D.-T. *et al.* (2017) OPA1 in lipid metabolism: function of OPA1 in lipolysis and thermogenesis of adipocytes. *Horm. Metab. Res.* 49, 276–285

8 Wu, J. *et al.* (2012) Beige adipocytes are a distinct type of thermogenic fat cell in mouse and human. *Cell* 150, 366–376

9 Sharp, L.Z. *et al.* (2012) Human BAT possesses molecular signatures that resemble beige/brite cells. *PLoS ONE* 7, e49452

10 Roh, H.C. *et al.* (2018) Warming induces significant reprogramming of beige, but not brown, adipocyte cellular identity. *Cell Metab.* 27, 1121-1137.e5

11 Grujic, D. *et al.* (1997) β3-Adrenergic Receptors on White and Brown Adipocytes Mediate β3-Selective Agonist-induced Effects on Energy Expenditure, Insulin Secretion, and Food Intake. *Journal of Biological Chemistry* 272, 17686–17693

12 Ahmadian, M. *et al.* (2011) Desnutrin/ATGL is regulated by AMPK and is required for a brown adipose phenotype. *Cell Metab.* 13, 739–748

13 Altshuler-Keylin, S. *et al.* (2016) Beige Adipocyte Maintenance Is Regulated by Autophagy-Induced Mitochondrial Clearance. *Cell Metab.* 24, 402–419

14 Nedergaard, J. and Cannon, B. (2013) UCP1 mRNA does not produce heat. *Biochim. Biophys. Acta* 1831, 943–949

15 Kazak, L. *et al.* (2015) A creatine-driven substrate cycle enhances energy expenditure and thermogenesis in beige fat. *Cell* 163, 643–655

16 Ikeda, K. *et al.* (2017) UCP1-independent signaling involving SERCA2b-mediated calcium cycling regulates beige fat thermogenesis and systemic glucose homeostasis. *Nat. Med.* 23, 1454–1465

17 Cypess, A.M. *et al.* (2009) Identification and importance of brown adipose tissue in

adult humans. *N. Engl. J. Med.* 360, 1509–1517
18 Saito, M. *et al.* (2009) High incidence of metabolically active brown adipose tissue in healthy adult humans: effects of cold exposure and adiposity. *Diabetes* 58, 1526–1531
19 Hanssen, M.J.W. *et al.* (2015) Short-term cold acclimation improves insulin sensitivity in patients with type 2 diabetes mellitus. *Nat. Med.* 21, 863–865
20 Emmett, M.J. *et al.* (2017) Histone deacetylase 3 prepares brown adipose tissue for acute thermogenic challenge. *Nature* 546, 544–548
21 Inagaki, T. *et al.* (2016) Transcriptional and epigenetic control of brown and beige adipose cell fate and function. *Nat. Rev. Mol. Cell Biol.* 17, 480–495
22 Ohno, H. *et al.* (2013) EHMT1 controls brown adipose cell fate and thermogenesis through the PRDM16 complex. *Nature* 504, 163–167
23 Sambeat, A. *et al.* (2016) LSD1 Interacts with Zfp516 to Promote UCP1 Transcription and Brown Fat Program. *Cell Rep.* 15, 2536–2549
24 Tateishi, K. *et al.* (2009) Role of Jhdm2a in regulating metabolic gene expression and obesity resistance. *Nature* 458, 757–761
25 Zeng, X. *et al.* (2016) Lysine-specific demethylase 1 promotes brown adipose tissue thermogenesis via repressing glucocorticoid activation. *Genes Dev.* 30, 1822–1836
26 Pastor, W.A. *et al.* (2013) TETonic shift: biological roles of TET proteins in DNA demethylation and transcription. *Nat. Rev. Mol. Cell Biol.* 14, 341–356
27 Chen, Q. *et al.* (2013) TET2 promotes histone O-GlcNAcylation during gene transcription. *Nature* 493, 561–564
28 Gao, J. *et al.* (2016) Non-catalytic roles for TET1 protein negatively regulating neuronal differentiation through srGAP3 in neuroblastoma cells. *Protein Cell* 7, 351–361
29 Tsai, Y.-P. *et al.* (2014) TET1 regulates hypoxia-induced epithelial-mesenchymal transition by acting as a co-activator. *Genome Biol.* 15, 513
30 Williams, K. *et al.* (2011) TET1 and hydroxymethylcytosine in transcription and DNA methylation fidelity. *Nature* 473, 343–348
31 Zhang, Q. *et al.* (2015) Tet2 is required to resolve inflammation by recruiting Hdac2 to specifically repress IL-6. *Nature* 525, 389–393
32 Yoo, Y. *et al.* (2017) TET-mediated hydroxymethylcytosine at the Pparγ locus is required for initiation of adipogenic differentiation. *Int J Obes (Lond)* 41, 652–659
33 Eguchi, J. *et al.* (2011) Transcriptional control of adipose lipid handling by IRF4. *Cell Metab.* 13, 249–259
34 He, W. *et al.* (2003) Adipose-specific peroxisome proliferator-activated receptor gamma knockout causes insulin resistance in fat and liver but not in muscle. *Proc Natl Acad Sci USA* 100, 15712–15717
35 Jeffery, E. *et al.* (2014) Characterization of Cre recombinase models for the study

of adipose tissue. *Adipocyte* 3, 206–211
36 Nguyen, K.D. *et al.* (2011) Alternatively activated macrophages produce catecholamines to sustain adaptive thermogenesis. *Nature* 480, 104–108
37 Boström, H. *et al.* (1996) PDGF-A signaling is a critical event in lung alveolar myofibroblast development and alveogenesis. *Cell* 85, 863–873
38 Chong, J.J.H. *et al.* (2013) Progenitor cells identified by PDGFR-alpha expression in the developing and diseased human heart. *Stem Cells Dev.* 22, 1932–1943
39 Karlsson, L. *et al.* (1999) Roles for PDGF-A and sonic hedgehog in development of mesenchymal components of the hair follicle. *Development* 126, 2611–2621
40 O'Neill, S.M. *et al.* (2014) Targeting adipose tissue via systemic gene therapy. *Gene Ther.* 21, 653–661
41 Chella Krishnan, K. *et al.* (2019) Sex-specific metabolic functions of adipose Lipocalin-2. *Mol. Metab.* 30, 30–47
42 Zhang, W. *et al.* (2016) Isoform switch of TET1 regulates DNA demethylation and mouse development. *Mol. Cell* 64, 1062–1073
43 Ito, S. *et al.* (2011) Tet proteins can convert 5-methylcytosine to 5-formylcytosine and 5-carboxylcytosine. *Science* 333, 1300–1303
44 Tahiliani, M. *et al.* (2009) Conversion of 5-methylcytosine to 5-hydroxymethylcytosine in mammalian DNA by MLL partner TET1. *Science* 324, 930–935
45 Yang, H. *et al.* (2014) TET-catalyzed 5-methylcytosine hydroxylation is dynamically regulated by metabolites. *Cell Res.* 24, 1017–1020
46 Huang, Z. *et al.* (2013) Bisulfite sequencing of cloned alleles. *Methods Mol. Biol.* 1049, 83–94
47 Zhang, Y. *et al.* (2009) DNA methylation analysis by bisulfite conversion, cloning, and sequencing of individual clones. *Methods Mol. Biol.* 507, 177–187
48 Li, L.-C. and Dahiya, R. (2002) MethPrimer: designing primers for methylation PCRs. *Bioinformatics* 18, 1427–1431
49 Itzhak, Y. *et al.* (2015) Long-term parental methamphetamine exposure of mice influences behavior and hippocampal DNA methylation of the offspring. *Mol. Psychiatry* 20, 232–239
50 Neri, F. *et al.* (2013) Genome-wide analysis identifies a functional association of Tet1 and Polycomb repressive complex 2 in mouse embryonic stem cells. *Genome Biol.* 14, R91
51 Wei, T. *et al.* (2015) An HDAC2-TET1 switch at distinct chromatin regions significantly promotes the maturation of pre-iPS to iPS cells. *Nucleic Acids Res.* 43, 5409–5422
52 Chandru, A. *et al.* (2018) Sin3A recruits Tet1 to the PAH1 domain via a highly conserved Sin3-Interaction Domain. *Sci. Rep.* 8, 14689
53 Galmozzi, A. *et al.* (2013) Inhibition of class I histone deacetylases unveils a

mitochondrial signature and enhances oxidative metabolism in skeletal muscle and adipose tissue. *Diabetes* 62, 732–742
54 Ye, J. (2013) Improving insulin sensitivity with HDAC inhibitor. *Diabetes* 62, 685–687
55 Li, F. *et al.* (2016) Histone deacetylase 1 (HDAC1) negatively regulates thermogenic program in brown adipocytes via coordinated regulation of histone H3 lysine 27 (H3K27) deacetylation and methylation. *J. Biol. Chem.* 291, 4523–4536
56 Yang, Q. *et al.* (2016) AMPK/α-Ketoglutarate Axis Dynamically Mediates DNA Demethylation in the Prdm16 Promoter and Brown Adipogenesis. *Cell Metab.* 24, 542–554
57 Gupta, R.K. *et al.* (2010) Transcriptional control of preadipocyte determination by Zfp423. *Nature* 464, 619–623
58 Shao, M. *et al.* (2016) Zfp423 Maintains White Adipocyte Identity through Suppression of the Beige Cell Thermogenic Gene Program. *Cell Metab.* 23, 1167–1184
59 Villanueva, C.J. *et al.* (2011) TLE3 is a dual-function transcriptional coregulator of adipogenesis. *Cell Metab.* 13, 413–427
60 Pearson, S. *et al.* (2019) Loss of TLE3 promotes the mitochondrial program in beige adipocytes and improves glucose metabolism. *Genes Dev.* 33, 747–762
61 Shapira, S.N. *et al.* (2017) EBF2 transcriptionally regulates brown adipogenesis via the histone reader DPF3 and the BAF chromatin remodeling complex. *Genes Dev.* 31, 660–673
62 Lim, Y.C. *et al.* (2016) Dynamic DNA methylation landscape defines brown and white cell specificity during adipogenesis. *Mol. Metab.* 5, 1033–1041
63 Sakamoto, H. *et al.* (2007) Cell type-specific methylation profiles occurring disproportionately in CpG-less regions that delineate developmental similarity. *Genes Cells* 12, 1123–1132
64 Mullican, S.E. *et al.* (2013) A novel adipose-specific gene deletion model demonstrates potential pitfalls of existing methods. *Mol. Endocrinol.* 27, 127–134
65 Karlsson, L. *et al.* (2000) Abnormal gastrointestinal development in PDGF-A and PDGFR-(alpha) deficient mice implicates a novel mesenchymal structure with putative instructive properties in villus morphogenesis. *Development* 127, 3457–3466
66 Lindahl, P. *et al.* (1997) Alveogenesis failure in PDGF-A-deficient mice is coupled to lack of distal spreading of alveolar smooth muscle cell progenitors during lung development. *Development* 124, 3943–3953
67 McCarthy, N. *et al.* (2016) Pdgfra and Pdgfrb genetically interact during craniofacial development. *Dev. Dyn.* 245, 641–652
68 Ljvak, K.J. (2001) Analysis of relative gene expression data using real time quantitative PCR and the 2^<-ΔΔCT> method. *Methods*

69 Dobin, A. *et al.* (2013) STAR: ultrafast universal RNA-seq aligner. *Bioinformatics* 29, 15–21

Chapter 3:

A necessary role of DNMT3A in endurance exercise by suppressing ALDH1L1-mediated oxidative stress

A necessary role of DNMT3A in endurance exercise by suppressing ALDH1L1-mediated oxidative stress

Abstract

Exercise can alter the skeletal muscle DNA methylome, yet little is known about the role of the DNA methylation machinery in exercise capacity. Here, we show that DNMT3A expression in oxidative red muscle increases greatly following a bout of endurance exercise. Muscle-specific *Dnmt3a* knockout mice have reduced tolerance to endurance exercise, accompanied by reduction in oxidative capacity and mitochondrial respiration. Moreover, *Dnmt3a* deficient muscle overproduces reactive oxygen species (ROS), the major contributors to muscle dysfunction. Mechanistically, we show that DNMT3A suppresses the *Aldh1l1* transcription by binding to its promoter region, altering its epigenetic profile. Forced expression of ALDH1L1 elevates NADPH levels, which results in overproduction of ROS by the action of NADPH oxidase complex, ultimately resulting in mitochondrial defects in myotubes. Thus, inhibition of ALDH1L1 pathway can rescue oxidative stress and mitochondrial dysfunction from *Dnmt3a* deficiency in myotubes. Finally, we show that *in vivo* knockdown of *Aldh1l1* largely rescues exercise intolerance in *Dnmt3a* deficient mice. Together, we establish that DNMT3A in skeletal muscle plays a pivotal role in endurance exercise by controlling intracellular oxidative stress.

Key words: DNA methylation, exercise, oxidative stress

Synopsis

- Muscle-specific Dnmt3a knockout mice display a reduced tolerance to endurance exercise.
- Dnmt3a knockout soleus muscle oververproduces ROS and exhibits mitochondrial dysfunction.
- ALDH1L1 acts as a downstream effector that mediate muscle dysfunction and exercise intolerance in loss of Dnmt3a

Introduction

Endurance exercise, an aerobic exercise, is generally characterized by high-frequency, long duration, and low power output activity, such as marathon running and swimming. Endurance exercise exerts many positive effects on health, prevents disease, and even acts as therapeutics for a wide range of non-communicable diseases [1,2]. Despite these benefits of exercise, there is very limited understanding in the regulatory factors that affect endurance exercise.

Mitochondria are the organelles where oxidation meets phosphorylation to generate ATP for contracting muscles [3]. In response to endurance exercise, skeletal muscle increases energy production through aerobic metabolism through involvement of enhancing mitochondrial oxidative capacity [4]. It has been suggested that the degree of mitochondrial health and adaptations can be dependent on ROS levels. Thus, a moderate increase in skeletal muscle ROS production in the acute phase of exercise is thought to activate signaling pathways that lead to cellular adaptation, thereby protecting against future stress [5]. On the other hand, excessive ROS can oxidatively damage macromolecules, such as DNA, lipids, and proteins, as well as modify cellular redox status and cellular functions. Consequently, ROS elevation is also associated with pathophysiological states of muscle and contractile dysfunction [5,6]. Mitochondria make a large contribution to ROS production at rest, but not during muscle contraction [7]. The majority of ROS produced during contraction arise from non-mitochondrial sources, such as NADPH oxidase (NOX), located in the microtubules [8–10]. The redox-mediated crosstalk between NOX and mitochondria exacerbates ROS production and disrupts redox homeostasis. For example, NOX-derived ROS promote the opening of mitochondrial ATP-sensitive K^+ channels [11–13]. The resultant potassium influx into the matrix lowers the mitochondrial membrane potential, which causes mitochondrial swelling, opening of permeability transition pores, and elevated ROS production [11–13]. In addition, NOX-derived ROS causes leakage of Ca^{2+} from the sarcoplasmic reticulum or entry of extracellular Ca^{2+}, resulting in mitochondrial Ca^{2+} overload and mitochondrial ROS emission, which ultimately results in muscle fatigue and dysfunction [5,14,15].

DNA methylation, a reversible epigenetic mark that usually occurs on a cytosine residue followed by a guanine (CpG), is mediated by a member of the DNA methyltransferase (DNMT) family [16]. Methylation prevents the binding of transcriptional machinery that requires interaction with cytosine, usually resulting in transcriptional silencing [17]. Exercise significantly alters the DNA methylation profile of skeletal muscle [18–26]. Acute and chronic forms of exercise induce both hyper- and hypo-CpG methylation of target loci [18–26], and some of these modifications are inversely correlated with gene expression [18,23,26]. For example, a single bout of aerobic endurance exercise in human subjects transiently induces hypomethylation at the promoter region of important mitochondria-related transcripts (e.g., *PPARGC1A*, *PDK4*, *TFAM*, and *PPARD*), followed by an increase in their expression [18]. Moderate-intensity exercise in humans has been reported to result in hypermethylation of *FABP3* and *COX4L1*, which is inversely associated with their gene expression [25]. As such, despite the obvious link between altered DNA methylation and

exercise-associated gene expression, the underlying function of DNMTs in exercise performance remains unclear.

Here, we report that skeletal muscle DNMT3A is a critical epigenetic modulator of endurance exercise. Muscle-specific *Dnmt3a*-deficient mice greatly reduced the exercise capacity accompanied by increased signs of myopathy. Remarkably, knockout (KO) muscles, especially soleus and gastrocnemius (GA) muscles exhibited a dramatic reduction in oxidative capacity and mitochondrial dysfunction accompanied by an increase in ROS during exercise. Our transcriptomic analysis identifies *Aldh1l1* as a key direct target of repression by DNMT3A in soleus muscle and GA muscles. Overexpression of ALDH1L1 was sufficient to recapitulate *Dnmt3a* KO–mediated mitochondrial dysfunction and oxidative stress by promoting accumulation of NADPH and thereby increasing NOX activity. Conversely, *Aldh1l1* KO or pharmacological inhibition of NOX rescued mitochondrial decline and oxidative stress caused by *Dnmt3a* deficiency. Lastly, we demonstrate that resolving oxidative stress with an anti-oxidant and *Aldh1l1* knock-down largely rescues exercise incapacity in *Dnmt3a* KO mice. Together, our results provide novel insights into the epigenetic regulation of the muscle response to exercise and reveal a surprising molecular target that is important for sustaining endurance exercise.

Results

DNMT3A level in the soleus muscle increases after endurance exercise

DNMT1 is the major enzyme involved in maintenance of the DNA methylation pattern following DNA replication, whereas DNMT3A and DNMT3B are primarily responsible for de novo DNA methylation [16]. Hence, we postulated that de novo DNMTs might be more important for adaptive responses to environmental changes. To begin to characterize the role of de novo DNMTs in endurance exercise, we examined their expression patterns in soleus, extensor digitorum longus (EDL), and GA muscles, which are red, white, and mixed muscles, respectively, at rest and after a bout of endurance exercise, in C57BL/6J wild-type mice. We also measured the mRNA expression of PPARγ-coactivator 1α (*Ppargc1a*), which is known to be induced by exercise in skeletal muscle [18,27].

Muscle-specific *Dnmt3a* ablation decreases the capacity for endurance exercise

Endurance exercise has been shown to lead to the greater relative increase in contractile activity in the soleus and red portion of the GA muscle relative to white muscles, such as EDL [28,29]. The increase of DNMT3A expression in soleus led us to hypothesize that DNMT3A plays an important role in endurance exercise. To test this, we generated muscle-specific *Dnmt3A* knockout mice (MCK-*Dnmt3a* KO) by using the well-characterized muscle creatine kinase (MCK)-Cre, which excises floxed alleles in muscle fibers but not satellite cells starting at embryonic day 17 [30].

To assess tolerance to endurance exercise, we employed two different regimens: (1) a low-intensity regimen (**Fig 1A**) that tested the ability to run steadily at relatively low speed (12 m/min) for an initial 40 min, followed by a gradual increase in speed until exhaustion [31], and (2) a high-intensity regimen (**Fig 1D**) that rapidly increased the running speed (6 m/min

and increased by 2 m/min every 5 min) to a maximal pace of 30 m/min, which persisted until exhaustion [31]. During low-intensity exercise, oxidative muscle fibers predominantly rely on fatty acid oxidation for their ATP production. On the other hand, high-intensity exercise raises the ATP utilization rate and induces a metabolic switch from fatty acid to glucose oxidation [31]. We tested the exercise performance of the MCK-*Dnmt3a* KO mice at 8 weeks of age under these two regimens. Remarkably, the running capacity of the MCK-*Dnmt3a* KO mice was greatly impaired: both distance and duration were reduced by 30–40% under both the low- and high-intensity regimens (**Figs 1B, C, E, F**).

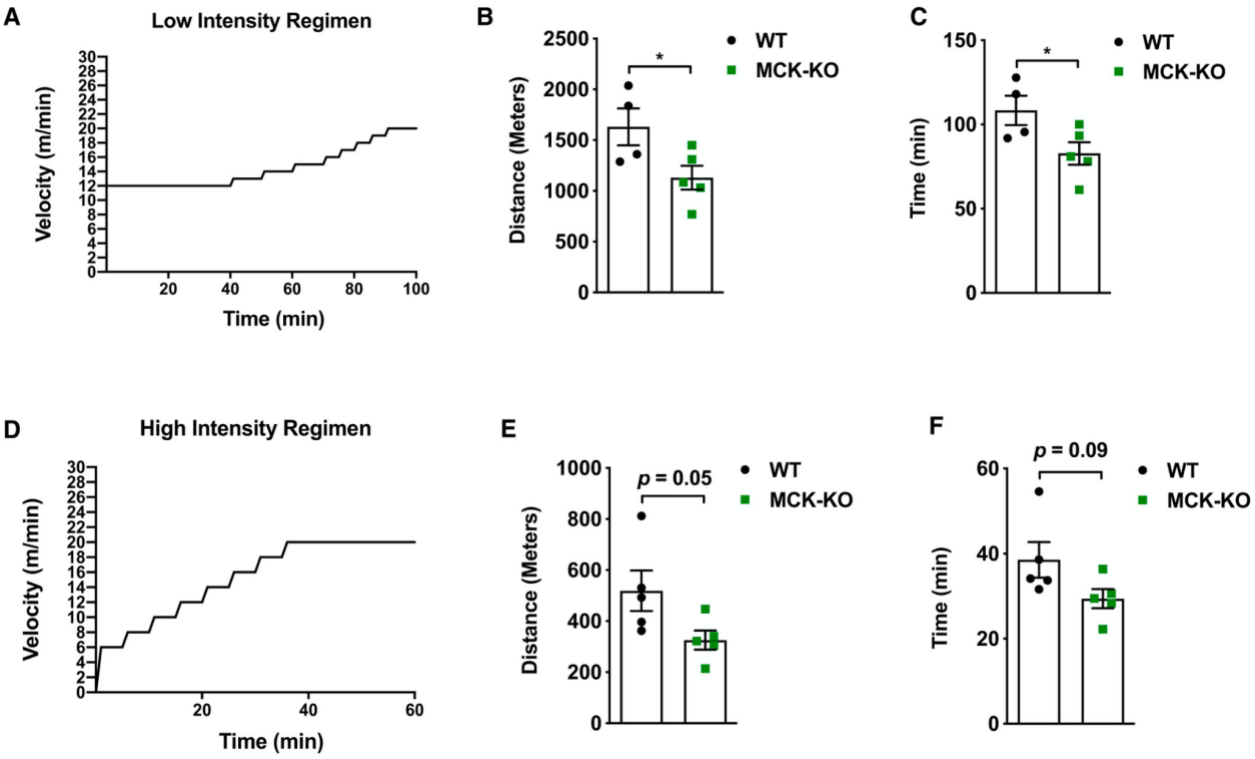

Figure 1. MCK-*Dnmt3a* KO mice display a reduced tolerance to endurance exercise.
(**A**) Schematic of low intensity exercise regimen.
(**B, C**) Exercise capacity of MCK-KO and WT mice from the low intensity regiment was conducted. (*n* = 4 WT, *n* = 5 KO mice, mean ±SEM, * p < 0.05, two-tailed student's t-test).
(**D**) Schematic of high intensity exercise regimen.
(**E, F**) Exercise capacity of MCK-KO and WT mice from the high intensity regiment (n = 5 mice, means ± SEM, two-tailed student's t-test).

Next, we investigated whether reduced exercise tolerance of MCK-*Dnmt3a* KO mice accompanies other morphological and biochemical changes as indications of muscle fatigue. First, nuclear dislocation is a hallmark of dysfunctional muscle with or without degeneration/regeneration [32]. Concordant with impaired exercise capacity, the KO muscles displayed an increased frequency of muscle damage, evidenced by an increased

number of dislocated nuclei in the soleus (2.4% vs 4.8% in WT vs. KO) and GA 2.3 vs. 3.5% muscles from 8-week-old mice (**Figs 2A–D**) after a single bout of low-intensity exercise for the same duration. Second, we measured ROS levels, as high levels of ROS are associated with contractile dysfunction and muscle fatigue [7]. Remarkably, we found that ROS levels greatly increased in red soleus and mixed GA muscles, but not in white EDL, at 8 weeks of age (**Figs 2E–G**). Lastly, we also measured blood lactate levels, which essentially serve as an indirect marker for biochemical events such as fatigue within exercising muscle [33]. As expected, blood lactate levels were also increased in exercised KO mice (**Fig 2H**). Together, these data indicate that *Dnmt3a* KO muscles display increased signs of muscle fatigue which was associated with reduced exercise capacity.

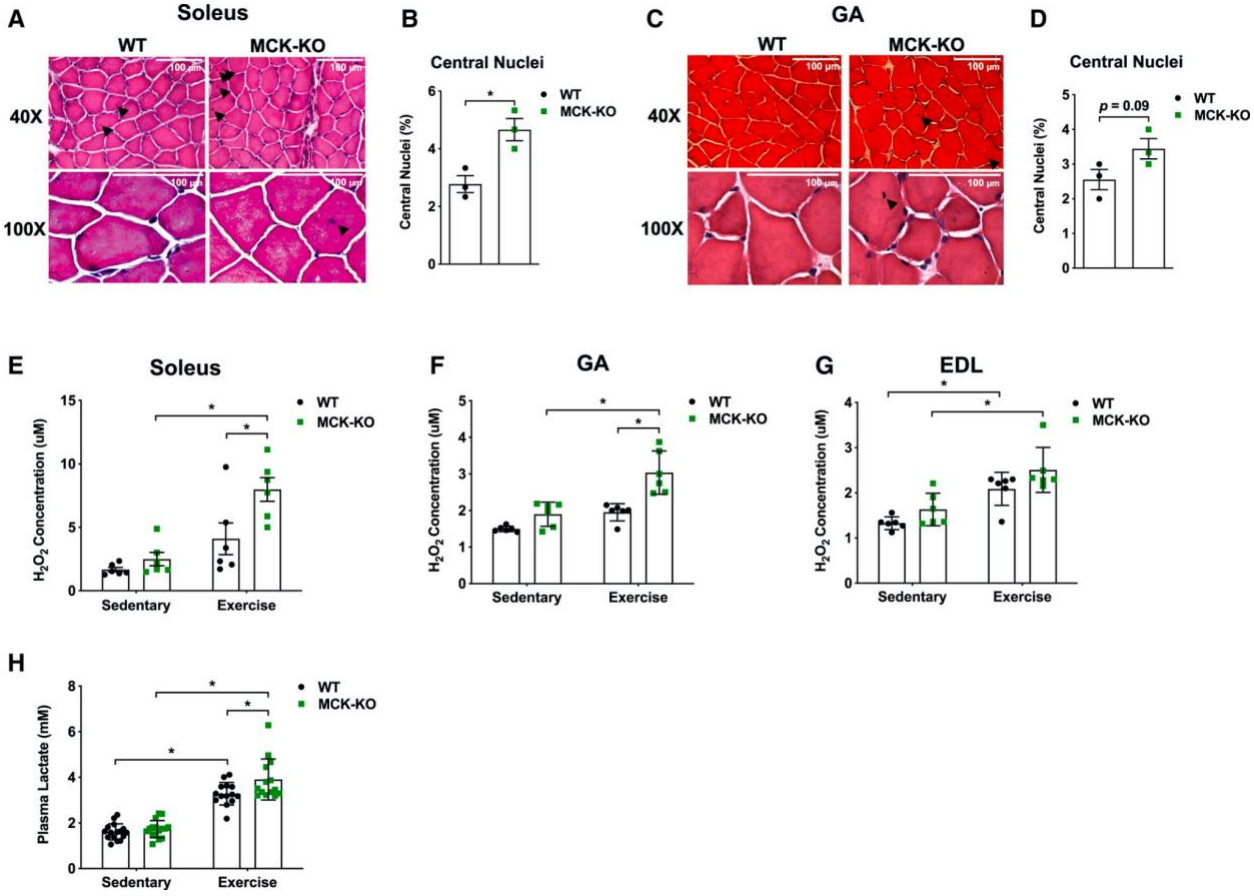

Figure 2. MCK-*Dnmt3a* KO mice display increased muscle damage following exercise. (**A**) The H&E staining of MCK-KO and WT soleus muscle after a bout of low intensity treadmill running (top 40X, bottom 100X magnifications). Black arrow indicates centralized nuclei.

(**B**) The percentage of myofibers with centralized nuclei was determined by manual counting 300 myofibers in 20X magnification. (n = 3, means ± SEM, * $p < 0.05$, two-tailed student's t-test).

(**C-D**) The analogous set of data is shown with WT and MCK-KO GA muscles. (n = 3, means ± SEM, two-tailed student's t-test. GA: Gastrocnemius)

(E-G) Hydrogen peroxide (H_2O_2) levels were measured in WT and MCK-KO soleus (E), GA (**F**), and EDL (**G**) at rest and after a bout of exercise (*n* = 6 per group, means ± SEM, * p < 0.05, two-tailed student's *t*-test and two-way ANOVA followed by Bonferroni post-hoc testing).

(**H**) Serum levels of lactate were measured before and after a bout of low-intense exercise for 50 mins in WT and MCK-KO mice (n = 16 for sedentary and n = 14 for exercise groups, means ± SEM, * p < 0.05, two-tailed student's *t*-test and two-way ANOVA followed by Bonferroni post-hoc testing).

Dnmt3a-KO muscle has reduced oxidative capacity and diminished mitochondrial respiration

High power of oxidative capacity and mitochondrial function of skeletal muscle is critical for supporting endurance exercise. Succinate dehydrogenase (SDH), located in the inner membrane of the mitochondrion, is responsible for oxidizing succinate to fumarate in the citric acid cycle [34]. Hence, we performed SDH staining to distinguish between oxidative and less-oxidative muscles. Remarkably, KO soleus muscles displayed ~20% less SDH activity relative to WT tissues even at the sedentary (**Figs 3A, B**) and that this difference became exacerbated after exercise showing a 50% decline in KO tissues from 8 weeks old mice (**Figs 3C, D**). KO GA muscles showed a similar pattern of SDH activity at rest and following exercise (**Figs. 3E-H**). By contrast, EDL muscles did not show marked differences between genotypes at both conditions (**Figs 3I–L**). We then assessed whether such differences of SDH activity is related to mitochondrial respiration rates and noted that KO soleus muscles exhibit a reduced oxygen consumption rate in both sedentary and exercise conditions (**Figs 3M, N**). We were also able to confirm that myotube-autonomous effect of DNMT3A loss of function in oxygen consumption rates (**Figs 3O–P**). Lastly, we performed H&E staining and SDH staining using successive tissue sections to examine whether damaged myofibers with centro-nucleation overlap with reduced SDH activity.

Skeletal muscle depots are composed of heterogeneous populations of muscle fibers, which are categorized largely as slow-twitch (type I) and fast-twitch (type II) based upon biophysical property of contractility [35]. Slow-twitch fibers are dense in mitochondria to allow high oxidative capacity and sustain long-term energy demands [36]. By contrast, fast-twitch fibers are subdivided into fast-oxidative (type IIA) or fast-glycolytic (type IIB/X), which correlate with their mitochondrial density [36]. The soleus muscle is rich in type I and some IIA myosin heavy chains (MHCs), whereas muscles like EDL are enriched in the faster MHC IIB fibers that are for the fast twitch property [37]. Previous studies suggest that shifting muscle fiber composition is engaged with altered exercise capacity and muscle dysfunction [38]. Collectively, our data suggest that DNMT3A is required for the full oxidative capacity of skeletal muscle and is not associated with fiber type determination.

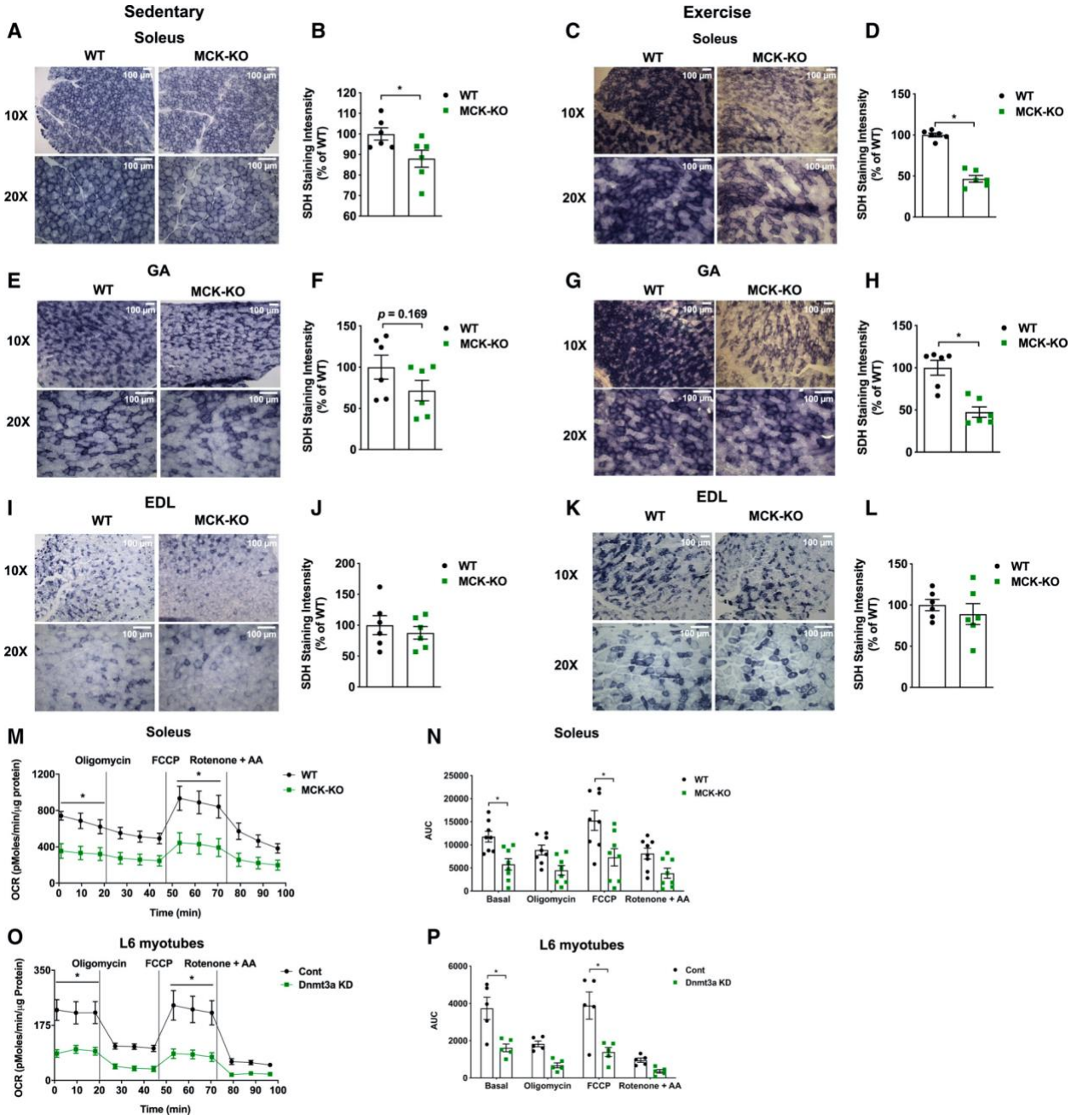

Figure 3. *Dnmt3a*-KO soleus muscle displays a decreased oxidative capacity with a reduced mitochondrial respiration.

(**A-D**) Succinate dehydrogenase staining was performed in WT and MCK-KO soleus at sedentary (**A, B**) and after a bout of low-intensity exercise for 50 min (**C, D**) (10X, 20X magnifications), and the staining intensity was quantified using ImageJ (n = 6, means ± SEM, * $p < 0.05$, two-tailed student's t-test).

(**E-H**) The analogous set of data is shown with WT and MCK-KO GA muscles. (n = 6, means ± SEM, * $p < 0.05$, two-tailed student's t-test).

(**I-L**) The analogous set of data is shown with WT and MCK-KO EDL muscles. (n = 6, means ± SEM, two-tailed student's t-test. EDL: Extensor digitorum longus)
(**M, N**) Mitochondrial respiration was measured in WT and MCK-KO soleus tissue after a bout of low-intensity exercise for 50 min under basal conditions and in response to 4 mM oligomycin (complex V inhibitor), 4 mM FCCP (uncoupler), or 4 mM each of rotenone and antimycin A (complex I inhibitor) (*n* = 8, means ± SEM, * $p < 0.05$, two-tailed student's t-test and two-way ANOVA followed by Bonferroni post-hoc testing).
(**O, P**) Mitochondrial respiration was measured in *Dnmt3a* knocked down L6 myotubes which were transduced with lentiviral under basal conditions and in response to 4 mM oligomycin (complex V inhibitor), 4 mM FCCP (uncoupler), or 4 mM rotenone and antimycin A (complex I inhibitor) (*n* = 5, means ± SEM, * $p < 0.05$, two-tailed student's t-test and two-way ANOVA followed by Bonferroni post-hoc testing).

Gene profiling identifies muscle-specific DNMT3A target genes
We and others have shown that DNMT3A regulates biological processes by regulating non-overlapping sets of cell type–specific target genes [39–41]. To elucidate the underlying molecular basis by which DNMT3A regulates exercise capacity, we performed RNA-Seq on WT and KO soleus muscle at rest and after exercise. The transcriptome profiles detected that 23 genes were upregulated, and 3 genes were downregulated in *Dnmt3a*-deficient soleus muscle at rest, while 18 genes were up and 17 genes were downregulated in the exercise condition (**Figs 4A, B**). While several of the upregulated genes in the KO overlapped conditions, none of the downregulated genes overlapped (**Figs. 4A, B**).

Our search to identify the targets responsible for the increase in ROS production led us to investigate *Aldh1l1*, which encodes aldehyde dehydrogenase 1 family member L1 (ALDH1L1), a cytosolic enzyme involved in folate and one-carbon metabolism. Specifically, ALDH1L1 oxidizes 10-formyltetrahydrofolate to tetrahydrofolate, simultaneously producing NADPH as a byproduct [42] (**Fig 4C**). Notably in this regard, NADPH plays a dual role in the regulation of oxidative stress. On the one hand, it is a reducing agent for glutathione, thioredoxins, peroxiredoxins, and glutathione peroxidases, which neutralize ROS [43]. On the other hand, it contributes to ROS generation, through the activity of the NADPH oxidase complex (NOX) (**Fig 4C**) located within the sarcoplasmic reticulum, transverse tubules, and sarcolemma in skeletal muscle fibers [44]. We hypothesized that ALDH1L1-mediated NADPH production feeds into NOX, thereby increasing intracellular ROS in *Dnmt3a* KO muscle.

First, we examined the regulation of *Aldh1l1* by DNMT3A. We measured the levels of *Aldh1l1* mRNA and ALDH1L1 protein to be elevated in KO muscle tissues (**Figs 4D–F**). Notably, ALDH1L1 expression was elevated only in the red soleus and mixed GA muscles, but not in the white EDL muscle (**Figs 4E, F**), suggesting that muscle depot-selective regulation of *Aldh1l1* by DNMT3A. To determine whether *Aldh1l1* is indeed a direct target of DNMT3A, we performed methylated DNA immunoprecipitation (MeDIP)-qPCR analysis of the CpG rich *Aldh1l1* promoter regions (**Fig 4G**). In KO soleus muscle, DNA methylation was greatly reduced in four of the five regions we examined, including the CpG island (P4) (**Fig 4H**). *In vivo* ChIP assay confirmed strong enrichment of DNMT3A at those differentially

methylated regions (**Fig 4I**). In fact, the DNA methylation and histone regulation machineries often engage in crosstalk [45]. Therefore, we also conducted a ChIP assay for H3K27ac, a histone modification marker of active promoters and enhancers, and detected strong signals at *Aldh1l1* promoter regions in KO soleus tissues (**Fig 4J**). Collectively, these data demonstrate that DNMT3A directly regulates expression of *Aldh1l1* by modifying the epigenetic profile at its regulatory regions.

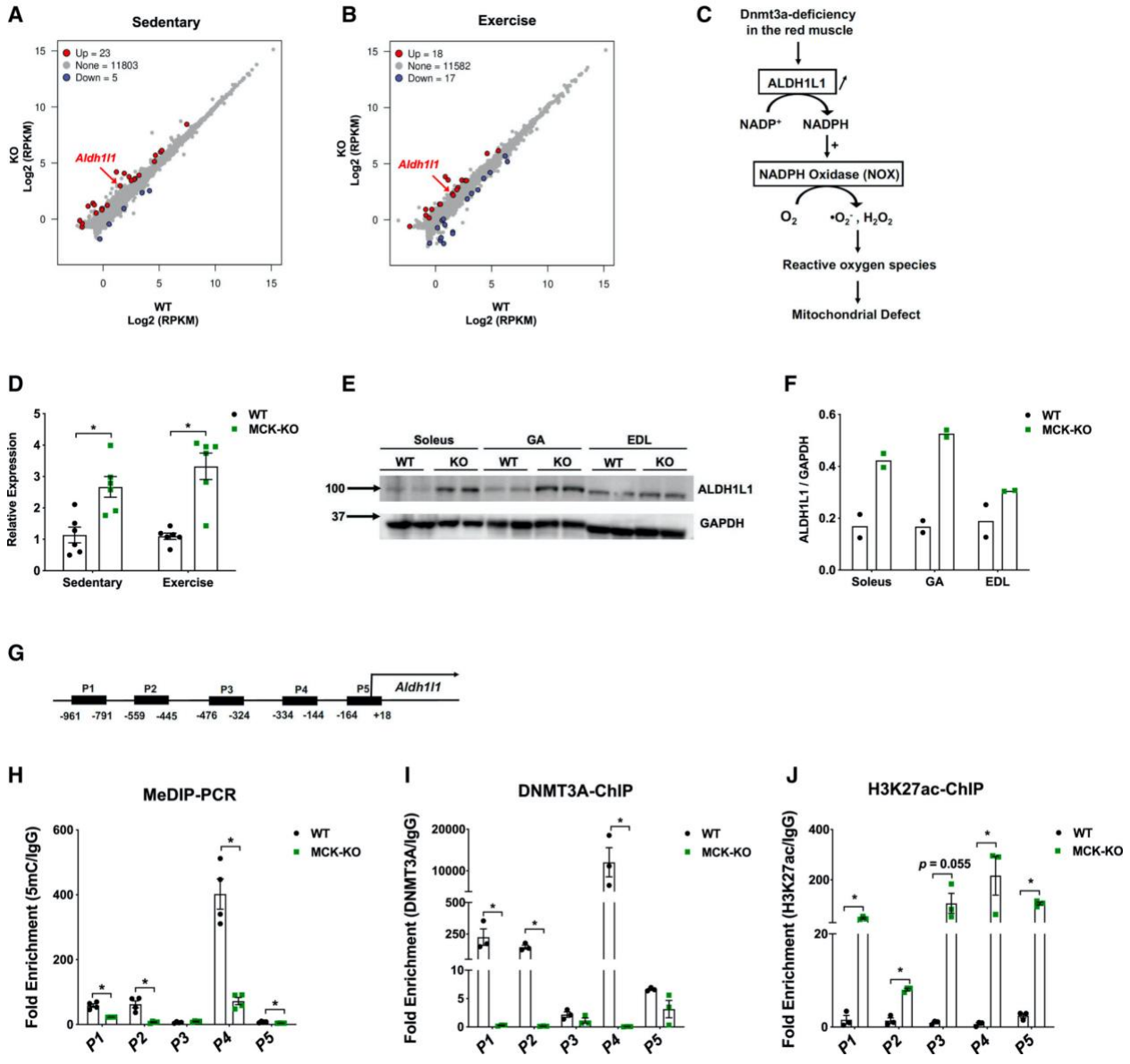

Figure 4. Transcriptome analysis identifies *Aldh1l1* as a key target gene of DNMT3A in the soleus muscle.

(A, B) (**A**) RNA-Seq was performed in WT and MCK-KO soleus muscle at rest. The scatter plots show differentially expressed genes in MCK-KO soleus muscle at sedentary (**A**) and after a bout of low-intensity exercise for 50 min (**B**) (FDR<0.05, p < 0.05).

(**C**) Proposed model for ROS regulation during loss of *Dnmt3a*. Loss of DNMT3A increases ALDH1L1 expression, thus leading to the increase in NADPH levels and increased activity of NADPH oxidase, leading to increased ROS levels. The increased oxidative stress contributes to mitochondrial dysfunction and muscle fatigue.
(**D**) Q-PCR validation of *Aldh1l1* at sedentary and after exercise for 50 min (n = 6, means ± SEM, * $p < 0.05$, two-tailed student's t-test).
(**E, F**) ALDH1L1 protein expression and the quantification in WT vs. MCK-KO soleus, GA and EDL muscles at sedentary and normalizing to GAPDH using ImageJ.
(**G**) The map of CpG-rich promoter regions of *Aldh1l1* and MeDIP and ChIP primers (P1-P5) that cover the CpG rich regions. The numbers correspond to the position from the transcriptional start site of *Aldh1l1*.
(**H**) MeDIP-qPCR was performed in WT and MCK-KO soleus muscle to assess differential methylation using primer sets from (**G**) (n = 4, means ± SEM, * $p < 0.05$, two-tailed student's t-test).
(**I**) DNMT3A ChIP-PCR was conducted in WT and MCK-KO soleus muscles using primer sets from (**G**) (n = 3, means ± SEM, * $p < 0.05$, two-tailed student's t-test).
(**J**) H3K27ac ChIP-PCR was conducted in WT and MCK-KO soleus muscles using primer sets from (**G)** (n = 3, means ± SEM, * $p < 0.05$, two-tailed student's t-test).

ALDH1L1 drives the increase in ROS and mitochondrial dysfunction in KO soleus muscle

To determine whether elevated ALDH1L1 expression is responsible for NADPH-dependent generation of ROS, we compared NADPH levels between WT and KO muscle. Indeed, NADPH levels were significantly increased in KO muscle (**Fig 5A**). To assess whether this in turn results in increased flux into NOX, [46,47] and, indeed, we detected elevated NOX level in KO tissues (**Fig 5B**). Next, to evaluate the functional significance of ALDH1L1, we performed an ALDH1L1 gain-of-function study in L6 rat myotubes in the presence and absence of apocynin, a specific NOX inhibitor [48]. Overexpression of ALDH1L1 had no effect on myogenesis, but remarkably, it was sufficient to recapitulate the redox changes in *Dnmt3a*-KO muscles, including the increases in the levels of NADPH (**Fig 5C**) and ROS (**Figs 5D, E**). More strikingly, ALDH1L1-overexpressing myotubes exhibited a reduced oxygen consumption relative to controls (**Figs 5F, G**). Importantly, all of these changes associated with ALDH1L1 overexpression were largely reversed by treatment with apocynin (**Figs 5C-G**). To obtain evidence that ALDH1L1 is required for the phenotype of the *Dnmt3a* loss-of-function model, we knocked out *Aldh1l1* in *Dnmt3a* knockdown L6 myotubes, which resulted in dramatic rescue of the oxidative stress that is mediated by *Dnmt3a* deficiency (**Figs 5H–K**).

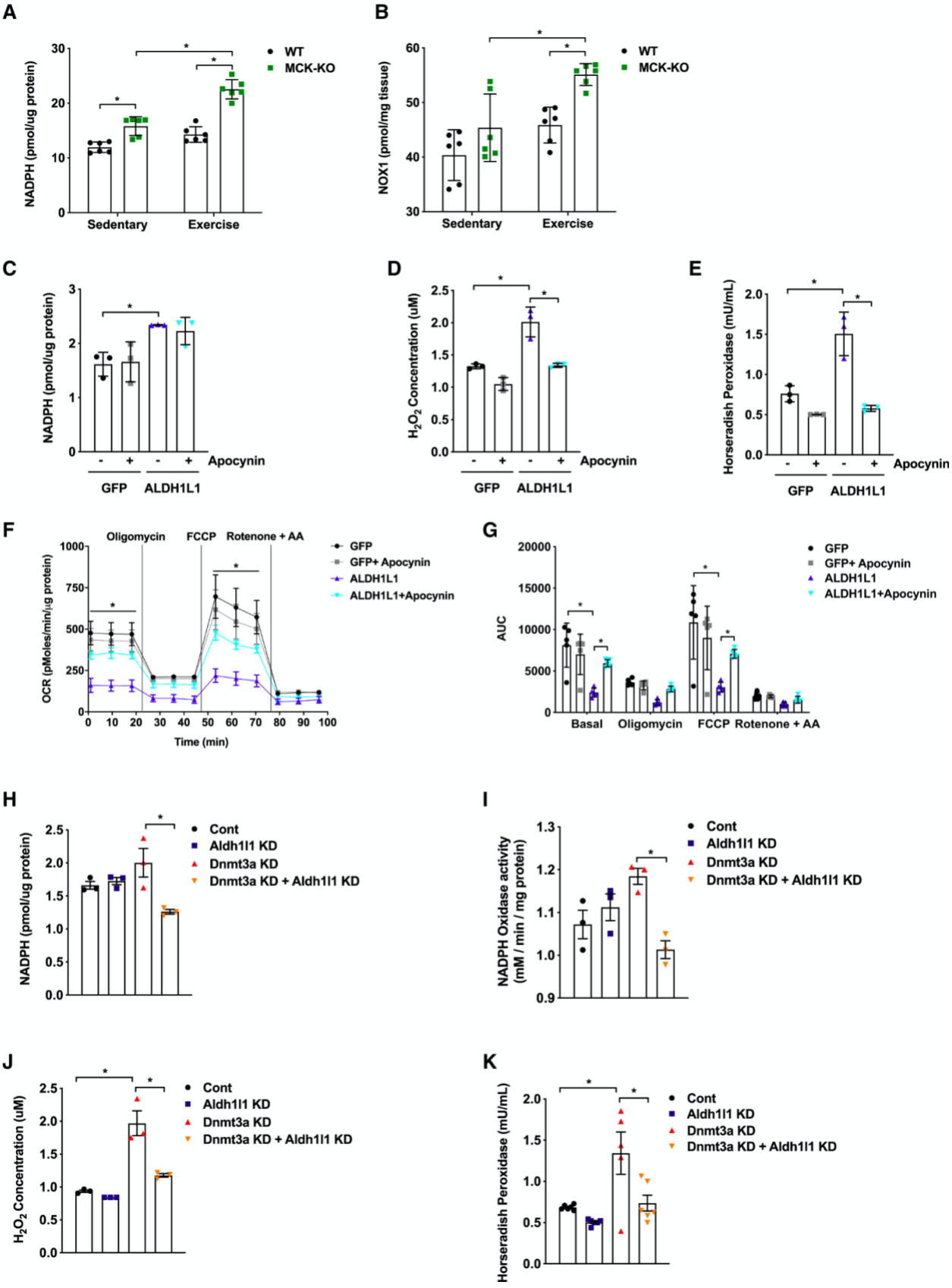
A
NADPH (pmol/ug protein)
WT
MCK-KO
Sedentary
Exercise
B
NOX1 (pmol/mg tissue)
C
NADPH (pmol/ug protein)
Apocynin
GFP
ALDH1L1
D
H2O2 Concentration (uM)
E
Horseradish Peroxidase (mU/mL)
F
Oligomycin
FCCP
Rotenone + AA
OCR (pMoles/min/ug protein)
Time (min)
GFP
GFP+ Apocynin
ALDH1L1
ALDH1L1+Apocynin
G
AUC
Basal
H
Cont
Aldh1l1 KD
Dnmt3a KD
Dnmt3a KD + Aldh1l1 KD
I
NADPH Oxidase activity (mM / min / mg protein)
J
K

Figure 5. ALDH1L1 contributes to the oxidative stress and mitochondrial defect in loss of *Dnmt3a*.

(**A, B**) NADPH levels (**A**) and NOX (**B**) level was measured in WT and MCK-KO muscles at rest and after a bout of low-intensity exercise for 50 min (*n* = 6, means ± SEM, * p < 0.05, two-tailed student's *t*-test and two-way ANOVA followed by Bonferroni post-hoc testing).

(**C-G**) L6 myotubes were transduced with lentiviral expression plasmids for Flag-ALDH1L1 and GFP. NADPH levels (**C**), H2O2 levels (**D, E**) , Mitochondrial respiration (**F, G**) were measured from these cells in the presence and absence of NADPH oxidase inhibitor apocynin (n = 3 per group, for (**C-E**) and n = 5 for (**F, G**), means ± SEM, * p < 0.05, two-tailed student's *t*-test and two-way ANOVA followed by Bonferroni post-hoc testing).

(**H-K**) Single and double knockdowns of *Dnmt3a* and *Aldh1l1* in L6 myotubes were achieved by lentiviral transduction. NADPH levels (**H**) and NOX activity (**I**) were measured in single and double knockdowns of *Dnmt3a* and *Aldh1l1* in L6 myotubes. (n = 3, means ± SEM, * p < 0.05, two-tailed student's *t*-test and two-way ANOVA followed by Bonferroni post-hoc testing). (**J, K**) H2O2 levels were measured in single and double knockdowns of *Dnmt3a* and *Aldh1l1* in L6 myotubes. (**J**: *n* = 3 and **K**: n = 6 for Control, Aldh1l1 KD, Aldh1l1 KD + Dnmt3a KD, n = 5 for Dnmt3a KD, means ± SEM, * p < 0.05, two-tailed student's *t*-test and two-way ANOVA followed by Bonferroni post-hoc testing).

Resolving oxidative stress and muscle-targeted *Aldh1l1* silencing in MCK-Dnmt3a KO mice partially rescues exercise intolerance

Since we hypothesized that excessive ROS production is a main driver of muscle dysfunction and exercise incapacity during loss of *Dnmt3a*, we sought to determine whether an antioxidant could resolve the issues. Remarkably, a single i.p. injection of N-acetylcysteine (NAC) rescued exercise capacity in KO mice by 43% but had no significant effect on WT's exercise performance (**Figs 6A, B**). Consistent with this data, we confirmed that NAC reduced ROS levels in *Dnmt3a* KD myotubes (**Fig 6C**) and significantly improved mitochondrial respiration (**Figs 6D, E**). Lastly, we sought to determine whether decreasing ALDH1L1 levels can rescue the exercise intolerance detected in *Dnmt3a* KO mice. To this end, we chose to use *in vivo* transfection method which allows us to specifically transfect the nuclei of terminally differentiated adult muscle fibers, but not the nuclei of satellite cells or connective tissue cells [49]. We delivered gRNA against *gAldh1l1* or control to the GA and soleus muscles in the KO mice and we achieved ~ 50% knock-down of *Aldh1l1* mRNA and protein in soleus and GA, but without a major change in EDL (**Figs 7A–C**). Remarkably, *Dnmt3a* KO mice that were delivered with *Aldh1l1* knock-down gRNA partially restored the ability of treadmill running by 47 % and 38% by time and distance, respectively, compared to the KO mice transfected with control gRNA (**Figs 7D, E**). Together, our results suggest that ALDH1L1 plays a critical role in producing muscle dysfunction and exercise intolerance arising from *Dnmt3a* deficiency.

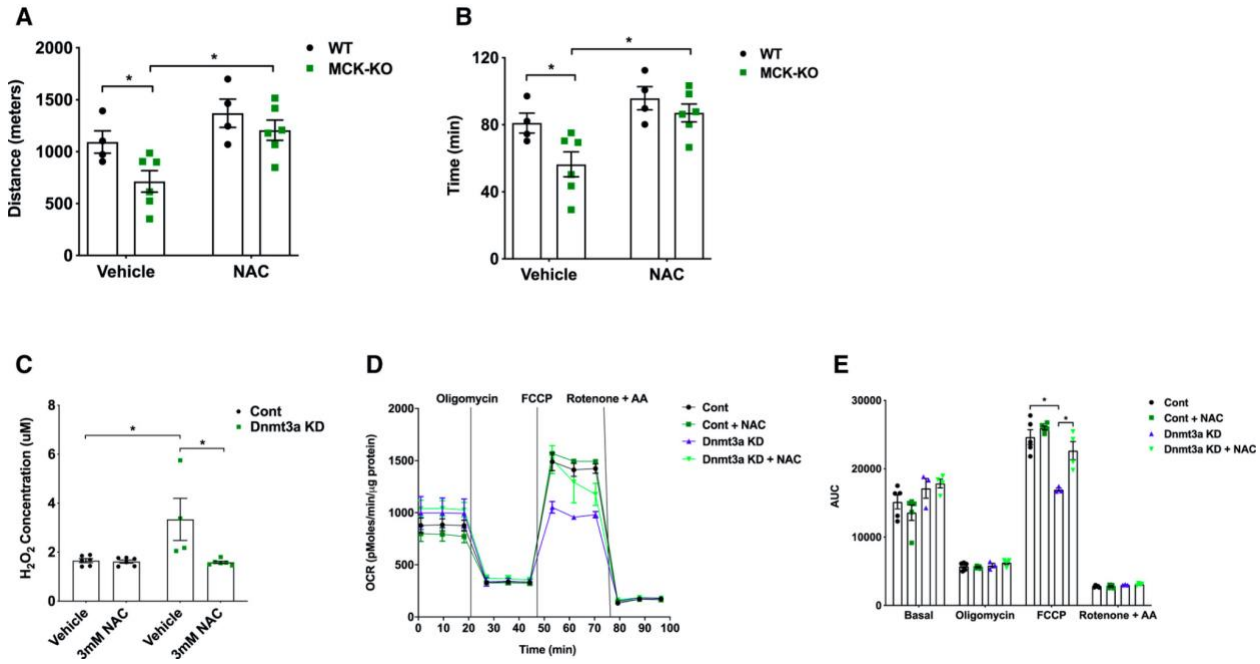

Figure 6. NAC treatment partially rescues reduced oxidative capacity in Dnmt3a KD myotubes and exercise intolerance in MCK-*Dnmt3a* KO mice.

(**A, B**) Exercise capacity of MCK-KO and WT mice treated with PBS (vehicle) or NAC (200mg/kg, i.p). (n = 4 WT and n = 6 MCK-KO , mean ±SEM, * $p < 0.05$, two-tailed student's t-test and two-way ANOVA).

(**C-E**) (**C**) Hydrogen peroxide (H_2O_2) levels (n = 6 for Control groups and Dnmt3a KD with NAC treatment group n = 4 Dnmt3a KD, means ± SEM, * $p < 0.05$, two-tailed student's t-test and two-way ANOVA followed by Bonferroni post-hoc testing).(**D, E**) mitochondrial respiration in *Dnmt3a* knockdown and control L6 myotubes treated with NAC (3mM) or vehicle treatment for 24hrs (n = 5 Control groups n = 3 Dnmt3a KD, n = 4 *Dnmt3a* KD with NAC treatment groups. means ± SEM, * $p < 0.05$, two-tailed student's t-test and two-way ANOVA followed by Bonferroni post-hoc testing).

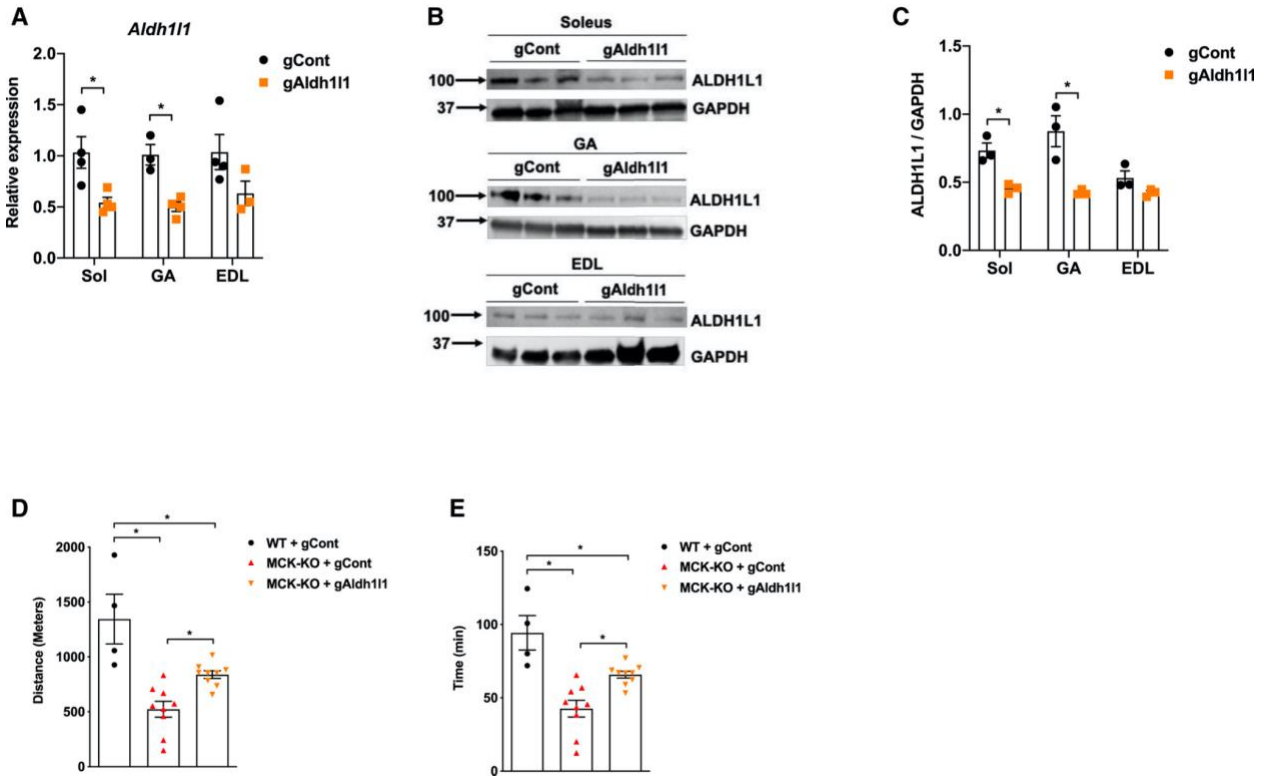

Figure 7. ALDH1L1 knockdown *in vivo* partially rescues exercise intolerance in MCK-*Dnmt3a* KO mice.

(**A**) *Aldh1l1* mRNA expression in various muscles in MCK-KO mice that were transfected with gRNA DNAs against Aldh1l1 or control. (n = 4 for Soleus, n = 3 GA gCont and n = 4 GA gAldh1l1, n = 4 EDL gCont and n = 3 EDL gAldh1l1 , means ± SEM, * p < 0.05, two-tailed student's t-test).

(**B, C**) ALDH1L1 protein expression and the quantification in MCK-KO muscles that were transfected with gCont vs. gAldh1l1 using ImageJ. (n = 3, means ± SEM, * p < 0.05, two-tailed student's t-test).

(**D, E**) Exercise capacity of WT and MCK- KO with or without transfection of gCont vs. gAldh1l1 under the low intensity regimen (*n* = 4 WT + gCont, *n* = 9 MCK- KO + gCont, and MCK- KO + gAldh1l1, *p<0.05, means ± SEM, two-tailed student's *t*-test and one-way ANOVA).

Discussion

Exercise significantly alters the DNA methylation profile of skeletal muscle [18–26], however, it has not been studied whether DNA methylation machinery has functional roles in exercise capacity. Here, we demonstrate that skeletal muscle DNMT3A plays an essential role for the full capacity to perform endurance exercise. Our findings indicate that

Dnmt3a deficiency in skeletal muscle leads to oxidative stress and muscle fatigue and consequently a dramatic reduction of exercise capacity. Surprisingly, our studies find that skeletal muscle DNMT3A is necessary to maintain mitochondrial function and oxidative capacity, which are critical to support endurance exercise. Our mechanistic studies reveal that ALDH1L1 as a key downstream effector of DNMT3A loss of function as evidenced by that knock-down of ALDH1L1 that can largely rescue defects from *Dnmt3a* deficiency *in vitro* and *in vivo*, while overexpression of ALDH1L1 recapitulates them. These findings demonstrate a surprising role for DNMT3A as an epigenetic modulator of endurance exercise by controlling intracellular oxidative stress and reveal ALDH1L1 as a key mediator.

Studies have reported that aerobic exercise changes DNA methylation profile. For example, a human study has shown that a single bout of aerobic exercise transiently induces promoter DNA hypomethylation of promoter regions of important mitochondria-related genes (e.g., *PPARGC1A*, *PDK4*, *TFAM*, and *PPARD*), followed by their induction [18]. on the basis of this human study, our results showing the requirement of DNMT3A in endurance exercise as counterintuitive. However, it should be noted that exercise affects DNA methylation profile in either direction depending on loci. As an example, another human study reported that moderate-intensity exercise results in hypermethylation of *FABP3* and *COX4L1*, which negatively correlated with their expression [25,50]. By the same token, genome-wide studies have reported that both acute and chronic exercise interventions produce profound changes in CpG methylation [18–26]. We did not observe that *Dnmt3a* deficiency in soleus alter the expression of the genes that were shown to be differentially methylated in association with exercise.

Mitochondria in skeletal muscle are highly dynamic organelles that exhibit remarkable plasticity, adapting their content, structure, and metabolism in response to a variety of physiological and pathophysiological stresses including exercise, disuse, and aging [51,52]. Exercise training increases mitochondrial biogenesis to satisfy elevated energy requirements by increasing oxidative capacity to ensure optimal ATP supply; this has the consequence of favoring lipid metabolism [53,54]. Thus, exercise represents a viable therapy, with the potential to reverse the impairment of mitochondrial function associated with diseases such as type 2 diabetes, and aging-related sarcopenia [55–57] . In this regard, a key link between exercise and control of mitochondrial biology was revealed by the observation that PGC-1α expression is transiently induced in skeletal muscle following an acute bout of exercise [58]. Since that discovery, a great deal of research effort has been devoted to elucidating the role of PGC1A in skeletal muscle mitochondrial biology and exercise. For example, transgenic expression of PGC1A increases mitochondrial content and function and the abundance of oxidative type I muscle fibers, while decreasing muscle fatigue. However, loss of PGC1A has only a mild effect on exercise capacity and does not alter fiber-type composition in muscle [59] or affect training-induced increase in the expression of genes involved in oxidative phosphorylation [60]. This suggests that PGC1A is sufficient, but not necessary, to mediate metabolic adaptations in response to exercise. We believe that the role of DNMT3A in the regulation of mitochondrial biology is likely to be PGC1A-independent as PGC1A mRNA and protein levels are not altered in *Dnmt3a* KO muscles.

Overproduction of ROS induced by unaccustomed, exhaustive exercise training or other stresses can lead to oxidative stress–related tissue damage and reduced contractility [61,62], involving impaired cellular function, macromolecule damage and apoptosis [63]. Mitochondria are highly susceptible to chronic high levels of ROS-mediated damage, and a heterogeneous class of human diseases, such as aging, cancer, neurodegenerative disorders, and diabetes, have been linked to mitochondrial defects and oxidative stress [63–65]. Despite the clinical significance, the molecular mechanisms involved in mitochondrial dysfunction and increased ROS production are not well understood. Recent studies have proposed a link between epigenetic factors and ROS-mediated adaptation in skeletal muscle [66–69]. Our results suggest DNMT3A is a critical epigenetic modulator of ROS and thereby helps to prevent oxidative stress–mediated myopathy. NADPH oxidases are major contributors to ROS production in skeletal muscle [70,71]. It has been shown that physical stretching can increase the activity of NADPH oxidase, especially NOX2, causing production of ROS in microtubule-dependent processes [72]. While that study described mechanotransduction-dependent activation of NADPH in cardiac muscles, here we identified ALDH1L1-dependent activation of NADPH oxidase as a contributor to ROS overproduction, especially in oxidative muscles, during loss of *Dnmt3a*. Our finding that inhibiting NADPH oxidase rescued both oxidative stress and mitochondrial dysfunction raises the possibility of repurposing these inhibitors to improve exercise trainability. Further understanding the epigenetic and molecular basis of DNMT3A to moderate ROS will help us address several critical health issues that are derived from exercise-induced high levels of ROS in the pathogenic processes of relevant human diseases.

ALDH1L1 is a folate-metabolizing enzyme that controls the overall flux of one-carbon groups in folate-dependent biosynthetic pathways, with simultaneous production of NADPH from NADP. Differential methylation of *ALDH1L1* has been reported with an implication in tumor development and progression in several cancer models [73–75] . Other than that, little has been known about physiological functions of ALDH1L1 in skeletal muscle biology. Here, we outline that ALDH1L1, whose transcriptional level is epigenetically regulated by DNMT3A especially in soleus and GA muscles, plays a determining role in *Dnmt3a* deficiency-induced oxidative stress and exercise intolerance.

Overall, we highlight the surprising role of DNMT3A in endurance exercise and skeletal muscle mitochondrial biology. Mechanistically, we reveal that ALDH1L1 serves as a novel molecular link that contributes to oxidative stress and mitochondrial dysfunction following the loss of *Dnmt3a* in red muscle. This is of great importance from the standpoint of exercise physiology, as physical activity is strongly encouraged as a key strategy for preventing and treating a wide range of human diseases. Understanding the epigenetic and molecular basis of exercise tolerance will help us to address critical health issues that arise from reduced ability to perform exercise.

Materials and Methods

Animals

Animal Care Mice were maintained under a 12-hr light /12-hr dark cycle at constant temperature (23°C) with free access to food and water. All mice were extensively back-crossed onto a C57BL/6J background. All animal work was approved by UC Berkeley ACUC. *In vivo* assays were done with 7- to 20-week-old littermate male mice.

Measurement of exercise capacity

All mice were acclimated to the treadmill prior to the exercise test session. For each session, food was removed 2 hr before exercise. Acclimation began at a low speed of 5 to 8 meters per minute (m/min) for a total of 10 min on Day 1 and was increased to 5 to 10 m/min for a total of 10 min on Day 2. The experiments were performed on Day 3. For the low intensity treadmill test, the treadmill began at a rate of 12 m/min for 40 min. After 40 min, the treadmill speed was increased at a rate of 1 m/min every 10 min for a total of 30 min, and then increased at the rate of 1 m/min every 5 min until the mice were exhausted. The high intensity treadmill test was conducted on the same open-field six-lane treadmill set at a 10% incline. Following a 5-min 0 m/min acclimation period, the speed was raised to 6 m/min and increased by 2 m/min every 5 min to a maximal pace of 30 m/min until exhaustion. Mice were considered exhausted when they were unable to respond to continued prodding with a soft brush. For the rescue experiment with *N*-Acetylcysteine (NAC, (Sigma, #A7250), mice were intraperitoneally injected with 200 mg/kg 4 hours prior to the exercise capacity test.

RNA-Seq library generation and analysis

RNA samples were extracted using the RNeasy Mini kit (Qiagen, 74104), and the quality of total RNA was assessed by the 2100 Bioanalyzer (Agilent) and agarose gel electrophoresis. Libraries were prepared using the BGI Library Preparation Kit, and sequencing was performed on the BGISEQ (BGI, China). RNA-Seq reads were aligned to the UCSC mm10 genome using HISAT2 (Hierarchical Indexing for Spliced Alignment of Transcripts [76], and mapping was done using Bowtie2 [76]. Differentially regulated genes were calculated using DEseq2 [77].

Measurement of NADPH

The NADPH measurement was performed on GA/Soleus or L6 myotube extracts using the NADP/NADPH assay kit (Cat#K347, BioVision) according to the manufacturer's instructions. Briefly, ~20 mg tissue samples or 4 x 10^6 cells were extracted in 400 µL of the given extraction buffer, and 50 µL was processed following instructions of the kit. OD450 measurements were made on a plate-reader (SpectraMAX i3 Plate reader) at 25°C, and the data was calculated using a standard curve.

Measurement of NADPH oxidase activity

NOX activity was measured by accessing oxidation of NADPH through Continuous Spectrophotometric Rate Determination [46,47]. Briefly, samples of tissue or cells were extracted in 500 µL and 200µL of potassium phosphate buffer, respectively. The tissues and cells were first homogenized and then sonicated. The homogenate was centrifuged at

top speed for 10 min, and the supernatant was used for reading. Oxidation of NADPH was monitored at 340 nm on the SpectraMAX i3 Plate Reader at 30°C [46,47].

MeDIP-qPCR

Genomic DNA was sheared using a Covaris S220 sonicator to an average of 200–600 bp. 600 ng of denatured DNA was incubated with 2 mg of 5-methylcytosine (5-mC) monoclonal antibody ([33D3] Diagenode, Cat No # C15200081) in IP buffer (0.1% SDS, 1 Triton X-100, 2 mM EDTA, 20 mM Tris-HCl pH 8.1, 150 mM NaCl) for 1 h at 4°C on a rotating wheel. Antibody-bound DNA was collected with 20 ml of protein A/G PLUS-Agarose (#sc-2003) for 1 h at 4°C on a rotating wheel and successively washed three times with IP buffer (0.1% SDS, 1 Triton X-100, 2 mM EDTA, 20 mM Tris-HCl pH 8.1, 150 mM NaCl). DNA was recovered in 100 ml of digestion buffer (50 mM Tris pH 8.0, 0.5% SDS, 35 mg proteinase K) and incubated overnight at 65°C. Recovered DNA was used for qPCR analysis. Primers for MeDIP-qPCR studies are listed in **Appendix Table S1**. All data were normalized to input.

ChIP-qPCR

Soleus muscles were homogenized in dounce homogenizer using Nuclei Preparation Buffer (10mM HEPES (pH7.5), 10mM KCl, 1.5mM MgCl2, 0.1% NP40) and crosslinked with 1% formaldehyde for 10 min, then neutralized with glycine and rinsed with cold phosphate-buffered saline. After nuclei isolation, samples were sonicated using an S220 Covaris to generate DNA fragments of ~200–500 bp. Inputs were taken from cleared lysates, and the rest were rotated O/N at 4°C with DNMT3A, H3K27ac, and IgG antibodies for immunoprecipitation. An aliquot of 20 µl of protein A/G PLUS-Agarose (#sc-2003) were added per IP and rotated 1 hr at 4°C. Beads were successively washed in low-salt RIPA buffer (20 mM Tris-HCl [pH 8.0], 1 mM EDTA, 1% Triton x-100, 0.1% SDS,140 mM NaCl, 0.1% Na deoxycholate), high-salt RIPA buffer (20 mM Tris-HCl [pH 8.0], 1 mM EDTA, 1% Triton x-100, 0.1% SDS, 500 mM NaCl, 0.1% Na deoxycholate), LiCl buffer (250mM LiCl, 0.5% NP40, 0.5% Na deoxycholate, 1 mM EDTA, 10 mM Tris-HCl [pH 8.0]) and TE buffer (10 mM Tris-HCl [pH 8.0] and 1 mM EDTA). Each reaction was then incubated in digestion buffer (50 mM Tris-HCl [pH 8.0], 1 mM EDTA, 100 mM NaCl, 0.5% SDS, proteinase K) for a minimum of 4 hr at 65°C to reverse cross-links. DNA was recovered using a phenol-chloroform extraction. Recovered DNA was used for qPCR analysis. Primers for CHIP-qPCR studies are listed in Appendix Table S1. All data were normalized to input.

Cell culture

L6 rat myoblasts (UCSF Cell Culture Facility Core) were maintained in Dulbecco's modified Eagle's medium (DMEM) supplemented with 10% fetal bovine serum, 100 U/ml penicillin, and 100 µg/ml streptomycin. Culture conditions were maintained in a humidified incubator under an atmosphere of 5% CO_2 at 37°C. Differentiation was carried out in DMEM supplemented with 2% horse serum. To generate lentivirus particles, lentiviral constructs were co-transfected with pMD2.G- and psPAX2-expressing plasmids into 293T cells. After 48 h, the virus-containing supernatant was collected, filtered through 0.45-mm filters, and added to mature L6 myotubes for 48 h along with 8 mg/ml polybrene. Transduction efficiency was determined by comparing to cells transduced in parallel with a GFP-expressing lentivirus.

In vivo electroporation

Mice were anesthetized by an IP injection of 91 mg/kg ketamine and 9.1 mg/kg xylazine, after which hindlimbs were shaved, and the GA muscles were injected with 30 µl hyaluronidase solution (which was prepared by resuspending bovine placental hyaluronidase (Sigma) in sterile injectable 0.9% NaCl at a concentration of 0.4 U/µl). Mice were anesthetized two hours later and the GAs were injected with 180ug plasmid DNA in sterile saline. After injection of plasmid DNA, the hind limbs were placed between two-paddle electrodes and subjected to 10 pulses (20 mSec) of 175 V/cm (with 480-mSec intervals between pulses) using an ECM-830 electroporator (BTX Harvard Apparatus, Holliston, MA).

ROS Measurement

Accumulation of hydrogen peroxide (H_2O_2) and horseradish peroxidase was measured using OxiSelect™ Hydrogen Peroxide/Peroxidase Assay Kit (Cell Biolabs, Inc., San Diego, CA), a sensitive quantitative fluorometric assay for hydrogen peroxide or peroxidase activity levels. To investigate H_2O_2 accumulation, the muscle tissues or L6 myotubes were homogenized in 1× assay buffer provided from the kit followed by centrifuging to remove debris. These lysates were then assayed according to the manufacturer's procedure.

Mitochondrial respiration

For tissue respiration, mice were allowed to run for 50 min on the low-intensity regime. Following this, WT and MCK-Dnmt3a KO soleus tissues were isolated and seeded in XF24 plates (catalog #101122-100,
Seahorse Bioscience). For cellular respiration, lentivirally transduced L6 were plated on XF24 Cell Culture Microplates catalog #100777-004, Seahorse Bioscience). Measurement of intact tissue and cellular respiration was performed using the Seahorse XF24 analyzer (Seahorse Bioscience). Oxygen consumption rates (OCRs) (picomoles of O2 per minute) were measured under basal conditions after three consecutive injections of the following: (1) oligomycin (ATP synthase inhibitor; 4 µM); (2) the electron transport chain accelerator ionophore FCCP (4 µM; FCCP treatment gives the maximal OCR capacity of the cells); and (3) the electron transport chain inhibitors Rotenone (4uM) and Antimycin A (4uM).

Data Availability

RNA-Seq data can be found GSE159105.

Statistical Analysis

Data are presented as means ± SEM and individual data points are plotted. Sample size was determined by our experience with inherent variability. No statistical method was used to predetermine sample size. Statistical analyses and the number of samples (*n*) were described in detail for each figure panel. Statistical analyses and the number of samples (*n*) is described in detail for each figure panel. Two-tailed unpaired Student's *t* test was

used for the comparison between two groups. One-way analysis of variance (ANOVA) or two-way ANOVA followed by the Bonferroni's test was used for the multiple comparisons. Statistical analyses were performed using excel and GraphPad Prism. All reported *p* values were two-sided and differences were considered significant at $p < 0.05$.

Author Contributions

SK supervised experiments and wrote the manuscript. SDV drafted the result, method, and legend sections. Experiments were carried out by SDV, DY, JK, HHP, BCC, and SK. HL analyzed RNA-Seq. SME and CMA contributed to mouse histology and *in vivo* transfection assays.

Acknowledgements

We thank Dr. Hei Sook Sul, Dr. Jen-Chywan Wally Wang, and Dr. Anders Näär for helpful conversations about the manuscript. We are very grateful to Dr. Brian Black and Emily Wilson for technical help with histology, Sarah Fung, Lilian Kim, Anna Pi, Tabitha Tcheau, Sarah, and Sarah Ampalloor, Mrinalini Jain, Pouya Amin, and Michelle Tampa for their technical supports.

Funding

Work was funded by AHA Award # 19POST34380834 to DY and R01 DK116008 to SK.

Conflict of interest

The authors declare no conflict of interest.

Appendix Table S1. Oligonucleotide sequences used in this manuscript

Hairpin	(m/r) shDnmt3a	CGCTCCGCTGAAGGAATATTT
gRNA	(r) gAldh1l1	CGAGGTGGTGGGTGTGTTCA
Q-PCR	(m) Cyclophilin_f	GGTGGAGAGCACCAAGACAGA
Q-PCR	(m) Cyclophilin_r	GCCGGAAGTCGACAATGATG
Q-PCR	(r) Cyclophilin_f	CCAAACACAAATGGTTCCCAGT
Q-PCR	(r) Cyclophilin_r	ATTCCTGGACCCAAAACGCT
Q-PCR	(m) Dnmt3a_f	GTGGAGCCTGAAGCAGCTG
Q-PCR	(m) Dnmt3a_r	CTGGCACATGCCTCCAATGAA
Q-PCR	(m) Dnmt3b_f	CCATGGTGGTGTCCTGGAAA
Q-PCR	(m) Dnmt3b_r	CAGGACTGCTGGAGAAGGTCT
Q-PCR	(m) Ppargc1a_f	AGCCGTGACCACTGACAACGAG
Q-PCR	(m) Ppargc1a_r	GCTGCATGGTTCTGAGTGCTAAG
Q-PCR	(m) Aldh1l1_f	GGTGACCCTGTTTTCCCTACT
Q-PCR	(m) Aldh1l1_r	GGGATCTGCTTTCCCATCCT
Q-PCR	(r) Myf5_f	TGAGGGAGCAGGTAGAGAAC
Q-PCR	(r) Myf5_r	CTGTTCTTTCGGGACCAGAC
Q-PCR	(r) Myh6_f	CGAGACGGTGGTGGGGCTGT
Q-PCR	(r) Myh6_r	CCTTTCCCACTGTCACCGGTATC
Q-PCR	(r) Myh7_f	GATGTTTTTGTGCCTGATGA
Q-PCR	(r) Myh7_r	CAGTCACCGTCTTGCCATTCT
Q-PCR	(r) Myog_f	CTACAGGCCTTGCTCAGCTC
Q-PCR	(r) Myog_r	TGGAGTTGCATTCACTGG
Q-PCR	(m) MHC1_f	GCCAACTATGCTGGAGCTGATGCCC
Q-PCR	(m) MHC1_r	GGTGCGTGGAGCGCAAGTTTGTCATAAG
Q-PCR	(m) MHCIIA_f	GGCACAAACTGCTGAAGCAGAGGC
Q-PCR	(m) MHCIIA_r	GGTGCTCCTGAGGTTGGTCATCAGC
Q-PCR	(m) MHCIIX_f	GGCAGCAGCAGCTGCGGAAGCAGAGTCTGG
Q-PCR	(m) MCHIIX_r	GAGTGCTCCTCAGATTGGTCATTAGC
Q-PCR	(m) MHCIIB_f	GAGCTACTGGATGCCAGTGAGCGC
Q-PCR	(m) MHCIIB_r	CTGGACGATGTCTTCCATCTCTCC
Q-PCR	(m) Ctxn3_f	GGGCATCCTCATTGTCAGGT
Q-PCR	(m) Ctxn3_r	TCAGCCCATGTTGAGGTTGG
Q-PCR	(m) Dnaic1_f	CGAACTTTTCAGCCACAGCC
Q-PCR	(m) Dnaic1_r	CCGTGTCCCACTGCAAAAAG
Q-PCR	(m) Mttp_f	GGAAGGCAGAGCTTCATGGT
Q-PCR	(m) Mttp_r	GGCTTCAGCCTTGTCCATCT
Q-PCR	(m) Plin3_f	GAGCGGGGTGGACACAGTGC
Q-PCR	(m) Plin3_r	CAAGGGATGTGGCGAGGCGG
Q-PCR	(m) Myh8_f	CAGGAGCAGGAATGATGCTCTGAG
Q-PCR	(m) Myh8_r	AGTTCCTCAAACTTTCAGCAGCCAA
Q-PCR	(m) Kcne1l_f	GGTCGTCCCTGACCCTTTC
Q-PCR	(m) Kcne1l_r	CGGCTAGGCAGGCATAGAA
Q-PCR	(m) Nos1_f	CTCGGGCATACCCTCACTTC
Q-PCR	(m) Nos1_r	ATGTTGACGTCATCCCCCAC
MeDIP/ChIP	(m) Aldh1l1-P1_f	TAAGGAGTCTCAGCGGTGGT

MeDIP/ChIP	(m) Aldh1l1-P1_r	TGGGCAGAGTCATTGTCCTA
MeDIP/ChIP	(m) Aldh1l1-P2_f	GGCATGCTAGGCAATGAACT
MeDIP/ChIP	(m) Aldh1l1-P2_r	CTCAGGTCATCCGTCCATTT
MeDIP/ChIP	(m) Aldh1l1-P3_f	GGTGAAGGAAATGACCCAAA
MeDIP/ChIP	(m) Aldh1l1-P3_r	ATGAGTGAGGAGGCAAGGAG
MeDIP/ChIP	(m) Aldh1l1-P4_f	CTGCTTCCTGCCTCCTTG
MeDIP/ChIP	(m) Aldh1l1-P4_r	CTAGCATGCCCGGAACCTA
MeDIP/ChIP	(m) Aldh1l1-P5_f	AAATGGACGGATGACCTGAG
MeDIP/ChIP	(m) Aldh1l1-P5_r	CCTCCAGGCAGAGAAGAGG

(m); mouse
(r); rat

References

1 Baskin, K.K. *et al.* (2015) Muscle as a “mediator” of systemic metabolism. *Cell Metab.* 21, 237–248

2 Hawley, J.A. *et al.* (2014) Integrative biology of exercise. *Cell* 159, 738–749

3 Huertas, J.R. *et al.* (2019) Stay fit, stay young: mitochondria in movement: the role of exercise in the new mitochondrial paradigm. *Oxid. Med. Cell. Longev.* 2019, 7058350

4 Clausen, J.P. and Trap-Jensen, J. (1970) Effects of training on the distribution of cardiac output in patients with coronary artery disease. *Circulation* 42, 611–624

5 He, F. *et al.* (2016) Redox mechanism of reactive oxygen species in exercise. *Front. Physiol.* 7, 486

6 Gomes, E.C. *et al.* (2012) Oxidants, antioxidants, and the beneficial roles of exercise-induced production of reactive species. *Oxid. Med. Cell. Longev.* 2012, 756132

7 Powers, S.K. *et al.* (2011) Reactive oxygen species: impact on skeletal muscle. *Compr. Physiol.* 1, 941–969

8 Di Meo, S. *et al.* (2016) Role of ROS and RNS sources in physiological and pathological conditions. *Oxid. Med. Cell. Longev.* 2016, 1245049

9 Panday, A. *et al.* (2015) NADPH oxidases: an overview from structure to innate immunity-associated pathologies. *Cell. Mol. Immunol.* 12, 5–23

10 Cross, A.R. and Segal, A.W. (2004) The NADPH oxidase of professional phagocytes--prototype of the NOX electron transport chain systems. *Biochim. Biophys. Acta* 1657, 1–22

11 Daiber, A. (2010) Redox signaling (cross-talk) from and to mitochondria involves mitochondrial pores and reactive oxygen species. *Biochim. Biophys. Acta* 1797, 897–906

12 Daiber, A. *et al.* (2017) Crosstalk of mitochondria with NADPH oxidase via reactive oxygen and nitrogen species signalling and its role for vascular function. *Br. J. Pharmacol.* 174, 1670–1689

13 Dan Dunn, J. *et al.* (2015) Reactive oxygen species and mitochondria: A nexus of cellular homeostasis. *Redox Biol.* 6, 472–485

14 Steinbacher, P. and Eckl, P. (2015) Impact of oxidative stress on exercising skeletal muscle. *Biomolecules* 5, 356–377

15 Görlach, A. *et al.* (2015) Calcium and ROS: A mutual interplay. *Redox Biol.* 6, 260–271

16 Jaenisch, R. and Bird, A. (2003) Epigenetic regulation of gene expression: how the genome integrates intrinsic and environmental signals. *Nat. Genet.* 33 Suppl, 245–254

17 Bird, A.P. and Wolffe, A.P. (1999) Methylation-induced repression--belts, braces, and chromatin. *Cell* 99, 451–454

18 Barrès, R. *et al.* (2012) Acute exercise remodels promoter methylation in human skeletal muscle. *Cell Metab.* 15, 405–411

19 Kanzleiter, T. *et al.* (2015) Exercise training alters DNA methylation patterns in genes related to muscle growth and differentiation in mice. *Am. J. Physiol. Endocrinol. Metab.* 308, E912-20

20 Widmann, M. *et al.* (2019) Physical exercise and epigenetic modifications in skeletal muscle. *Sports Med.* 49, 509–523

21 Valenzuela, N. *et al.* (2017) HIRA deficiency in muscle fibers causes hypertrophy and susceptibility to oxidative stress. *J. Cell Sci.* 130, 2551–2563

22 Li, F. *et al.* (2017) Study of HSPB6: Insights into the Properties of the Multifunctional Protective Agent. *Cell. Physiol. Biochem.* 44, 314–332
23 Nitert, M.D. *et al.* (2012) Impact of an exercise intervention on DNA methylation in skeletal muscle from first-degree relatives of patients with type 2 diabetes. *Diabetes* 61, 3322–3332
24 Song, S. *et al.* (2019) The HDAC3 enzymatic activity regulates skeletal muscle fuel metabolism. *J. Mol. Cell Biol.* 11, 133–143
25 Seaborne, R.A. *et al.* (2018) Methylome of human skeletal muscle after acute & chronic resistance exercise training, detraining & retraining. *Sci. Data* 5, 180213
26 Brown, W.M. (2015) Exercise-associated DNA methylation change in skeletal muscle and the importance of imprinted genes: a bioinformatics meta-analysis. *Br. J. Sports Med.* 49, 1567–1578
27 Gouspillou, G. *et al.* (2014) The relationship between muscle fiber type-specific PGC-1α content and mitochondrial content varies between rodent models and humans. *PLoS ONE* 9, e103044
28 Haizlip, K.M. *et al.* (2015) Sex-based differences in skeletal muscle kinetics and fiber-type composition. *Physiology (Bethesda)* 30, 30–39
29 Laughlin, M.H. *et al.* (2006) Exercise training produces nonuniform increases in arteriolar density of rat soleus and gastrocnemius muscle. *Microcirculation* 13, 175–186
30 Brüning, J.C. *et al.* (1998) A muscle-specific insulin receptor knockout exhibits features of the metabolic syndrome of NIDDM without altering glucose tolerance. *Mol. Cell* 2, 559–569
31 DeBalsi, K.L. *et al.* (2014) Targeted metabolomics connects thioredoxin-interacting protein (TXNIP) to mitochondrial fuel selection and regulation of specific oxidoreductase enzymes in skeletal muscle. *J. Biol. Chem.* 289, 8106–8120
32 Roman, W. and Gomes, E.R. (2018) Nuclear positioning in skeletal muscle. *Semin. Cell Dev. Biol.* 82, 51–56
33 Finsterer, J. (2012) Biomarkers of peripheral muscle fatigue during exercise. *BMC Musculoskelet. Disord.* 13, 218
34 Old, S.L. and Johnson, M.A. (1989) Methods of microphotometric assay of succinate dehydrogenase and cytochrome c oxidase activities for use on human skeletal muscle. *Histochem. J.* 21, 545–555
35 Talbot, J. and Maves, L. (2016) Skeletal muscle fiber type: using insights from muscle developmental biology to dissect targets for susceptibility and resistance to muscle disease. *Wiley Interdiscip. Rev. Dev. Biol.* 5, 518–534
36 Bourdeau Julien, I. *et al.* (2018) Metabolic networks influencing skeletal muscle fiber composition. *Front. Cell Dev. Biol.* 6, 125
37 Arany, Z. *et al.* (2007) The transcriptional coactivator PGC-1beta drives the formation of oxidative type IIX fibers in skeletal muscle. *Cell Metab.* 5, 35–46
38 Handschin, C. *et al.* (2007) Skeletal muscle fiber-type switching, exercise intolerance, and myopathy in PGC-1alpha muscle-specific knock-out animals. *J. Biol. Chem.* 282, 30014–30021
39 Challen, G.A. *et al.* (2011) Dnmt3a is essential for hematopoietic stem cell differentiation. *Nat. Genet.* 44, 23–31
40 Nguyen, S. *et al.* (2007) Ablation of de novo DNA methyltransferase Dnmt3a in the nervous system leads to neuromuscular defects and shortened lifespan. *Dev. Dyn.* 236, 1663–1676

41 Nishikawa, K. *et al.* (2015) DNA methyltransferase 3a regulates osteoclast differentiation by coupling to an S-adenosylmethionine-producing metabolic pathway. *Nat. Med.* 21, 281–287
42 Krupenko, S.A. (2009) FDH: an aldehyde dehydrogenase fusion enzyme in folate metabolism. *Chem. Biol. Interact.* 178, 84–93
43 Fernandez-Marcos, P.J. and Nóbrega-Pereira, S. (2016) NADPH: new oxygen for the ROS theory of aging. *Oncotarget* 7, 50814–50815
44 Ferreira, L.F. and Laitano, O. (2016) Regulation of NADPH oxidases in skeletal muscle. *Free Radic. Biol. Med.* 98, 18–28
45 Du, J. *et al.* (2015) DNA methylation pathways and their crosstalk with histone methylation. *Nat. Rev. Mol. Cell Biol.* 16, 519–532
46 Reusch, V.M. and Burger, M.M. (1974) Distribution of marker enzymes between mesosomal and protoplast membranes. *J. Biol. Chem.* 249, 5337–5345
47 Hidalgo, C. *et al.* (2006) A transverse tubule NADPH oxidase activity stimulates calcium release from isolated triads via ryanodine receptor type 1 S -glutathionylation. *J. Biol. Chem.* 281, 26473–26482
48 Petrônio, M.S. *et al.* (2013) Apocynin: chemical and biophysical properties of a NADPH oxidase inhibitor. *Molecules* 18, 2821–2839
49 Welle, S.L. (2009) *Myostatin and muscle fiber size* . Focus on “Smad2 and 3 transcription factors control muscle mass in adulthood” and “Myostatin reduces Akt/TORC1/p70S6K signaling, inhibiting myoblast differentiation and myotube size.” *American Journal of Physiology-Cell Physiology* 296, C1245–C1247
50 Lane, S.C. *et al.* (2015) Effects of sleeping with reduced carbohydrate availability on acute training responses. *J. Appl. Physiol.* 119, 643–655
51 Hood, D.A. *et al.* (2019) Maintenance of skeletal muscle mitochondria in health, exercise, and aging. *Annu. Rev. Physiol.* 81, 19–41
52 Gouspillou, G. and Hepple, R.T. (2016) Editorial: mitochondria in skeletal muscle health, aging and diseases. *Front. Physiol.* 7, 446
53 Kuzmiak-Glancy, S. and Willis, W.T. (2014) Skeletal muscle fuel selection occurs at the mitochondrial level. *J. Exp. Biol.* 217, 1993–2003
54 Boushel, R. *et al.* (2014) Mitochondrial plasticity with exercise training and extreme environments. *Exerc. Sport Sci. Rev.* 42, 169–174
55 Kim, Y. *et al.* (2017) Impact of aging and exercise on mitochondrial quality control in skeletal muscle. *Oxid. Med. Cell. Longev.* 2017, 3165396
56 Yoo, S.-Z. *et al.* (2018) Role of exercise in age-related sarcopenia. *J. Exerc. Rehabil.* 14, 551–558
57 Picca, A. *et al.* (2019) Targeting mitochondrial quality control for treating sarcopenia: lessons from physical exercise. *Expert Opin. Ther. Targets* 23, 153–160
58 Safdar, A. *et al.* (2011) Exercise increases mitochondrial PGC-1alpha content and promotes nuclear-mitochondrial cross-talk to coordinate mitochondrial biogenesis. *J. Biol. Chem.* 286, 10605–10617
59 Zechner, C. *et al.* (2010) Total skeletal muscle PGC-1 deficiency uncouples mitochondrial derangements from fiber type determination and insulin sensitivity. *Cell Metab.* 12, 633–642
60 Rowe, G.C. *et al.* (2012) PGC-1α is dispensable for exercise-induced mitochondrial biogenesis in skeletal muscle. *PLoS ONE* 7, e41817

61 Tidball, J.G. and Wehling-Henricks, M. (2007) The role of free radicals in the pathophysiology of muscular dystrophy. *J. Appl. Physiol.* 102, 1677–1686
62 Bowen, T.S. *et al.* (2015) Skeletal muscle wasting in cachexia and sarcopenia: molecular pathophysiology and impact of exercise training. *J. Cachexia Sarcopenia Muscle* 6, 197–207
63 Simioni, C. *et al.* (2018) Oxidative stress: role of physical exercise and antioxidant nutraceuticals in adulthood and aging. *Oncotarget* 9, 17181–17198
64 Lejay, A. *et al.* (2014) Mitochondria: mitochondrial participation in ischemia-reperfusion injury in skeletal muscle. *Int. J. Biochem. Cell Biol.* 50, 101–105
65 Di Meo, S. *et al.* (2017) Skeletal muscle insulin resistance: role of mitochondria and other ROS sources. *J. Endocrinol.* 233, R15–R42
66 Dimauro, I. *et al.* (2020) Exercise, redox homeostasis and the epigenetic landscape. *Redox Biol.* 35, 101477
67 Radak, Z. *et al.* (2013) Oxygen consumption and usage during physical exercise: the balance between oxidative stress and ROS-dependent adaptive signaling. *Antioxid. Redox Signal.* 18, 1208–1246
68 Radak, Z. *et al.* (2011) Age-dependent changes in 8-oxoguanine-DNA glycosylase activity are modulated by adaptive responses to physical exercise in human skeletal muscle. *Free Radic. Biol. Med.* 51, 417–423
69 Rasmussen, M. *et al.* (2014) Dynamic epigenetic responses to muscle contraction. *Drug Discov. Today* 19, 1010–1014
70 Henríquez-Olguin, C. *et al.* (2019) Cytosolic ROS production by NADPH oxidase 2 regulates muscle glucose uptake during exercise. *Nat. Commun.* 10, 4623
71 Sakellariou, G.K. *et al.* (2013) Studies of mitochondrial and nonmitochondrial sources implicate nicotinamide adenine dinucleotide phosphate oxidase(s) in the increased skeletal muscle superoxide generation that occurs during contractile activity. *Antioxid. Redox Signal.* 18, 603–621
72 Prosser, B.L. *et al.* (2011) X-ROS signaling: rapid mechano-chemo transduction in heart. *Science* 333, 1440–1445
73 Oleinik, N.V. *et al.* (2011) Epigenetic silencing of ALDH1L1, a metabolic regulator of cellular proliferation, in cancers. *Genes Cancer* 2, 130–139
74 Kang, J.H. *et al.* (2016) Aldehyde dehydrogenase is used by cancer cells for energy metabolism. *Exp. Mol. Med.* 48, e272
75 Krupenko, S.A. and Krupenko, N.I. (2019) Loss of ALDH1L1 folate enzyme confers a selective metabolic advantage for tumor progression. *Chem. Biol. Interact.* 302, 149–155
76 Kim, D. *et al.* (2015) HISAT: a fast spliced aligner with low memory requirements. *Nat. Methods* 12, 357–360
77 Love, M.I. *et al.* (2014) Moderated estimation of fold change and dispersion for RNA-seq data with DESeq2. *Genome Biol.* 15, 550

Chapter 4:
Conclusion

By 2030, metabolic diseases will be the number one noncommunicable disease on a global scale with one billion people suffering from metabolic disorders and their consequences (1). Metabolic disorders are caused by a lot of known risk factors such as dietary intake, lack of exercise and other lifestyle behaviors (2). Recently, a rising number of studies have linked differential epigenetic modifications with metabolism (2). The most relevant epigenetic modifications involved in gene activity regulation are DNA methylation, histone modifications, and non-coding RNAs (3). Out of these, DNA methylation is the most extensively studied epigenetic mark in relation to gene expression regulation (3). Despite the efforts taken to unravel the specific contributions of writers (DNA methyltransferases) and erasers (TET methylcytosine dioxygenases) of DNA methylation, the underlying molecular mechanisms remained previously unknown. My thesis work focuses on identifying the specific roles of TET1 and DNMT3A in metabolic regulations.

Chapter 1 provides a review on the detailed understanding of DNMT3a and TET2 mechanisms, which may lead to identifying novel targets for the treatment of IR and relevant human diseases.

Chapter 2 reports the role of Tet1 as a potent beige-selective epigenetic breaker of the thermogenic gene program. TET1 expression was increased during white adipogenesis and reduced during beige and brown adipogenesis, displaying an anti-correlation with UCP1 levels. TET1 also suppresses adipocyte thermogenesis in a cell-autonomous manner in beige adipocytes. Furthermore, adipose specific TET1 KO mice were more glucose tolerant and insulin sensitive than controls, having reduced insulin levels at fed and fast states on HFD. Finally, TET1-mediated suppression of the thermogenic gene program is largely done in a DNA demethylase-independent manner and in large part due to HDAC1. These findings advances our understanding of how thermogenesis is regulated by epigenetics and lead to a therapeutic strategy to increase energy expenditure in obesity and related metabolic disorders.

Chapter 3 shows that DNMT3A plays a necessary role in endurance exercise by suppressing ALDH1L1-mediated oxidative stress. Muscle-specific *Dnmt3a* ablation decreases the capacity for endurance exercise, shows reduced oxidative capacity and diminished mitochondrial respiration. Importantly, gene profiling studies identified *Aldh1l1* as a key target gene of DNMT3A in the soleus muscle. Furthermore, ALDH1L1 drives the increase in ROS and mitochondrial dysfunction in KO soleus muscle. Finally, resolving oxidative stress and muscle targeted *Aldh1l1* silencing in Dnmt3a KO mice partially rescues exercise intolerance. Together, our results provide novel insights into the epigenetic regulation of the muscle response to exercise and reveal a surprising molecular target that is important for sustaining endurance exercise.

Overall, my work not only advances our understanding of the epigenetic regulations in metabolism but also provides novel insights into the development of improved therapeutic strategy in the future.

References

1. Kelly T, Yang W, Chen CS, Reynolds K, He J. Global burden of obesity in 2005 and projections to 2030. Int J Obes (Lond). 2008 Sep;32(9):1431–7.
2. Tzika E, Dreker T, Imhof A. Epigenetics and metabolism in health and disease. Front Genet. 2018 Sep 18;9:361.
3. Samblas M, Milagro FI, Martínez A. DNA methylation markers in obesity, metabolic syndrome, and weight loss. Epigenetics. 2019 Mar 27;14(5):421–44.